

Master Thesis, Department of Geosciences

# **Spatial and temporal analysis of Holocene coastal development: applications to erosion assessment and cultural heritage mitigation in Svalbard**

**Evangeline Sessford**



**UNIVERSITY OF OSLO**

**FACULTY OF MATHEMATICS AND NATURAL SCIENCES**



# **Spatial and temporal analysis of Holocene coastal development: applications to erosion assessment and cultural heritage mitigation in Svalbard**

**Evangeline Sessford**

This thesis was carried out in connection with:









Master Thesis in Geosciences

Discipline: Physical Geography, Hydrology and Geomatics

Department of Geosciences

Faculty of Mathematics and Natural Sciences

University of Oslo

May 2013

© **Evangeline Sessford, 2013**

This work is published digitally through DUO – Digitale Utgivelser ved UiO

<http://www.duo.uio.no>

It is also catalogued in BIBSYS (<http://www.bibsys.no/english>)

All rights reserved. No part of this publication may be reproduced or transmitted, in any form or by any means, without permission.

## **Abstract**

High geomorphic and climatic variability in Arctic coastlines makes evaluating future coastal erosion in a changing climate a challenge. Predictions must, among other things, incorporate modifications to sediment supply and accommodation space, changes in the permafrost regime, climate variability including rising air and sea temperatures, stronger winds, less sea ice, and increased precipitation. This thesis explores processes and climate variables associated with coastal development throughout the Holocene and within modern times. In so doing, it illustrates how research builds upon itself and can be extended into applied science sectors concerning coastal protection and mitigation strategies.

In response to the need for more detailed surface maps in coastal regions on Svalbard, a combination of geomorphological field observations, differential GPS measurements, and aerial image analysis were used to produce detailed Quaternary maps for two field sites in Central Spitsbergen, Skansbukta and Fredheim. These provide the basis for further study, as mapping in itself is not sufficient for future projections relevant to mitigation strategies and cultural heritage protection. One site of significant value to the cultural memories of Svalbard was chosen for further investigations. The development of Fredheim's unconsolidated coast has been reviewed in relation to climatic changes during the Holocene, sediment supply and accommodation space, and geomorphic processes such as: beach aggradation, unconsolidated sediment coastal erosion, bedrock erosion, ice push and melt out, and longshore drift.

The relation between coastal processes and climatic variability are reviewed using relative and absolute chronology through spatial analysis and radiocarbon dating. Results from this study are compared to published data from other locations in Central Spitsbergen. Incorporation of rates and age restraints has produced a shoreline displacement curve providing relative time constraints on uplift and thereby understanding of climatic influences on coastal processes in the past. Present day coastal processes are used as a key to past shoreline development and when the past processes are seen from the context of the present, it is possible to outline possible future changes that may threaten the cultural heritage.

To further assess the modern processes and current state of the coastline at Fredheim, the new Digital Shoreline Analysis System tool (DSAS) was used to quantify coastal erosion rates. Three other sites with unconsolidated coastlines, showing variations in

geomorphology, sedimentology, and exposure to environmental forces, are also reviewed to illustrate disparities in erosional response. Results reveal that even within a single site, such as the 290 m long coastal section at Fredheim, large variations in erosion rate occur. This implies that spatial differences are significant in coastal development and need to be assessed in combination with temporal variability for future assessments and cultural heritage mitigation.

The spatial and temporal analysis of Holocene coastal development and modern erosion rates are applied to erosion protection within the field of engineering in the final chapter of this thesis. Having examined the mechanisms behind coastal erosion, in relation to sediment type and bedrock stability, it is suggested that a wooden barricade using posts drilled into the permafrost be built at Fredheim to protect the coast from further erosion. Such a barricade has previously been used on Svalbard and has shown to be extremely resistant to erosion and sea ice impacts and will also prevent sediments from washing away due to fluvial activity through relict channels.

## Preface

Throughout my life I have made quick decisions concerning life changing circumstances, especially in regards to my education. I have never, even as a child dreamed to be anything in particular but always jumped at that which interested me at the time and stuck with the consequences no matter what. Fortunately, the majority of such decisions have led to a remarkably exciting, productive, and fulfilling education (and I dearly hope it continues!). I have bitterly fought with administrative boards to be given permission to do the unusual. In secondary school I went to Germany on an unorganized exchange, during my bachelors no one was aware of UNIS, and did not want to give me credit for study there. And during my master studies I decided to complete the entirety of my fieldwork and writing on Svalbard and opt out of the mandatory courses at UiO in exchange for those at UNIS. This, along with the final written style of my thesis are options that most master students, if not all at UiO, are unaware of.

I aspired to write my thesis as an assemblage of two scholarly papers and include an introduction to set the scene, scope and aim for the papers and closing chapters to tie the work together, in replacement of the traditional style format. Having discussed this idea with my supervisors we were under the impression that directing my thesis in such a manner would allow the project to be explored in more detail and be beneficial to us all. The Quaternary maps and their descriptions are first author work, the second chapter is the main focus of my work of which I am also first author, I am second author of the third chapter which describes present coastal erosion on Svalbard, and chapter four of which I am co-author is a representation of how this study is applicable to engineers and government interests alike. My part in the methods and writing process is clearly explained in the thesis introduction, along with the motives and scope of the study.

I wished to use this writing style for a number of reasons. The first is that I had been asked to co-author the paper, "Time-lapse aerial photography reveals significant coastal erosion on Svalbard, Norwegian high Arctic", with PhD candidate, Emilie Guegan, at the Norwegian Institute for Science and Technology (NTNU). This paper is directly related to my thesis work. I decided to take the opportunity to broaden my research capabilities and strengthen my ability to work as a team toward a common research goal. It is also an accepted and encouraged form of thesis manuscript in Canada where I am originally born and raised. As I may one day return to Canada, it seemed the most logical step forward for continuation of my studies or in the working field. In my opinion the presentation of such a thesis is more

distinguished, organized and pleasing to read. It also provides me with a sturdier foundation for article submission in the future, as I intend on furthering my studies as a PhD candidate.

Conducting my thesis in such a way gave me the opportunity to work with a broader group of people and research groups. It opened doors for contract work with SINTEF and collaboration with the Governor of Svalbard. In so doing, it has also widened my areas of interest and knowledge to that of coastal engineering in arctic environments and thereby blooming new friendships. It is my hope that future students at UiO, and other Norwegian universities will become aware of the plethora of opportunities available to master students and that sticking to the norm may be the simplest option, but not necessarily the most inspiring, thrilling, or passion filled as breaking away can be.

## Author contributions

As there are one or more co-authors in chapters ten through thirteen, I would like to specify my contributions to the work.

Chapter ten: These map descriptions are written by me as was the cartographic work drawn. Anne Hormes initiated the process for publication in the Norwegian Polar Institute Report Series and contributed through fieldwork, discussions, and editorial review. Final editorial review and mapping guidance was contributed by Winfried Dallmann of the Norwegian Polar Institute. Special thanks to Lena Rubensdotter for advice on mapping techniques.

Chapter eleven: I was responsible for the bulk of the research, fieldwork and writing of this paper. Anne Hormes contributed through field work, writing of the sedimentology and radiocarbon paragraphs, drawing of log Figures, writing guidance, and editorial review. Additional support and guidance were given by Henrik Rasmussen and Bernd Etzelmüller. Intended article submission is to *The Holocene* within some months after thesis submission.

Chapter twelve: This paper was initialized and directed by Emilie Guegan. I was responsible for the aerial image analysis, erosion rate calculations and writing of everything pertaining to the field sites, Fredheim and Skansbukta. Initial editing of the paper was completed by me. Emilie Guegan focused on the remaining two field sites and Anders Schomacker guided the writing process and contributed insight on image and Figure presentation along with editorial review. Anne Hormes completed the editorial review. It has been submitted to *Geology* on 17 April 2013.

Chapter thirteen: This report was a collaborative effort led by Jomar Finseth with contributions by Anne Hormes and myself. It has been added to the thesis as an example of the applicability of this research to engineers for use in mitigation and protection strategies. The report is presented in its original portable document format as originally published and edited by SINTEF. All sections in English and associated Figures pertaining to the geology of Fredheim are written and produced by me. Field data collection for 2011 and 2012 was conducted by me with contributions by field assistants and SINTEF colleagues, Håkon Tangen and Joar Justad, and has been used in other sections of the report.

## Acknowledgements

This thesis would not have been possible to complete without the never-ending help and encouragement from many professors, colleagues, friends and family. For this reason I'd like to give a shout out to those who were particularly abundant with their support.

Anne Hormes, you are truly the best supervisor I could have had. Without your offer to me to take this master position, I would likely not have been able to come back to Svalbard and live. You were always available for me when I came knocking on your office door and constantly had so many new ideas, journal articles and field advice for me that it was difficult to keep up with your enthusiasm! But, not only have you been wonderful to me in my studies, but also in my personal life, always helping out with the next new climb and ready with skis, dogsledding, a night out, and a place to crash afterward. To Bernd Etzelmüller, as an internal contact at UiO, far away in the big city you have always been available answering e-mails in record time and sure not to leave me hanging when a question came your way. Thank you both.

Emilie Guegan, I would not have written my thesis as an assemblage of articles if not for you. It has been a pleasure working with you and Anders Schomacker in writing our paper and look forward to more opportunities in the future! Jomar Finseth, you have opened my eyes to the opportunities available within arctic technology and hope to collaborate again in the future. I never would have gotten through the problems presented to me by ArcGIS, aerial images and differential GPS data if it had not been for the constant support of Harald Faste Aas at Norwegian Polar Institute who replied to e-mails, met with me and gave constant support.

I have been fortunate to have had many field assistants with varying abilities and skills and would also like to acknowledge them. Hanna Hassberg, you are my survival suit. To this day I would likely still be floating around Billefjorden in a zodiac with a non-responsive engine if you were the type to get sea-sick. Fortunately, you had the ability to keep calm and in good spirits with me on fieldwork for both seasons. Your delicious cooking, witty humour, knowledge as a fellow geographer/geologist and skills as a button pusher and DGPS holder were the true reasons behind the successful collection of data. I have Håkon Tangen and Joar Justad to thank for my skills at operating DGPS in the field. Ole Patrick Larsen and Stefán Benediktsson, I'll recommend you any day to walk the GPR line. I have Alexander Hovland to thank for my constant supply of coffee both in the field, and when suffering in the office.



A thank you must also go out to SINTEF, Svalbard Science Forum and Sysseimann for financial and field support. Without your aid fieldwork would have been lacking.

Benni, Mer, Ingrid, Ivar, Vidar, Steve, Dani and Jonathan, your friendship has been crucial in many ways and I would not be as I am without you. And lastly but most assuredly not least, thank you to my family and all other friends and colleagues who have not been mentioned by name here. Your faces and names are in my heart and I shall remember you as long as I am mentally able!

Longyearbyen, April 2013

## Contents

Abstract.....	i
Preface .....	iii
Author contributions .....	v
Acknowledgements .....	vi
List of Figures .....	x
List of Tables.....	xv
Chapter 1 - Introduction.....	1
1.1 Motivation .....	1
1.2 Scientific rationale .....	1
1.3 Objectives and scope.....	3
Chapter 2 - Literary background.....	5
2.1 Coastal erosion in the Arctic .....	5
2.2 Holocene climatic development in the Arctic .....	6
2.3 Svalbard climate development from 1912 to present.....	7
2.4 Uplifted marine terraces as indicators for climate and geomorphic development.....	9
Chapter 3 – Study sites .....	12
3.1 Svalbard Geological overview .....	12
3.1.1 Fredheim .....	13
3.1.2 Skansbukta.....	14
3.2 Cultural heritage on Svalbard .....	15
3.2.1 Fredheim .....	16
3.2.2 Skansbukta.....	17
Chapter 4 – Methodology .....	19
4.1 Differential GPS measurements.....	19
4.2 Manual erosion measurements .....	19
4.3 Active layer detachment slide measurements .....	20
4.4 Automatic camera .....	20
4.5 Radiocarbon samples .....	21
4.6 Mapping (ArcGIS) .....	21
4.7 Aerial images and Digital Shoreline Analysis System.....	21
4.8 Unused data collection.....	22
4.9 Changes and additions to field investigations.....	22
Chapter 5 – Summary of results.....	24
5.1 Sessford, E.G. and Hormes, A. (2013) NP Report Series .....	24
5.2 Sessford, E.G. and Hormes, A. (unpublished).....	24

5.3 Guegan, E.M., Sessford, E.G. and Schomacker, A. (submitted) Geology .....	25
5.4 Finseth, J., Sessford, E.G. and Hormes, A. (2012) SINTEF .....	26
Chapter 6 – Discussion .....	27
6.1 Spatial and temporal variation affecting coastal development .....	27
6.4 Implications for future coastal development .....	30
6.5 Effects of coastal processes on cultural heritage mitigation .....	31
Chapter 7 – Conclusions .....	32
Chapter 8 – Future work.....	34
Chapter 9 – References .....	36
Chapter 10 – Map descriptions of Fredheim and Skansbukta .....	43
10.2 Fredheim: Quaternary superficial deposits .....	45
10.3 Skansbukta: Quaternary superficial deposits .....	56
Chapter 11 – Holocene reconstruction and spatial analysis of coastal development in Svalbard.....	66
Chapter 12 – Time-lapse aerial photography reveals significant coastal erosion on Svalbard, Norwegian high Arctic .....	89
Chapter 13 – Erosjonssikring av Fredheim; visualiseringsprosjekt (Erosion protection at Fredheim; visualization project).....	101
Appendix – (external disc).....	149

## List of Figures

### Chapters 1 – 9

Figure 1: Temperature and precipitation data from Longyearbyen airport (Data acquired from met.no).....	09
Figure 2: Suggested pattern and magnitude of isostatic uplift for Svalbard subsequently to LGM retreat. The red dot notes the location of Fredheim, the main field site in this thesis. (Figure adapted from Ingolfsson and Landvik 2013).....	10
Figure 3: Geological overview map of Svalbard indicating the BFZ and fieldsite locations in respect to the bedrock geology and Longyearbyen. (Figure adapted from Norwegian Polar Institute online resources, <a href="http://geonet.npolar.no/items-general/frame.html">http://geonet.npolar.no/items-general/frame.html</a> ).....	12
Figure 4: Field site locations relative to Svalbard and the circumpolar north. (Image adapted from <a href="http://geology.com/world/arctic-physical-map.jpg">http://geology.com/world/arctic-physical-map.jpg</a> , Photos: Sessford 2011).....	15
Figure 5: Overview of eastern Isfjorden indicating Fredheim and Skansbukta in relation to the fjords and valleys (Figure adapted from Norwegian Polarinstitute Interaktive Kart, <a href="http://toposvalbard.npolar.no">http://toposvalbard.npolar.no</a> ).....	16
Figure 6: The cultural heritage buildings at Fredheim showing A: Gammelhytta, B: Villa, C: Nødhytta, and D: Outhouse (Sessford, May 2012).....	17
Figure 7: Hilmar Nøis standing with the presumed burnt down building in the foreground and the remaining buildings in the background (Photo taken in 1965, from archive belonging to John-Eldar Pedersen.).....	17
Figure 8: The remains of the crushed boats where the black line indicates the extent of ice floe thrusting as indicating by sediment push (Photo: Sessford, August 2012). Inset image of Hilmar Nøis with the boats in 1965 (From archive of John-Eldar Pedersen).....	17
Figure 9: Cultural heritage structures at Skansbukta (Photo: Sessford, August 2011).....	18
Figure 10: Looking southeast over Skansbukta with the cultural heritage boat on land in the centre of the image (Sessford, August 2011).....	18
Figure 11: The hunting and fishing hut as depicted by Arne Nøis in 1961-64 and as seen in August, 2009 (Photo: Sessford, drawing from archive belonging to John-Eldar Pedersen).....	18
Figure 12: Simplified sketch of buildings at Fredheim indicating manual measurement locations. Eastern points are used in analysis for the SINTEF report (i.e. F1e).....	19
Figure 13: Simplified sketch of active layer detachment slide measurements. The curved black line represents the scarp along the backwall as delineated by the change in angle, and discolouration of beach terrace stones. Slope gradients are a) top, b) middle, c) bottom with the average gradient represented as g). Measurements took place approximately every 2 m along the scarp (Sessford, June 2012).....	20

### Chapter 10

Figure 1: Aerial image 13824_00048 of Fredheim (Norwegian Polar Institute, 2009).....	44
Figure 2: Aerial image 13822_00081 of Skansbukta (Norwegian Polar Institute, 2009).....	44
Figure 3: Excerpt from map C9Q, Adventdalen Geomorphological and Quaternary Geological Map indicating the glaciofluvial material identified at Fredheim, from Tolgensbakk et al. 2000.....	45
Figure 4: Fluvially dominated sedimentation affected by longshore drift and fjord circulation at Fredheim. (Aerial Image S90, Norsk Polarinstitutt, 1990).....	46
Figure 5: Beach ridges on MT3, note linearity and spacing. Image taken from the northeast of the map facing south west, Nordbekken can be seen in the bottom right corner of the photo. (Sessford, 2012).....	48
Figure 6: Ice ride up/pile up from 1999 (Image from Sysselmannen på Svalbard, 2000).....	48
Figure 7: Pre-recent fluvial plain with recent fluvial sediments indicated in yellow. The limit between the pre-recent Nøis alluvial plain and the recent Sassen estuary is a sharp boundary seen clearly with vegetated river channels on the pre-recent delta (Sessford, June 2012).....	49
Figure 8: Backcutting of relict channel due to spring meltwater flow (Sessford, June 2012).....	50
Figure 9: MT3 with beach ridges overlain by alluvial fan containing some vegetated relict channels (Sessford, June 2012).....	50
Figure 10: Organic material below Nordbekken alluvial fan and relict channels leading away from the fan toward the buildings and the fjord (Sessford, June 2012).....	50

Figure 11: Strong backcutting and erosion where relict channels meet the coastal escarpment due to concentrated groundwater flow (note groundwater at base of escarpment) (Sessford, August 2011).....	50
Figure 12: Examples of a gelifluction lobe where the line indicates the front lip (Sessford, June 2012).....	51
Figure 13: Non-vegetated area on the slope of MT3 consisting of colluvium. The shovel shows the boundary between the present day surface and colluvium. At this particular location (nearby to the radiocarbon sample), one can see cracking where the initialization of a possible slope failure may occur in the future. (Sessford, October 2011).....	51
Figure 14: Bedrock exposure on MT3, note well rounded-ness (Sessford, June 2012).....	53
Figure 15: Mechanical (wind) and chemically eroded boulders that have undergone frost shatter (Sessford, June 2012).....	53
Figure 16: Terraces and bedrock mounds as indicated, purple line delimits the beach deformation by sea ice (Sessford, August 2012).....	53
Figure 17: Buildings at Fredheim from left to right: Nødhytta (emergency hut), Outhouse, Villa, Gammelhytta (Old hut) (Sessford, May 2012).....	54
Figure 18: Setting up the thermistor string (Hassberg, June 2012).....	55
Figure 19: Location of automatic camera and direction of photos taken by camera (Sessford, July 2012) .....	55
Figure 20: Colluvium undergoing erosion through slumping. Location of radiocarbon samples for MT3 (Sessford, June 2012).....	55
Figure 21: Steep shoreface at Skansbukta (Sessford, August 2011).....	56
Figure 22: The beach at Skansbukta where stones overlying wooden structures and half burying mining buckets indicate progradation (Kelley, September 2011).....	56
Figure 23: Approximate division of beach material at Skansbukta. Recent beach material is above the light blue line, vegetated material is below the dark blue line and lichen covered material is between the two. (Sessford, August 2011).....	57
Figure 24: Seasonal pond, note steep gradient toward coast and lack of vegetation. (Sessford, August 2011).....	57
Figure 25 (right): Vegetated beach and colluvial sediments, note rock fall material lying on surface. (Sessford, August 2011).....	57
Figure 26: Sea ice thrust on shore during winter (Sessford, April 2012).....	57
Figure 27: Beach hummocks from the south side of Skansbukta (Sessford, June 2012).....	57
Figure 28: Skansbukta slopes from the bay, note the rapid mass movement deposit in the middle of two debris flow accumulations (Hassberg, June 2012).....	58
Figure 29: Rock fall accumulation at the base of gully below cliff and above debris flow run-out (Sessford, August 2011).....	58
Figure 30: Elongated debris flow accumulations overriding each other with well-defined levees covering the snow avalanche deposits (Sessford, August 2011).....	58
Figure 31: Rapid mass movement deposit showing less active rock fall on the left where gelifluction is the more predominant slope movement, and the right side where rock fall is predominantly active. (Sessford, September 2011).....	59
Figure 32: Gelifluction steps to the side and above mine entrance. Note how rock fall is caught on the surface of each step (Sessford, June 2012).....	59
Figure 33: Large rock fall boulder stopped in bog area (Sessford, August 2011).....	60
Figure 34: Rock fall debris comes to stop on gelifluction steps, vegetation and cultural heritage material at mine entrance (Sessford, June 2012).....	60
Figure 35: Small rock fall and aeolian debris caught on snow patch surface (Sessford, June 2012).....	60
Figure 36: Patterned ground as seen from the slopes above the mine entrance (Sessford, August 2011).....	60
Figure 37: Bog north of cultural heritage zones and below debris flow accumulation (Sessford, August 2011).....	60
Figure 38: Man made path with small drainage opening (Sessford, July 2011).....	61
Figure 39: Waterfall over cliff from gully (Sessford, August 2011).....	62
Figure 40: Lowermost bedrock of the Gipshuken Fm. upper cliff exposures of the Kapp Starostin Fm. Both showing autochthonous weathering (Sessford, August 2011).....	62

Figure 41: The loading boat (Sessford, August 2011).....	62
Figure 42: The hunting and fishing cabin (Sessford, August 2011).....	62
Figure 43: All cultural heritage zones as seen from the slopes above (Sessford, August 2011).....	62

## Chapter 11

Figure 1: Map of Svalbard with an inset of Inner Isfjorden indicating the field site, Fredheim as well as the locations for radiocarbon samples in Salvigsen, (1990) (S1990 a: Erdmannflya, b:Bohemanflya), in western Isfjorden, and , Salvigsen, (1984), and Feyling-Hanssen, (1965), on the eastern coast of Billefjorden, (S 1984) and (FH 1965) at (c:Teltfjellbekken, d: Ekholmvik, e: Kapp Ekholm, f: Phantomvik, g: Mytilusbekken, and h: Gåsodden).....	69
Figure 2: Aerial images of Fredheim from 1977, 1990, and 2009 indicating fjord surface circulation toward the west. Note deltaic growth toward the east. (Images adapted from Norwegian Polar Institute).....	69
Figure 3: Sedimentological log of MT4 indicating radiocarbon sample depths and changes in depositional environment.....	73
Figure 4: Sedimentological log of MT3 with radiocarbon sample depths and indications of a transgression between Unit 1 and Unit 2.....	73
Figure 5: Inferred shoreline displacement curves as indicated by recalibrated radiocarbon dates from Feyling-Hanssen, (1965), Salvigsen, (1984), and Salvigsen, (1990). Results from this study, for Fredheim, are shown in relation to the others. The blue dashed boxes indicated the time frame elevation change used in emergence rate calculations. The transgression noted in the Sessford and Holmes curve is indicated by the sedimentological observations on MT3.....	74
Figure 6: Hummocky beach on MT3, note the rounded boulders from mechanical weathering through wave action, and holes from chemical weathering (Photo: Sessford, June 2012).....	76
Figure 7: Modern beach reach as delineated by the solid line, and hummocks outlined by the dashed line (Photo, June, 2012).....	76
Figure 8: Ice thrust ridge on MT3 during deposition of MT2 and cooler times within the Holocene (Photo, June 2012).....	77
Figure 9: Modern ice thrust ridge (marked as deformation by ice in Figure 3) (photo, June, 2012).....	77
Figure 10: Fair weather beach ridges on MT3. The Black backpack dimensions are approximately 60 by 20 cm.....	79

## Chapter 12

Figure 1: Location of the study sites on Svalbard. LYR indicates the main settlement, Longyearbyen. 1: Vestpynten, 2: Fredheim, 3: Skansbukta, 4: Svea.....	91
Figure 2: Coastal erosion and aggradation of the river delta from Sassendalen at Fredheim in 1977, 1995 and 2009. The limits of deltaic aggradation and fluvial erosion were measured by Digital Shoreline Analysis System tool (DSAS) and plotted in ArcGIS on the referenced aerial photograph from 2009 (Norwegian Polar Institute).....	93
Figure 3: Erosion rates for A) Vestpynten and B) Fredheim, and total erosion distance for C) Skansbukta and D) Svea.....	94

## Chapter 13

Figur 1: Fredheim sett fra sør-vest.....	107
Figur 2: Typisk plott etter DGPS undersøkelse.....	110
Figur 3: Typisk plott fra kornfordelingsanalyse; velgradert sand.....	110
Figur 4: Forenklet skisse av bygningene på Fredheim. Målene er oppgitt i meter og er utført i 14. juni 2012 (Tangen og Justad et al. 2012).....	111
Figur 5: Sone med vannkanaler i jorden og utvasking.....	112
Figur 6: Iskart 1. februar 2011 and 1. mars 2011.....	113
Figur 7: Iskart 1. februar 2012. and 1. mars 2012.....	113
Figur 8: Forklaring til iskart.....	113
Figur 9: Gjennomsnittlige erosjonsrater pr år i cm (venstre side), plottet mot sommertemperatur Svalbard (skala høyre side). (Temperaturer er hentet fra <a href="http://www.climate4you.com">www.climate4you.com</a> ).....	113

Figur 10: Presentasjon av målepunkt utført med DGPS, 2010, 2011 og 2012 (Tangen og Justad et al. 2011 og 2012).....	114
Figur 11: Red points mark geological outcrops made up of the Gipshuken Fm. at Sveltihel, Storgjelet in the Nøis Valley and Fredheim. The main river is Sassen River, flowing from Sassen Valley. Image adapted from Norsk Polarinstitutt, Interaktiv Kart TopoSvalbard.....	117
Figur 12: Geological map excerpt of Fredheim as created by Norsk Polarinstitutt (Lauritzen et al. 1989). Dark green is the Gipshuken Fm. and light green is the Kapp Starostin Fm. above. The off white areas represent fluvial and marine unconsolidated deposits. Note how there is no bedrock described at Sveltihel or Fredheim.....	117
Figur 13: Showing sediment deposits and sample locations. The buildings are marked as Outhouse (O), Main Villa (V), Emergency Hut (E) and Danielbu (D). Inside of the beach deformation area are two crushed boats. Note bedrock at the base of Marine deposit slopes. (Figure adapted from Sessford 2012, Master Thesis in Preparation).....	119
Figur 14: Aerial image from 1990 displaying sediment plume from Nøiselva carried by longshore drift toward the east. Orange line indicates extent of the delta and coastal cliff in 2009 as measured with DGPS. (Image adapted from Norsk Polarinstitutt image S90 2207).....	120
Figur 15: Bedrock outcrop at 16°56'2,214" E, 78°21'19,763" N, used for Q-system rock quality evaluation and samples C1 (detached from top of outcrop) and B2 (previously detached and found on beach below outcrop. (Photo: Sessford, July 2012)....	120
Figur 16: Samples C1 (left) and B2 (right) .....	121
Figur 17: Sample B1.....	121
Figur 18: Chemical and mechanical weathering on bedrock outcrops on terraces (photo: Sessford 2012).....	121
Figur 19: Bedrock outcropping on marine terrace (Photo: Sessford 2012).....	121
Figur 20: Spring melt-water flowing from snowpack along relict river and flowing over escarpment edge (Photo: Sessford, June 2012).....	122
Figur 21: Surface water flowing from spring meltwater into bog and then out toward the fjord along vegetated relict river channel (Photo: Sessford, June 2012).....	122
Figur 22: The Nøis River prograding delta has extended toward the east by approximately 125 metres in the last two decades (Photo: Sessford, August 2011).....	122
Figur 23: Unconsolidated bimodal fluvial sediments that make up the coastal escarpment. Note the positioning of the stones indicated by the curved line in the cliff section (marked in red) which show a distinct channel deposition above which vegetation is growing. The blue section is scree deposits from erosion of the escarpment. (Photo: Sessford, October 2011).....	124
Figur 24: Grain size analysis results for samples taken approximately 30 cm below escarpment top. Series labels correspond to DGPS measurement locations as shown in Figur 13.....	125
Figur 25: Grain size analysis results for samples taken in the middle of the escarpment approximately 1m above the base and directly above scree accumulation. Series labels correspond to DGPS measurement locations as shown in Figur 13.....	125
Figur 26: A relict channel that reaches the coastal escarpment and is undergoing higher erosion than inter-channel zones (un-vegetated). (Photo: Sessford, August 2011).....	126
Figur 27: Oblique photo of Fredheim distinctly showing snow catchment areas in vegetated relict fluvial channels (Photo: retrieved from Pedersen Archives approx. date of image 1965).....	126
Figur 28: Grain size results for fjord floor sediments in front of Fredheim where FF5, FF6 and FF7 are the blue, red and green lines respectively.....	127
Figur 29: Sea and glacier ice pushed up onto delta from the east (photo taken approximately 30 m from delta edge) (Photo: Sessford, March 2012).....	128
Figur 30: Ice piling up on edge of delta in front of Fredheim. Note the absence of sea ice in March (Photo: Sessford, 2012).....	128
Figur 31: Active layer detachment slides behind buildings. Note channel like vegetated areas below scarps with high gelifluction and vegetation. (Photo: Sessford 2011).....	128
Figur 32: Waves do not hit coastal escarpment even at high tide. (Photo: Sessford, June 2012).....	130
Figur 33: Ice foot attached to coastal escarpment possibly acting as an eroding agent through plucking of sediments. (Photo: Sessford March, 2012).....	130
Figur 34: Precipitation and temperature data for Svalbard from 1912 to 2012 (Accessed on 27.11.2012 from <a href="http://www.climate4you.com">www.climate4you.com</a> ).....	131

Figur 35: Prinsippskisse av erosjonssikring ved Fredheim.....	133
Figur 36: Moment på stolpe uten forsterkning og forankring, eksempel.....	133
Figur 37: Moment på stolpe med forsterkning og forankring, eksempel.....	134
Figur 38: Erosjonssikring mellom to pirer i Barentsburg.....	135
Figur 39: Visualisering: Sett fra nord, Tempelfjorden.....	135
Figur 40: Visualisering: Sett fra vest, tempelfjorden.....	136
Figur 41: Visualisering: Sett med fugleperspektiv fra sør.....	136
Figur 42: Visualisering: Sett med fugleperspektiv fra sør.....	137
Figur 43: Motiv fra Coles Bay, nordligste pir.....	138
Figur 44: Visualisering: Sett fra Vest, Sassenfjorden.....	138
Figur 45: Visualisering: Sett fra sør-vest, Sassenfjorden.....	139
Figur 46: Visualisering: Sett fra nord, Tempelfjorden.....	139
Figur 47: Visualisering: Kaikonstruksjon i Pyramiden etter senkekaske-prinsippet. ....	140
Figur 48: Visualisering: Sett fra Vest, Sassenfjorden. ....	141
Figur 49: Visualisering: Sett fra sør-vest, Sassenfjorden.....	141
Figur 50: Visualisering: Sett fra nord, Tempelfjorden.....	142
Figur 51: Visualisering: Sett fra Vest, Sassenfjorden.....	143
Figur 52: Visualisering: Sett fra sør-vest, Sassenfjorden.....	143
Figur 53: Visualisering: Sett fra nord, Tempelfjorden.....	144
Figur 54: Skisse med erosjonssikring av Fredheim (Bridget Thodesen, 2012). ....	145

## External Disc

Map 1: Fredheim, Isfjorden, Svalbard Quaternary geology and geomorphology map, 1:3000

Map 2: Skansbukta, Billefjorden, Svalbard Quaternary geology and geomorphology map, 1:2000

Figure DR1: Guegan et al., (submitted, Geology) supplementary material



## List of Tables

### Chapter 11

Table 1: Radiocarbon ages referred to in the text and used in the inferred shoreline displacement curve.....	71
--	----

### Chapter 13

Tabell 1: Beskrivelse av jord knyttet til kornfordeling (ISO 14688-1).....	111
Tabell 2: Resultat fra målinger utført ved Fredheim I perioden 1987-2012. Målingene i meter er i hovedsak utført med målebånd mellom det nord-østre hjørnet på de enkelte bygg og erosjonskanten.....	111
Tabell 3: Erosjonsrater presentert i cm basert på målinger vist i tabell 2.....	112
Tabell 4: Tabell med beskrivelse av jordprøver.....	114
Tabell 5: Beregnet antall år før bygninger er tatt av kysterosjon forutsatt konstante erosjonsrater i årene fremover. Tabellen viser tre scenarioer basert på de tre gjennomførte studiene.....	115
Tabell 6: Maksimum gjennomsnittlig erosjonsrate og minimum antall år før husene er tatt av erosjon.....	115
Tabell 7: Rock mass quality Q-system results for bedrock outcrop at Fredheim.....	123
Tabell 8: Quality classes for Q-values as described by Barton (personal communication). From this table one can see that at Fredheim there is extremely poor Class F rock.....	124
Tabell 9: Percentage of fine grains in fjord sediment samples.....	127

### External Disc

Guegan et al., (submitted, Geology): DR2 Supplementary material

## **Chapter 1 - Introduction**

### **1.1 Motivation**

In 2008/2009 and in response to the Governor of Svalbard's request, the Norwegian Institute for Cultural Heritage Research (NIKU) in collaboration with the University Centre in Svalbard (UNIS), initialized research on the threats coastal erosion poses on cultural heritage sites (Flyen, 2009). Results of the initial study established, among other things, the following:

1. Few geological maps of Svalbard show the surface layers of coastal regions
2. Existing images, aerial photographs and maps are not detailed enough to identify active coastal erosion
3. Sites are not only threatened by coastal erosion, but also other geohazards such as solifluction, river erosion and others whose magnitude is unknown

The resolve of the study proposed more extensive fieldwork to be absolutely essential and to "visit each individual historical site in order to evaluate the risk and effects of geothreats in short, medium and long term", in order to produce detailed surface maps of the areas (Flyen, 2009 p.13).

Undoubtedly this study conducted by NIKU and UNIS has left room for further investigations which need to be addressed scientifically. In order to evaluate the risks that coastal erosion poses on cultural heritage, it is necessary to understand the history of coastal development at the sites in question. Therefore the mapping in itself is not sufficient for future projections relevant to mitigation strategies and cultural heritage protection. Palaeo climate data and knowledge of coastal development is essential to understand the roles space and climate have on coastal development (Nichol, 2002). The Holocene history of the field sites, age constraints for timing of events and Quaternary mapping are imperative. It is also necessary to understand what implications coastal erosion has on the Arctic and future climate in general. The driving forces behind coastal erosion and spatial and temporal variability within the Arctic are crucial to the development of Arctic coastal research.

### **1.2 Scientific rationale**

Coastal erosion studies in the Arctic have increasingly come into focus as of the past couple of decades; a considerably shorter time period than studies of temperate coastlines (Lantuit 2008). However, it is becoming clear that the consequences of eroding coasts in the Arctic have a significant impact on climate warming due to the presence of onshore and offshore permafrost that when thawed releases excessive amounts of carbon dioxide, nitrous oxide

and methane into the atmosphere (Anisimov, 2007; Walter et al., 2007; Elberling et al., 2010; Shakhova et al. 2010). Thawing permafrost thereby pushes the Arctic into the position of having the most rapid environmental change experienced on earth, change which is expected to increase in the coming years (Anisimov, 2007; Romanovsky et al., 2010). Permafrost is rapidly thawing and studies suggest that coastal erosion may have more impact than given credit for (Rachold et al., 2005; Lantuit 2008).

During their investigation of 61 000 km of Arctic coasts, Lantuit et al. (2012) reported an average erosion rate of 0.5 m/ yr. This average is derived from a number of regional rates of which Svalbard is the lowest and the American Beaufort Sea the highest, returning 0 m/yr and 1.15 m/yr, respectively (Lantuit et al., 2012). This difference is suggested to come directly from the observation that Svalbard coasts have an “overwhelmingly rocky nature” with “virtually no visible ground ice” (Lantuit et al., 2012; 393, 391) and tidewater glaciers make up a large portion of coastal margins whereas the American Beaufort Sea has extensive unconsolidated coastlines containing massive ground ice thereby contributing through active layer detachments and retrogressive thaw slumping (Lantuit and Pollard 2005, Lantuit and Pollard 2008). However, these observations for Svalbard have been made from only 8,782 km of coast making up only 8.7 % of the total coastline length (Lantuit et al., 2012). Quaternary studies of sedimentary deposition which focus on the west and north coasts and all the inner fjord areas of Svalbard show that there are extensive sectors of coastline that are made up of unconsolidated sediments (Mangerud et al., 1992). Considering Svalbard’s apparent lack of coastal erosion, the relatively high weighted mean organic carbon content of 2.86 % (Lantuit et al., 2012) should not be considered negligible in regards to sediment budget and release of greenhouse gases. Results from the IPY 2007-2009 year showed that the warmest permafrost so far north in the northern hemisphere is present on Svalbard, suggesting that the vulnerability of coastlines is increasing (Christiansen and Etzelmüller 2010). It may be that the sediment and carbon increase are negligible in Svalbard, but cultural heritage buildings and present day infrastructure are threatened by increasing erosion rates. Very small scale variations in coastline alter the rates of erosion significantly. Assessments concerning the magnitude of erosion and accumulation of arctic coasts are monitored by The Arctic Coastal Dynamics (ACD) project (Rachold et al. 2005, Wangensteen et al. 2007). However, assessments mainly concern present day changes and there is little knowledge of past coastlines which provide valuable insight into future amplitudes of change (Woodroffe and Murray-Wallace, 2012).

To better understand these spatial differences between coastlines it is of interest to reconstruct Holocene landform development and review past climates to strengthen models simulating warmer scenarios in the future. Therefore, the Holocene climatic development

sheds light on the temporal and spatial changes that arctic coastlines have undergone in the past and what they might be facing in the future. This study attempts to use past shorelines as analogues for future changes in shoreline and coastal development and to assist in mitigation strategies for cultural heritage protection. It also reviews the present day land, sea and ice characteristics affecting coastal erosion.

### **1.3 Objectives and scope**

This thesis is intended to review the Holocene and climatic history of Svalbard and its effects on landform and hazard development, specifically coastal erosion. Two main field sites, Fredheim and Skansbukta, were chosen to approach this aim. In the process special attention is given to the following topics:

- Quaternary geological and geomorphological mapping and its use in:
  - past coastal processes and landform development
  - current erosion measurements and rates
  - cultural heritage mitigation strategies
- Shoreline displacement and the development of marine terraces in relation to the Holocene Thermal Maximum and coastal processes
- Land, sea, and ice influence on coastal erosion and aggradation

The chapters in this thesis are designed to replicate a logical workflow method and to illustrate how papers build upon each other within the scientific world and are assembled to further use within the public and applied science sectors. It begins with Quaternary mapping and map descriptions, the first step in a methodological approach to research and applied science pertaining to the earth's surface. It is necessary to begin with an overview of the research area and what earth processes have taken place in the past and are present now. The next step is using the mapping methods for relative chronology of landform development by using relative and absolute dating methods like radiocarbon dating to reconstruct coastal history to better understand future coastal characteristics within a changing climate. The third article continues to narrow down the focus by looking specifically into coastal erosion rates in Svalbard at the present time. The final chapter takes the scientific research work and illustrates how it can be used in the applied field for engineers and mitigation planning for cultural heritage in Svalbard.

There are a total of four field sites in this thesis; however, priority is given toward the Skansbukta and specifically the Fredheim site. The thesis is written from a Quaternary

geology perspective and directed towards persons studying or working with arctic coastal and near coast processes – in particular geologists, geographers and engineers.

## **Chapter 2 - Literary background**

### **2.1 Coastal erosion in the Arctic**

Present day Arctic coasts vary greatly in morphology and geological history but are characterized by the presence of both onshore and offshore permafrost and a short (3 to 4 months) period of open water where waves can reach and erode the coasts (Lantuit et al., 2012). For the remaining part of the year sea ice and shorefast ice generally hug the coastline thereby protecting it from wave based erosion. However with the present warming circumstances sea ice extent is in decline and coasts are becoming more vulnerable to wave action, thermal erosion, and melt out of ground ice (Aré, 1988, Nicholls et al., 2007; Lantuit and Pollard, 2008; Lantuit et al., 2011; Lantuit et al., 2012). Variability in coastlines alters the extent of erosion significantly as it alongside temporal variability control the depth of the active layer and ground ice content. Temporal variability in erosion rates is governed by climatic forcing which affects storminess and the presence of sea ice, and glacial proximity whereas spatial variability concerns cliff and beach morphology, proximity to river systems, cryology and lithology (Aré, 1988; Rachold et al., 2005; Solomon, 2005; Lantuit et al., 2011). These factors contribute greatly to coastal erosion rates.

The Arctic Coastal Dynamics (ACD) project is currently leading studies concerning Arctic coasts. It aims at estimating the quantity of sediments originating from coasts and entering the sea by assessing the rates and magnitudes of erosion (Rachold et al. 2005; Wangenstein et al. 2007; Lantuit 2008). During their investigation of 61 000 km of Arctic coasts, Lantuit et al. (2012) reported an average erosion rate of 0.5 m/yr. This average is derived from a number of regional rates of which Svalbard is the lowest and the American Beaufort Sea the highest, returning 0 m/yr and 1.15 m/ yr, respectively (Lantuit et al., 2012). These rates are comparable to others around the Arctic such as 0.59 m/yr on the Bykovsky Peninsula in the Russian Laptev Sea during the 1951 – 2006 period (Lantuit et al., 2012), 0.6 m/yr for the Beaufort Mackenzie region of Canada between 1972 and 2000 (Solomon, 2005), on Herschel Island in the Canadian Beaufort Sea 0.61 m/yr and 0.45 m/yr were calculated by Lantuit and Pollard (2008) for the 1952 - 1970 and 1970 - 2000 periods, respectively, and 0.31 m/yr for the 1949 – 1976 period near Barrow Alaska on the American Chuckchi Sea (Harper, 1978). The highest rates are associated with unconsolidated coasts with exceptionally high ice content; the lowest rates usually pertain to bedrock cliffs.

Present day rates are of importance in understanding the current health of coastlines, however the morpho-dynamics of coasts will alter as temperatures increase and coasts are subjected to warmer temperatures such as occurred during the Holocene Thermal Maximum.

Changes in the permafrost regime, sea ice extent, increased spring runoff, increased precipitation will indubitable have an effect on coastal retreat and growth.

Using the past as a proxy for future coastal development is crucial, especially when the Arctic is becoming a more active region both anthropogenically and geomorphically.

## **2.2 Holocene climatic development in the Arctic**

The transition from the Last Glacial Maximum (LGM) to the Holocene is generally attributed to the abrupt termination of the Younger Dryas (YD) 11,700 years BP (Miller et al., 2010). However, it is apparent that the start of the Holocene and significant events within it have not happened simultaneously through space and time (Kaufman et al., 2004). Svendsen and Mangerud, (1997) suggests that the onset of the Holocene in Svalbard began 10,000 cal BP, when glaciers became smaller than modern sizes. Observations of marine sediment cores by (Jessen et al., 2010), support this time frame as indicated by continued deposition of ice rafted debris (IRD), starting the Holocene warming 10,100 cal BP. Nevertheless, the variability in Holocene climate can essentially be divided into five periods (Miller et al., 2010); the Holocene Thermal Maximum (HTM) 10,100-8000 cal BP (Salvigsen, 2002; Jessen et al., 2010), gradual cooling after 8000 cal BP and establishment of cooler Neoglaciation after 4000-3000 cal BP (Salvigsen, 2002; Hald et al., 2004), Medieval Warm Period (MWP) between 1200-950 cal BP (Salvigsen, 2002; Miller et al., 2010), Little Ice Age (LIA) 550 cal BP-early 1900s (Miller et al., 2010; Berner et al., 2011) and modern years 1912-2012 (Miller et al., 2010; Humlum et al., 2011).

Open water proxies suggest that the HTM coalesced with increased mass of warm Atlantic and Pacific water moving northward (Miller et al., 2010). This, along with increased summer insolation, decreased perennial sea-ice cover and the northward advance of the Polar front were major contributing factors to rise in surface temperatures (Hald et al., 2004; Jessen et al., 2010; Miller et al., 2010; Berner et al., 2011). Miller et al., 2010, (p. 1703), suggest that, "quantitative estimates of HTM summer temperature anomalies around Svalbard range from 1 to 3° Celsius... and sea-surface temperatures were as much as 4-5 ° Celsius". Macrofossil studies on Bjørnøya suggest an enhanced seasonality with July temperatures of about 9°C and January temperatures of -12°C (Wohlfarth et al., 1995). Sea ice extension was at its minimum between 8500 and 7000 cal BP in Fram Strait (Müller et al., 2012). Some records indicate the beginning of a gradual cooling from about 8000 cal BP. On Bjørnøya pollen and macrofossil studies on lake sediments were used to reconstruct a temperature decrease (Wohlfarth et al., 1995). In Van Mijenfjorden sea-surface temperature (SST) decreased most likely due to decrease in summer insolation (Hald et al., 2004). The SST fall was likely influenced by an increase in Polar Water or freshwater runoff. Svendsen and Mangerud

(1997), suggest that glacier expansion began on Svalbard 5000 years ago but that continuous and sustained growth did not dominate glacier mass balance until 3000 years ago.

Evidence from *in situ* mosses beneath Longyearbreen glacier indicate that the glacier was at least 2 km shorter in length between 1900 and 1100 cal BP (Humlum et al., 2005). Summer temperatures declined in the last 1800 years, but were still relatively high until 1000 AD according to chironomid transfer functions from Lake Skardtjørna (Velle et al., 2011). Higher winter temperatures were reconstructed for the last 1200 years from ice core records, indicating a declining trend until about 1820 AD (Divine et al., 2011).

There is little evidence of the Medieval Warm Period (MWP) (1200 - 950 cal BP) in Svalbard, but the presence of *Mytilus edulis* found in fjords as described by (Salvigsen, 2002) suggest that a warming did occur. The ice core records indicate the warmest inter temperatures during the last 1800 years for  $870 \pm 140$  AD (Divine et al., 2011). The MWP period is generally credited to a reduction in sulfate aerosols due to increased volcanic activity (Miller et al., 2010). Shorelines during the MWP were approximately 2 metres higher than at present (Salvigsen, 1984). Though, proxy records based on chironomids and alkenones do not indicate any significantly higher summer temperatures during MWP (D'Andrea et al., 2012, Divine et al., 2011).

The Little Ice Age (LIA) is the last glacial cold period on Svalbard (550 cal BP - early 1900s). During this time period it is supposed that glaciers on Svalbard advanced further than during Neoglaciation. In western Spitsbergen neoglacial moraines were documented from several glacier forefields and dated by lichenometry and radiocarbon dating (Werner et al., 1993). The average temperature inferred for the Northern Hemisphere during LIA was 1° Celsius cooler than today (Miller et al., 2010). Modeling studies suggest that the negative phase of the North Atlantic Oscillation may have been amplified during this time (Miller et al., 2010). Cooling may also have been intensified by alterations in atmospheric circulation. It is well known that cooling during the LIA was mainly dominated by a decrease in Northern Hemisphere summer insolation (Miller et al., 2010). Insolation was affected by orbital changes, increased volcanism and decreased solar activity. Sea level in Svalbard was approximately one metre higher than today (Salvigsen, 1984).

### **2.3 Svalbard climate development from 1912 to present**

Svalbard has a highly sensitive climate which is likely the result of three main mechanisms as described by Humlum et al., (2003):



1. the archipelago is located within the main pathway for air masses in the Arctic Basin
2. Svalbard lies at the confluence of air masses and ocean currents with very different temperature characteristics such as the meeting of the Warm Atlantic Current and cold arctic waters (Nilsen et al. 2008)
3. Sea ice extent around Svalbard undergoes rapid variations coupled with atmospheric and oceanic circulation

Svalbard has the longest meteorological data record from the High Arctic which dates back to 1912 (Figure 1). The climate in Svalbard has long been of interest because of its dynamic variability. Between 1917 and 1922, a significant increase in temperature occurred which changed the mean annual air temperature (MAAT) from -9 Celsius to -4 Celsius at sea level (Humlum et al., 2011). This jump in temperature, (though disputed by Kohler et al., (2011) as being a gradual change rather than a step-like change) ended the LIA. A warming period took precedence lasting until approximately 1955 when the temperature dropped about 5° Celsius, followed by another cold period until 1990 and now the present stage of renewed warming (Humlum et al., 2011; Humlum et al., 2003). It appears as though a decadal-scale variation in temperature is superimposed on this general changing pattern and is forced by changes in winter temperature as opposed to large scale variations described in section 2.2 where summer insolation was a main driving force. Bednorz, (2011), describes a 1.65° Celsius increase in mean winter temperature per decade since 1975/1976 and that negative extremes are becoming less frequent. Such negative extremes are generally associated with high sea ice concentrations in mid-late winter. On the other hand, positive extremes are increasing, though not yet at a significant rate, and tend to coincide with low pressure troughs over the Fram Strait, bringing warm air masses from the south (Bednorz, 2011). During the winter, when there is no solar insolation, atmospheric circulation accounts for 95 percent of warm air to the Arctic, whereas only five percent is due to oceanic circulation (Bednorz, 2011).

The weather on Svalbard is heavily controlled by high and low pressure systems that are considered semi-permanent (Humlum et al., 2003). When the Siberian High pressure system extends over Russia, warm southerly air masses are advected over Svalbard causing heavy precipitation and warm temperatures even during winter. For example, in late January and early February in 2012, record amounts of precipitation, high temperatures (+6.6°C on February 8<sup>th</sup>), and melting occurred in Svalbard, causing overflow of the dammed lake, Isdammen, and large slush avalanches to be released in Longyearbyen and Barentsburg ([www.yr.no](http://www.yr.no), personal observation). It is not unlikely that other such events happened elsewhere on Svalbard at the same time.

Average precipitation is approximately 15-20 percent (per 100 m) in coastal regions but only about 5-10 percent in central areas (Humlum et al., 2003). These differences are allocated to orographic effects.

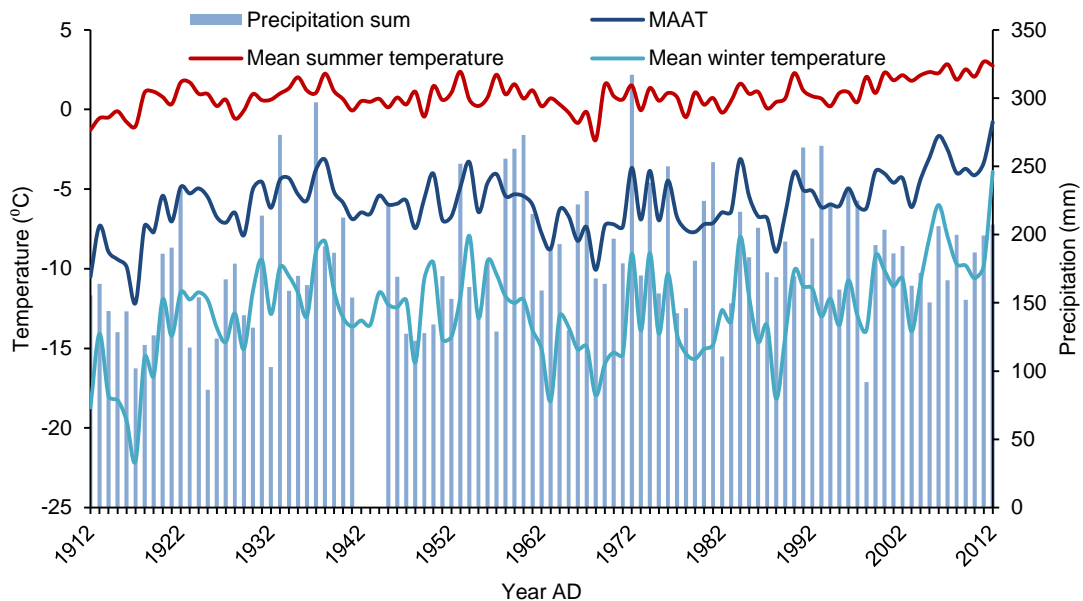


Figure 1: Temperature and precipitation data from Longyearbyen airport (Data acquired from met.no).

## 2.4 Uplifted marine terraces as indicators for climate and geomorphic development

It has long been acknowledged that uplifted marine terraces, (also known as raised beaches) are of primary importance in regards to glacial reconstruction and are considered isostatic fingerprints of past ice volume expansions (Feyling-Hanssen 1965, Boulton 1979, Forman and Miller 1984, Salvigsen 1984, Landvik et al. 1987, Salvigsen et al. 1990, Landvik et al. 1992, Ziaja and Salvigsen 1995, Salvigsen et al. 2005, Ingolfsson 2011, Ingolfsson and Landvik 2013, Long et al. 2013). Extensive investigations of maximum elevations and marine terrace locations in the Svalbard and Barents Sea region have led to the consensus that the Barents Sea Ice-Sheet (BSIS) of the Last Glacial Maximum (LGM) has inferred differential loading on the land surface (Salvigsen and Slettemark 1995, Ziaja and Salvigsen 1995, Forman et al. 2004, Ingolfsson 2011). The modern theory revolves around a multi-domed BSIS of varying ice thicknesses and thereby variations in differential loading and isostatic rebound (Hogan et al. 2010, Hormes et al. 2011, Ingolfsson and Landvik 2013). Therefore, the marine limit of one area in Svalbard for example, may alter from another location within the same fjord.

Vertical shoreline displacement combined with radiocarbon dating of whale bones, shells and driftwood can be used for reconstruction of the timing of deglaciation, the rate of isostatic uplift and for spatial and temporal comparison between shorelines (Ziaja and Salvigsen

1995). Collection of fossils from uplifted sediments of marine terraces, provided they have remained in situ, may correspond with relative sea level (RSL) synchronous with the time material was deposited (Feyling-Hanssen 1965, Forman et al. 1987). Age of material can easily be over or under estimated due to re-deposition by waves, rivers, glaciations, and periglacial processes. Shoreline displacement curves assist in reconstruction of the magnitude and pattern of postglacial isostatic uplift such as that for Svalbard seen in Figure 2 (Ingolfsson and Landvik 2013). They are created from mapping of marine terraces in association with dated material. The Holocene shoreline displacement curve as described by (Salvinsen, 1984) gives inner Isfjorden a displacement from approximately 70 m a.s.l. to 15 m a.s.l. between 10,000 and 6000 cal years BP suggesting an isostatic rebound of about 55 m during the HTM. Isostatic rebound was along the order of 8 m during neoglaciation, and 2 m during the MWP (Salvinsen, 1984). Therefore, it is apparent that glacier growth following the LGM was not extensive enough to depress the surface of Svalbard significantly.

By using ages of marine terraces in combination with surface topography, it is possible to hypothesize on climate variations at the time of uplift furthermore, associate changes in climatic forcing with the development of the shoreline. This is a branch of study which has only briefly been touched upon (Møller et al., 2002; Nichol, 2002)).

The surface topography of marine terraces i.e. beach ridge amplitude and wavelength, and shore gradient, serve as indicators of processes acting upon the shoreline during emergence and thereby record vertical and horizontal movement of the shoreline. Resulting beach plains will slope so that forelands prograde and older beach ridges will be more elevated than those that are younger (Feyling-Hanssen 1965). The

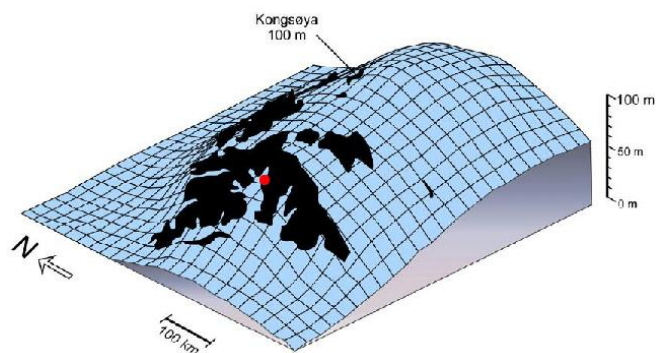


Figure 2: Suggested pattern and magnitude of isostatic uplift for Svalbard subsequently to LGM retreat. The red dot notes the location of Fredheim, the main field site in this thesis. (Figure adapted from Ingolfsson and Landvik 2013).

slope gradient therefore depends upon the rate of emergence and progradation of the shoreline, resulting in rapid ( $\sim >100$  cm/century) or slow ( $\sim 10$ -100 cm/century) displacement (inferred from Feyling-Hanssen and Olsson 1960). Beach ridges are formed along the top of the forelands due to dominant longshore beach drift, often producing storm ridges (Feyling-Hanssen 1965). A fair weather beach, also known as a berm ridge, might be characterized by low amplitude ( $<0.5$ m) beach crests with wavelengths of approximately 5m and are flat crested (Mason, 2010; Long et al. 2012). Beaches may be clear and defined as ridges or disrupted as hummocks/pits. The surface materials and sediment type making up beach

terraces gives insight into the dominant sediment supply source. Hilaire-Gravel et al., (2010, 215) suggest that there are five main controls on gravel beach morphology in the Arctic; sediment source and supply, rate and direction of sea-level change, basement topography, wave climate and sea ice. Areas with large beach ridge complexes have often been formed where sediment supply is abundant and longshore currents effective and can form under the rise or fall of RSL (Hilaire-Gravel et al., 2010). Therefore the surface topography of marine terraces can provide valuable information regarding relative sea-level changes, sea ice extent, storminess and variations in sediment supply (Møller et al., 2002; Hilaire-Gravel et al., 2010; Long et al. 2012).

Uplifted marine terraces should then be useful tools not only as indicators of isostasy due to differential loading and unloading of ice sheets and glaciations but also as clues into past shoreline development and climatic forcing.

## Chapter 3 – Study sites

### 3.1 Svalbard Geological overview

Svalbard contains an exceptionally good record of geological time as it documents sediment deposition from Precambrian to present day Quaternary landforms. It also reveals at least four major tectonic events recognized in the pre-Devonian, Late Devonian (the Svalbard equivalent to the Caledonian Orogeny), Carboniferous and Tertiary (Lauritzen, 1989). The Billefjorden Fault Zone (BFZ) is a north-south trending half-graben structure that formed in the Precambrian and during the middle Carboniferous (323 Ma) was reactivated as a normal fault and the Billefjorden trough sank (Steel, 1984). It is the most relevant fault to this study (Figure 3). The most recent earthquake of larger magnitude along the BFZ happened in

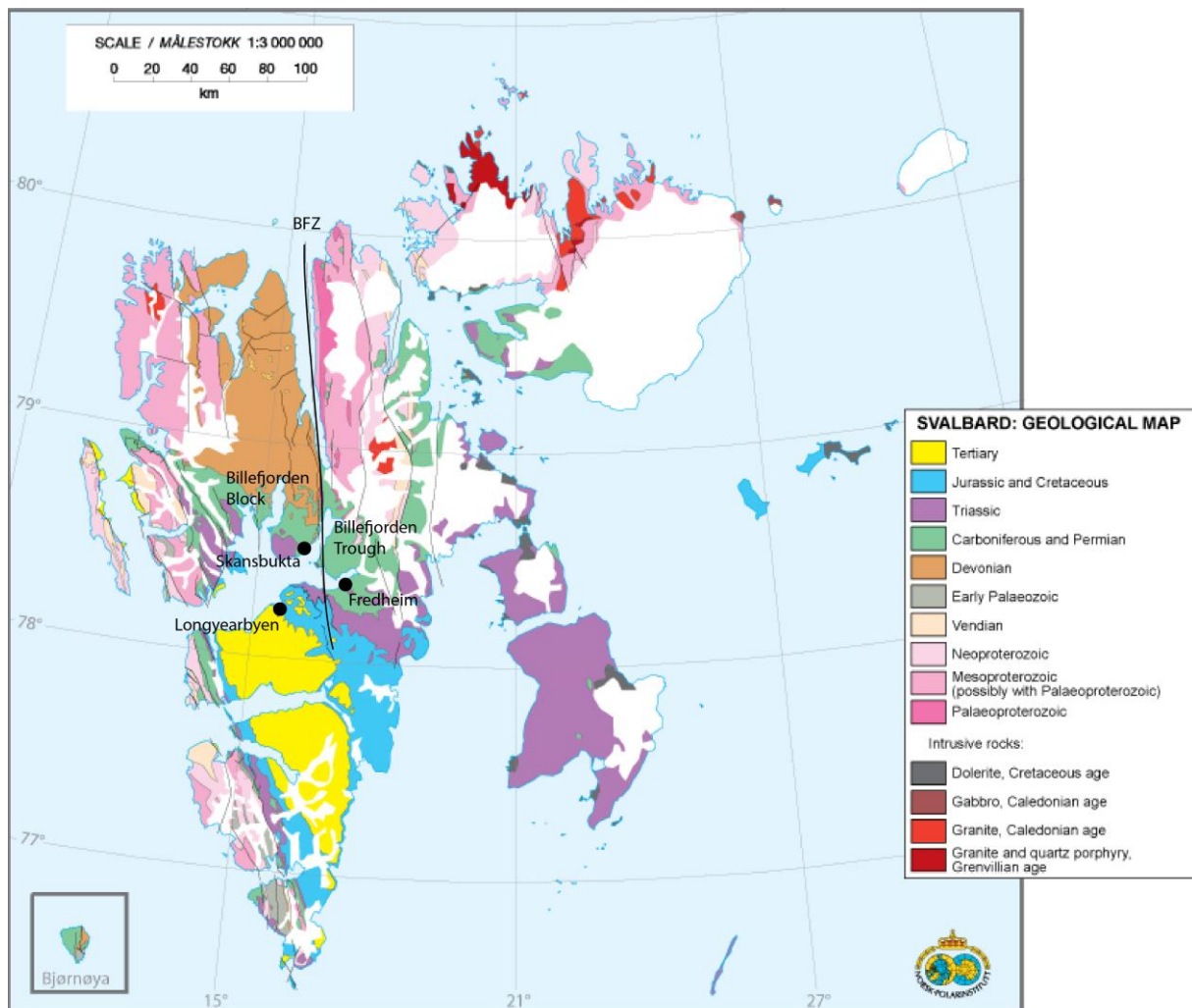


Figure 3: Geological overview map of Svalbard indicating the BFZ and fieldsite locations in respect to the bedrock geology and Longyearbyen. (Figure adapted from Norwegian Polar Institute online resources, <http://geonet.npolar.no/items-general/frame.html>)

February of 2008 and reached 6.2 on the Richter scale. During the Carboniferous, uplift of the half-graben occurred in the west an area known as the Nordfjorden Block and infill to the east, the Billefjorden Trough. Toward the end of the Carboniferous, sediment deposition was fairly uniform across the Svalbard central basin leading to platform deposition of Permian sediment to both the west and east of the BFZ (Dallmann, 1999). Toward the end of the Lower Permian, the Gipshuken Formation (Fm.) of Artinskian age was deposited. It is predominantly made up of interbedded dolomite and anhydrite in the lower part and fine-grained, algal dolomites in the upper (Lauritzen, 1989). Interpretation of the Gipshuken Fm. is sabkha deposits overlain by lagoonal, algal limestones (Lauritzen, 1989). The Kapp Starostin Fm. rests conformably above the Gipshuken Fm., dates to the Upper Permian and is lithologically composed of cherts, siltstones, siliceous sandstones and spiculitic shales (Lauritzen, 1989). Its resistance to weathering produces a distinct marker boundary between it and the lower Gipshuken Fm. The base of Kapp Starostin Fm. is made up of the Vøringen Member (Mb), a bioclastic, coarse grained limestone containing brachiopod and bryozoan fauna, marking the large scale transgression of Late Artinskian-Early Kungurian age (Lauritzen, 1989). The entire system has been uplifted in the north during the Tertiary therefore producing older exposed bedrock in the north and younger in the south. This left the central zone surrounding the confluence between Billefjorden and Tempelfjorden to contain Permian bedrock overlain by Quaternary sediments.

### **3.1.1 Fredheim**

The study area description is, unless otherwise stated, from observations taken during this study and expanded upon in Chapter 10 of this thesis. Fredheim lies directly on the eastern edge of the Billefjorden Fault Zone (BFZ) and within the Billefjorden Trough (Lauritzen, 1989) approximately 32 km east of Longyearbyen, as the crow flies (Figure 3). The entire region is covered by unconsolidated Holocene sediments except for a few locations where bedrock outcrops on the beach, coastal escarpment and between some marine terraces. Fredheim appears to sit on a strand flat and is covered by pre-recent fluvial sediments. To the west of the buildings are more recent fluvial deposits that cut through the pre-recent deposits and a river delta that originates from the River Nøis. The delta is actively building out toward the east and Fredheim. It contains an active lagoon that is changing its shape and drainage regularly. Southeast of Fredheim, are five marine terraces produced by isostatic rebound. All of the terraces have beach ridges on their surfaces. The terraces are separated by steep slopes containing gelifluction processes on the surface and sometimes vegetation, in particular the species *Salix Polarix*. Eleven active layer detachment slides are seen on the slopes between terraces. To the south of Fredheim is an active alluvial fan that is fed by a small melt water river coming from Fjordnibba (mountain to the east of Fredheim and not

shown in maps). This alluvial fan is surrounded by a small bog and the water is drained as ground water, below the surface and within the active layer. It appears that the groundwater follows relict rivers; braided river-like depressions that appear within the pre-recent fluvial deposits often sprouting much vegetation. Groundwater emergence is seen at the escarpments mostly west of Fredheim where they have incised the edge of the escarpments.

Sea ice is generally present 6-7 months a year, though in recent years sea ice extent has been in decline and has not been present at all over the last two winters (Norwegian Ice Service, 2012; personal observation). However, an ice foot generally forms along the coast from repeated freezing of waves along the shore and ice berg accumulation. Dominant wind directions have not been measured specifically for Fredheim. The dominant wind direction for all of Svalbard during the winter is from the southeast to the northwest; however regional disparities are likely present (Humlum et al., 2005). Permafrost is present and has an active layer depth of approximately 90 cm, as determined when installing thermistor stings in the active layer.

### **3.1.2 Skansbukta**

Unless otherwise stated, descriptions are from observations taken during this study and are expanded upon in Chapter 10. Like Fredheim, Skansbukta sits on the edge of the active Billefjorden Fault Zone (BFZ), only on the uplifted west rather than the trough in the east. It is approximately 35 km north of Longyearbyen if measured in a direct line (Figure 3). The lowermost geologic unit of the towering cliff of Skansen, is the Gipshuken Fm. of Lower Permian Age. Anhydrite dominates the lowermost regions but is overlain with intermittent layers of dolomite. Skansen has a very well exposed, 115 m thick, continuous section of finely-laminated algal dolomites above the anhydrite. These uppermost deposits are suggested by (Lauritzen, 1989) to be sabkha deposits lain down as a Permian karstic surface and terminates with caliche horizons, a sedimentary deposit of hardened calcium carbonates. Above the caliche horizons is the Kapp Starostin Fm. The cliff base begins at an altitude of 232 m a.s.l. and rises straight up to approximately 250 m a.s.l. It is split periodically by gullies which contain buildups of allocthonous weathering material and seasonal flow of water. Gullies are located above debris flow run-out zones. Colluvial fans are situated below fairly flat sections of cliff with no gully. The angle of the slope leading from the cliff base to the beach varies having a steeper gradient on colluvial fans and more of a concave shape within the debris flow zones. Rock fall is common, though much of it is caught amongst the vegetation that grows within the gelifluction lobes. The beach area below the cliffs is divided into four types of surface cover: recent beach sediments, sediments with lichen cover, beach and colluvial sediments with vegetation cover and bog. The latter two are very similar but the water content in the bog is higher, therefore producing greater quantity of



vegetation. Some depressions in the beach area are present and are described as Seasonal Ponds. Patterned ground can be seen from above when looking down on the beach. The seasonal water flow from the gullies is as waterfalls over the cliff and then groundwater until outflow at the edge of the recent beach, resurfacing for a brief time at the base of the slope as bog and intermittent rivers.

The same sea ice, wind and permafrost conditions are present at Skansbukta as are at Fredheim. However, the bay is more protected and rarely has large waves as it is protected on three sides and only really open to winds from the southeast.

### 3.2 Cultural heritage on Svalbard

Svalbard is an Arctic archipelago governed by Norway as established by the Spitsbergen Treaty of February 9, 1920 and is located between Northern Norway and the North Pole. To its East lies the Barents Sea and to the West, the Fram Strait (Figure 4). Though Icelandic annals suggest that Svalbard was first discovered in 1194, the first recorded discovery of Spitsbergen (the largest and central island within the archipelago), was by a Dutch crew in 1596 piloted by Willem Barentsz

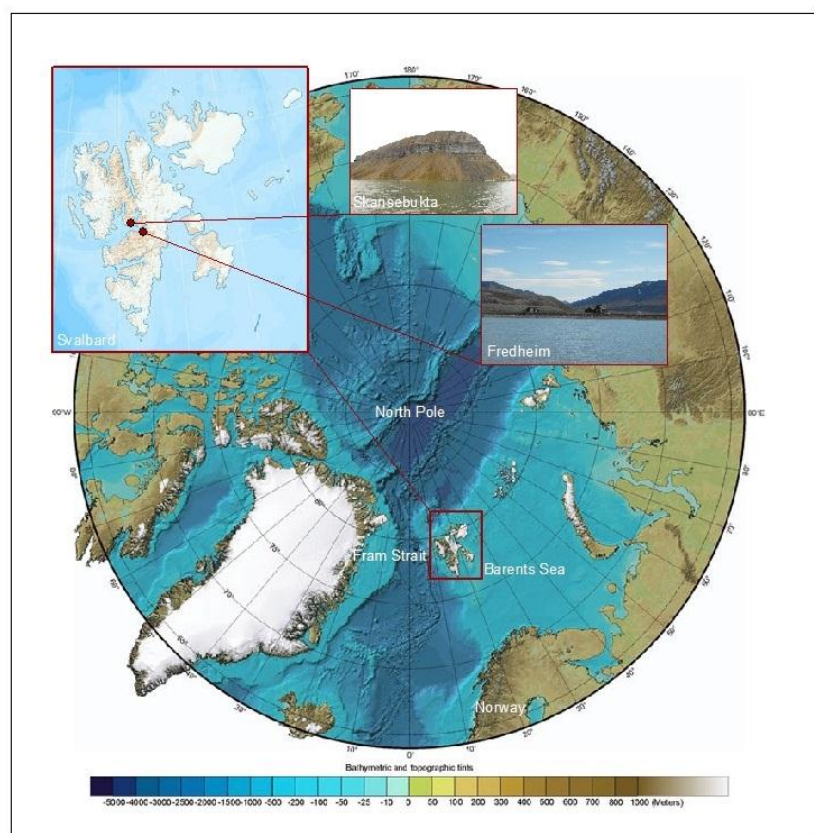


Figure 4: Field site locations relative to Svalbard and the circumpolar north. (Image adapted from <http://geology.com/world/arctic-physical-map.jpg>, Photos: Sessford 2011)

(Schilder, 1984). This discovery led to a flux of Europeans and Russians who for the sake of fame, glory and money braved the treacherous north and sailed to Svalbard. During the 17<sup>th</sup> century, whaling was the predominant rationale for heading to Svalbard and in the 18<sup>th</sup> century it was joined by hunting and scientific exploration (Arlov, 1994). The 19<sup>th</sup> and 20<sup>th</sup> centuries brought industrialization. Scientific enterprises had revealed that not only could Svalbard be exploited for its biological resources, but also for its geological wealth (Arlov, 1994). Coal mining led the terrestrial based economic activity that continues to this day to pilot the Svalbard economy alongside tourism. Over the centuries, some of those who



attempted a career or life in Svalbard were rather successful, while others less so but all left an imprint on the land resulting in what is now deemed "cultural heritage" by the Governor of Svalbard, in the Environmental Protection Act of 15 June 2001, chapter 5 section 39 (Government of Norway 2001). It states that all structures and sites containing traces of human activity dating from 1945 and earlier are protected by law. Therefore it is of great interest to examine those locations where such artifacts stand and determine if they are endangered by geological hazards. To do so it is necessary to conduct research on the present day landforms existing on Svalbard that have been formed by geohazards and attempt to correlate their cause with changes in climate that have occurred during the Holocene.

### 3.2.1 Fredheim

Unless otherwise stated, the historical events and knowledge concerning Fredheim that are presented in this section are from the historical pamphlet "Villa Fredheim" by (Johannessen, 1997). Fredheim (Peaceful Home) is located on the southern banks of Sassendalen in central Spitsbergen at the mouth of Sassendalen (Figure 5). It is a central location, easily



Figure 5: Overview of eastern Isfjorden indicating Fredheim and Skansbukta in relation to the fjords and valleys (Figure adapted from Norwegian Polar Institute Interaktive Kart, <http://toposvalbard.npolar.no>).

accessible from Longyearbyen by boat, ski and dog sledge. Fox, reindeer, seal, and polar bear frequent the area regularly. It is therefore of no great surprise that the "King of Sassen" made it his home base for hunting and trapping. Hilmar Nøis had an extended residency of an accumulated 38 years of overwintering in Svalbard as a hunter and trapper. He first came to Svalbard in 1909 when he was 18 years old. He died in 1975 at the age of 72. His uncle, Daniel Nøis, built Gammelhytta (Old Hut) in 1911/12 (Figure 6). It was built in a style similar

to that of the Norwegian hunting period prior to World War One, which used moss to fill cracks in the walls and roof and piled up squares of peat as insulation, birch bark was laid on the outside to keep out the wind and rain. Gammelhytta was relocated away from the escarpment in 2001 because coastal erosion. The main Villa, Nødhytta (Emergency Hut) and Outhouse were built in 1924 (Figure 6). Nødhytta is a recent term used for the hut as it was originally built as a storage shed for tools and equipment. These were built in the more modern style using wooden boards.

It is written in the pamphlet that the foundation of a burnt-down building lies approximately 50 m to the west of the main villa, but this has failed to be seen during fieldwork though may be the building seen in the foreground of Figure 7. It is not mentioned where precisely this hut was located, but unless this was it, the probability that the remains have now fallen into the sea due to coastal erosion, is quite high. The same fate became of a Russian hunting station which stood approximately 140 m to the west of the main villa. The remains of two fishing/hunting boats, destroyed by an ice flow in 1999, are also present at Fredheim (Figure 8).

Today, Fredheim is no longer used as a hunting and trapping station but rather a tourist destination for both locals and non-residents of Svalbard. Every winter thousands of scooters, hundreds of dog teams, and tens of skiers travel from Longyearbyen over the snow to visit the cultural heritage site of

Fredheim. The Villa is used by the Governor of Svalbard and often opened up in a lottery for locals to use during special holidays. Nødhytta is always open and can be used as an emergency hut for those in need. Gammelhytta is generally locked and not available for the public. However, every April the Governor's office has an open house where people may come and learn about the cultural memories stored at Fredheim.

### 3.2.2 Skansbukta

Unless otherwise stated, the historical events and knowledge concerning Skansbukta that are presented in this section are from the historical pamphlet "Isfjorden" by (Prestvold,



Figure 6: The cultural heritage buildings at Fredheim showing A: Gammelhytta, B: Villa, C: Nødhytta, and D: Outhouse. The black outline shows the old position of Gammelhytta prior to moving in 2001 (Sessford, May 2012).



Figure 7: Hilmar Nøis standing with the presumed burnt down building in the foreground and the remaining buildings in the background. (Photo taken in 1965, from archive belonging to John-Eldar Pedersen.)



Figure 8: The remains of the crushed boats where the black line indicates the extent of ice floe thrusting as indicating by sediment push (Sessford, August 2012). Inset image of Hilmar Nøis with the boats in 1965 (From archive of John-Eldar Pedersen).



2003). Below the large tabletop mountain known as Skansen, lies Skansbukta, one of the most sheltered bays in Svalbard (Figure 5). Surrounded by mountains on three sides, it is only open to South-easterly winds. The towering cliffs above the bay have been the instigating factor for human activity in the area. Layers of anhydrite visible at the lower reaches of the cliffs lured the Dalen Portland Cement Works to begin mining excavations for gypsum in 1918. The enterprise was short-lived, and after one year the project was

abandoned. A second attempt at mining was undergone in the 1930s but was again forsaken, leaving a wealth of cultural monuments for future generations.

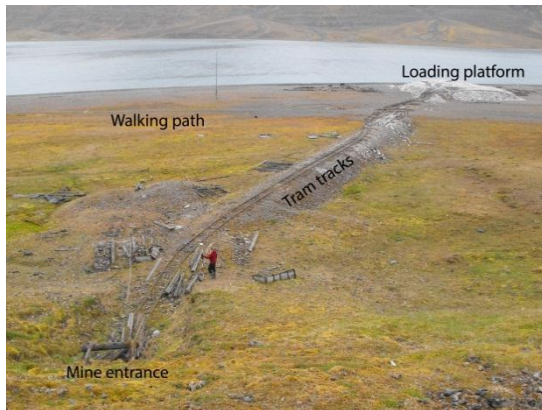


Figure 9: Cultural heritage structures at Skansbukta (Sessford, August 2011)



Figure 10: Looking southeast over Skansbukta with the cultural heritage boat on land in the centre of the image (Sessford, August 2011).

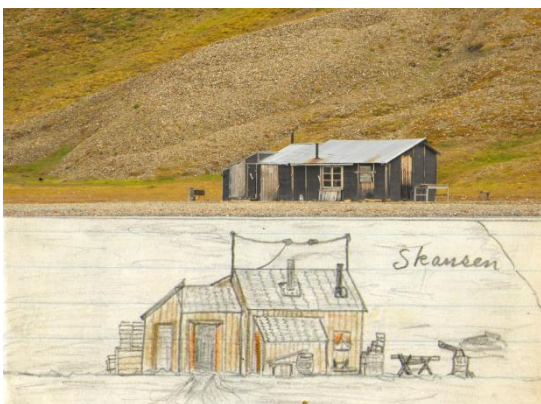


Figure 11: The hunting and fishing hut as depicted by Arne Nøis in 1961-64 and as seen in August, 2009 (Photo, Sessford, drawing from archive belonging to John-Eidar Pedersen).

Large structures associated with the mining installation are still in decent tact. A cargo installation or loading platform lies near the shore of the bay and is linked to the mine entrance by tram tracks (Figure 9). A small boat, likely used as a transport vessel for gypsum is battered but still in good condition and is on the Northern end of the beach (Figure 10). Towards the southern end of the beach are in situ building posts and foundations from various structures along with a path leading from one such ex-building to the tram tracks. One hut, now owned by the Hunting and Fishing Club of

Longyearbyen is still in very good condition, and is used regularly by Longyearbyen residents (Figure11). However, it is unknown from which period the hut was originally built. A drawing done by Arne Nøis (a nephew of Hilmar Nøis) in 1961-64, is shown in Figure 11 and differs from the hut as seen today. As suggested by the presence of Arne, Skansbukta was not only used for mining operations, but also as hunting and trapping station by the Nøis family. Therefore it holds ever more cultural memories of Svalbard heritage.

## Chapter 4 – Methodology

This master study has been built off a combination of field based methods and computer based analysis of aerial images. A total of 38 days were spent in the field over the course of the two year study period from August 2011 – March 2013. All field work was carried out with the help of field assistants and/or supervisors and colleagues. Efforts were often combined with field work for SINTEF and undergraduate teaching assistance during field excursions. Aerial images were provided by the Norwegian Polar Institute and analyzed using ArcGIS software and combined with differential GPS points using Leica GeoOffice software.

### 4.1 Differential GPS measurements

Differential GPS measurements were taken on a number of occasions at both field sites (Appendix: Raw DGPS). The same field parameters were used while points were collected, though the ground control points (GCP) were at different locations. GPS and GLONASS satellite systems were used with a cutoff angle of  $10^0$ . All data points were collected and registered in the WGS1984 datum using the UTM33X projection. Real time processing was unable to be used in the field due to a failure in radio communications between the base station and rover. However, post-processing was easily done using the Leica Geo Office software.

### 4.2 Manual erosion measurements

Manual measurements of the distance between the buildings and the top of the coastal escarpment at Fredheim were completed on each visit (Appendix: ErosionRates\_Fredheim). This results in a total of six measurements for each building covering the span of two years. Measurements were taken with a hand held cloth tape measure from the north east corner of each building to follow the same methods used previously in Tangen and Justad (2012), (Figure 12).

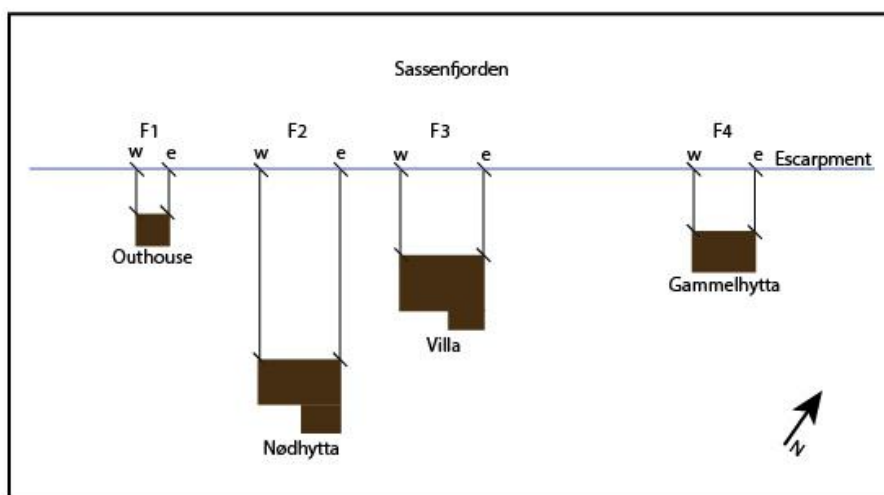


Figure 12 (left): Simplified sketch of buildings at Fredheim indicating manual measurement locations. Eastern points are used in analysis for the SINTEF report (i.e. F1e).

### 4.3 Active layer detachment slide measurements

Active layer detachment slides have been measured at the Fredheim site in an attempt to find the back wall height at the time of detachment. The idea being that the back wall height should give insight into the depth of the active layer at the time of detachment. They have been simplified so that each measurement mimics a right angle triangle in an attempt to reconstruct the back wall height at the time of release using the Pythagorean Theorem (Figure 13). Measurements were taken every two metres along the back wall. The length of the hypotenuse along the slope of the slide has been measured using a cloth tape measure, and the gradient of the back wall slope measured using a hand held compass at the top, middle, and base to find an average gradient. The base of the slope is considered to be at a  $10^\circ$  gradient. As most of the slides have post-detachment gelifluction on their surface, it is difficult to determine where the base of the detachment is located. All measurements are found in the appendix section of this thesis.



Figure 13: Simplified sketch of active layer detachment slide measurements. The curved black line represents the scarp along the backwall as delineated by the change in angle, and discolouration of beach terrace stones. Slope gradients are a) top, b) middle, c) bottom with the average gradient represented as g). Measurements took place approximately every 2 m along the scarp (Sessford, June 2012).

### 4.4 Automatic camera

An automatic SLR camera has been installed at Skansbukta and taken images every day at noon from the 23 August 2011 to the 11 April 2012 (with a gap where the battery died between 12 January 2012 and 4 April 2012). This was placed across the bay from Skansbukta in the attempt to monitor slope processes, snow accumulation, and sea ice changes. The same camera was then placed at Fredheim between the 5 July 2012 to the 2 February 2013 to observe sea ice changes and build-up of the ice foot and snow accumulation over the winter.

#### **4.5 Radiocarbon samples**

Radiocarbon samples were only collected at the Fredheim site. Detailed sedimentological logs were measured in the marine terraces MT4 and MT3. Sedimentological descriptions are used to describe the depositional environments (Nichols, 1999; Krüger and Kjær, 1999). Mollusk samples were collected in MT4 75 cm and 100 cm below surface (64.25 and 64 m a.s.l., respectively). On MT3 mollusk samples were collected at 50 cm and 2.57 m below surface (50.5 and 48.40 m a.s.l.).

Both mollusk fragments and paired shells were identified before chemical preparation following techniques of Feyling-Hanssen, (1965). The radiocarbon analyses were determined with the Uppsala EN-tandem accelerator (Possnert, 1990). Radiocarbon ages are reported as conventional dates with 1 standard deviation and as calibrated ages. In the text all radiocarbon ages are calibrated given as cal BP (before present: 1950 AD). The radiocarbon dates were calibrated to calendar ages using a reservoir age of  $440 \pm 52$  years). This is based on two different recommendations using a marine reservoir effect of  $450 \pm 52$  (Mangerud in Mangerud et al. 2006) and  $438 \pm 52$  years (Bondevik and Gulliksen in Mangerud et al. 2006) for mollusks and foraminifera in Spitsbergen. The calibration is based on the Fairbanks '0107' calibration curve with the online calibration software (<http://radiocarbon.ldeo.columbia.edu/research/radcarbcal.htm>) (Fairbanks et al., 2005) as this curve uses only coral U/Th dates. All terrestrial material was calibrated with Calib 6.0 and INTCAL09 (Reimer et al., 2009).

#### **4.6 Mapping (ArcGIS)**

Landforms and sediments have been mapped and identified through field observations in August 2011 and June 2012 and supported by analysis of a 2009 panchromatic orthorectified aerial image. Field work consisted of differential GPS measurements and observational study. Leica GeoOffice software was used to post process DGPS points and later combined with the aerial image in ArcGIS to visualize the Quaternary maps. The majority of landforms on the Skansbukta map have been identified and measured in the field using the DGPS and filled in with support from the aerial image. For Fredheim, only the following were measured with DGPS: coastal escarpment, active layer detachment slides, alluvial fan, delta extent, lagoon and buildings. The rest of the landforms have been identified in the field, but mapped using the 2009 aerial image.

#### **4.7 Aerial images and Digital Shoreline Analysis System**

The United States Geological Survey (USGS) design tool DSAS (Digital Shoreline Analysis System; Thieler et al., 2009), was implemented for the third manuscript (Chapter 12). Transects at 10 m intervals and perpendicular to the oldest coastlines were constructed at



every site. The coastal erosion rates were obtained by dividing the retreating distance by the number of years between each photo survey. Coastline positions for Fredheim, Vestpynten, Skansbukta and Svea were delineated on aerial photographs from 1969 to 2012. Aerial photographs from 1998, 2006, and 2009, were orthorectified and served as a base to georeference remaining datasets in ArcGIS. Coastlines were mapped on the aerial photographs for each year. Wherever possible, coastal bluffs or cliffs were used as markers for mapping the coastline as this provided better accuracy in terms of identification on the aerial photographs and is not subject to error due to tidal variations.

#### **4.8 Unused data collection**

In October 2011, ground penetrating radar data was collected at Fredheim using the Malå Professional Explorer console and the RAMAC RTC unshielded Rough Terrain Antenna of 50 MHz. Data were intended to be used to determine depths of active layer detachments and bedrock beneath pre-recent fluvial material. However, due to time constraints it was decided to focus on the coastal erosion at Fredheim, rather than the active layer detachments. The data is still available, and if used in collaboration with manual measurements of the active layer detachments, could provide valuable insight into past active layer depths and reconstruction of permafrost growth during the Holocene (Appendix: Raw GPR).

In May 2012, each of the fens (marked in brown as organic material in the Fredheim map described in Chapter 10) was drilled in the attempt to date onset of biological growth. As each of the fens is located on a different terrace, the hope was to provide time constraints for when marine terraces became terrestrial and vegetation growth was possible. This, alongside the radiocarbon ages would then have provided a clearer picture of uplift rate. However, all dates were returned as modern.

Two Geoprecision data loggers were placed in the active layer, one at Fredheim and the other Skansbukta, to gain understanding of when the active layer begins to thaw and freeze at both locations. Unfortunately data would not download while in the field due to faulty equipment. It may be that data will be able to be collected over the following summer; however, it is not included in this thesis work.

#### **4.9 Changes and additions to field investigations**

As the focus of this thesis changed a few times over the course of the two years, there were a number of field techniques that proved unneeded and others which may have been of significant use. If field work were to be done over again a number of changes would have been implemented. As dating of the fens turned out modern, terrace uplift rates are left less constrained. It would have been beneficial to measure the distance between beach ridge crests and their elevations to gain understanding of uplift rates in terms of sediment

deposition through longshore drift. Considering the cm accuracy of the DGPS, it would have worked well for these measurements. Likely measurements would have taken a couple of days.

There are also a couple of small lakes located further south in Sassendalen as seen in aerial images, and are located on the different marine terraces. These lakes, if drilled may be able to be used as analogues for uplift through both sedimentation rates and macrofossil/microfossil dating as has been conducted on the Kola Peninsula by Corner et al., (2001).

Less time would have been spent at Skansbukta in terms of the coastal erosion investigations. Skansbukta instead holds valuable insight into the development of slope processes. The debris flow accumulations there are unlike most others observed on Svalbard and need further investigation into their sedimentological structure. Time constraints on debris flows and understanding the extreme event intervals are something which has not been done to great extent on Svalbard, however, has been touched upon by André (1986, 1995).



## **Chapter 5 – Summary of results**

Short summaries of the results from each of the included manuscripts are given in this chapter.

### **5.1 Sessford, E.G. and Hormes, A. (2013) NP Report Series**

Two Quaternary geological maps have been completed in cultural heritage sites from Inner Isfjorden. Fredheim has been conducted in 1:3000 for a 0.8 km<sup>2</sup> area and a 0.5 km<sup>2</sup> area at Skansbukta has been mapped in 1:2000. The maps serve as a base to reconstruct Holocene landform development. Map descriptions review the landforms and their process of development and are divided up into the following sections:

For Fredheim:

- Glacial deposits and glacial history
- Marine deposits and Holocene emergence
- Fluvial deposits
- Slope deposits
- Periglacial features
- Bedrock
- Anthropogenic structures and recent events

For Skansbukta:

- Marine material
- Slope deposits
- Periglacial features and hydrology
- Bedrock
- Anthropogenic structures

Maps are used in the remaining manuscripts as supporting data.

### **5.2 Sessford, E.G. and Hormes, A. (unpublished)**

Spatial analysis, mapping, sedimentological descriptions and radiocarbon samples allowed for reconstruction of palaeo coastline processes during the development of the Holocene, and present day assessment of coastal erosion and aggradation. Results suggest that MT5 is pre-LGM and MT4 and MT3 underwent rapid uplift during the HTM between 11 235 and 9100 cal BP. There was a small transgression during the uplift of MT3 as indicated by sedimentological analysis. Emergence of MT2 and MT1 was significantly slower than the

upper terraces, and were completed during the cooling period before establishment of Neoglaciation between 7200 and 6800 cal BP, and 4200 and 3770 cal BP, respectively. The last uplift of the relict alluvial plain probably happened during the MWP (1200-950 cal BP). Present coastal erosion and progradation of the Nøis river delta are modern (1912-2012). The uplifted marine terraces are interpreted as having formed during predominantly calm periods where sediment accumulation was rapid. The steep scarps dividing each major uplift event are thought to represent short-lived periods of beach erosion which have more recently undergone periglacial processes (gelifluction and active layer detachment sliding). Hummocky and pitted beach sections on MT3 are interpreted to have been developed due to lack of accommodation space and the presence of boulders disrupting clear beach formation. However, on MT2 and MT1 these sections may have been more influenced by ice-push as they were deposited during cooler times and are predominantly in areas where accommodation space was not lacking. Due to the recent erosional period during modern times present accommodation space has been created. Now as Svalbard is entering a warm period, growth rate of the Nøis river delta has increased, replicating the same processes that have been exhibited throughout the Holocene. It shows both beach ridge accumulation as well as hummocky/pitted areas where sea ice has been thrust on land by wind.

### **5.3 Guegan, E.M., Sessford, E.G. and Schomacker, A. (submitted)**

#### **Geology**

Four study sites, Vestpynten, Fredheim, Skansbukta and Svea, in central Spitsbergen and within Isfjorden were accessed for present coastal erosion and aggradation rates. Basic results found that erosion at the Vestpynten site is highly variable with erosion rates ranging between 0.75 m/yr and 0 m/yr. At Fredheim the coastline has been continuously eroding since 1977 with an average rate of 0.33 m/yr. However, average erosion rates were higher between 1977 and 1995 (0.4 m/yr) and have decreased between 1995 and 2009 (0.23 m/yr). This change runs in parallel with the prograding delta system where growth began to increase in 1995. The total area of sediment loss from the coastal cliff is 3085 m<sup>2</sup> totaling a volume of approximately 6170 m<sup>3</sup> when multiplied by the average cliff height of 2 m. At Skansbukta the average erosion rate is minimal of only 0.04 m/yr which is mostly caused by significant aggradation of one section equalling 18.7 m in 19 years. At Svea, the annual erosion rate is 0.11 m/yr with a maximum eroded distance of 4.7 m over 42 years.

Erosion rates are considerably variable between sites but also within each site suggesting that local coastal morphology plays the largest role in erosional processes.

#### **5.4 Finseth, J., Sessford, E.G. and Hormes, A. (2012) SINTEF**

This SINTEF report reviews the geology and coastal erosion at Fredheim that are significant in relation to the risk of destruction of the cultural heritage buildings situated there. Manual distance measurements from the buildings to the coastal cliff which were collected between 1987 and 2012 are presented where the maximum change in distance is approximately 9 m of sediment loss. Results show that total erosional distance varies from building to building yet if rates continue as they have all the buildings risk being washed to sea within the next 160 years, however, the outhouse which is closest to the cliff may be affected within the next six years. Both the outhouse and Danielbu (Gammelhytta) have previously been moved back away from the coast to avoid such circumstances.

Geological results show that the outcropping bedrock cliff to the east (outside measurement area) and the bedrock which has recently become exposed on the shore face below the buildings is made up of poor quality rock as described subjectively through the Q-system analysis (Barton and Choubey 1977). Results from marine sediment analysis show a significantly high silt fraction, whereas terrestrial sediments are bimodal consisting mainly of sand and gravel sediments. This is particularly the case for relict channels where fines are washed out during spring melt.

All results point toward the need for cultural heritage protection through mitigation. This report suggests that the optimum way to do this is by coastal protection.

## Chapter 6 – Discussion

The discussion section reviews the four manuscripts and connections between them that have allowed for the assessment of palaeo land, sea and ice processes with those presently acting today. As there are a number of factors which may have influenced the erosion rates spatially and temporally, it is necessary to address the possibilities that future studies may focus on the contributing factors of specific processes. By addressing these issues now in a more theoretical sense, it is hoped that more thorough research may be conducted in the future. Such is the discussion laid out and intended to review the spatial and temporal development of landforms and sediments at Fredheim and their influence on coastal erosion and cultural heritage mitigation strategies.

### 6.1 Spatial and temporal variation affecting coastal development

By combining the manuscripts together observations show that the development of palaeo beaches as shown by the uplifted marine terraces was rapid, sedimentation was dominated by sand and pebbles and wave action through longshore drift was eminent. The beach ridges and pitted beaches show a distinct difference in accommodation space availability. In the north, toward the bedrock exposures and higher gradients there is no space for beach ridges to form, instead they spread out toward the south where space is available. Hummocks and pits are instead present closer to the bedrock. When observing the present day beach, hummocks and pits appear where the ice foot sits during the winter, suggesting that as the ice is present sediment is deposited around the ice chunks and when melt out occurs hummocks are left from the spaces between ice, and pits where the ice was sitting (Rodzik and Zagórski, 2009). However, as the terraces were developed during the HTM (Sessford and Hormes, unpublished) it seems unlikely that sea ice would be present due to higher sea surface and air temperatures (Miller et al., 2010). So the hummocks are likely a result of lack of accommodation space or possibly from ice berg ride up (Girjatowicz, 2001). It is also possible that the hummocks are created because of large boulders falling onto the shoreline through erosion of the bedrock. Sediments would then not build smoothly as ridges, but around the boulders in hummocks. Evidence of these boulders is clearly seen on MT3 where they have noticeably been affected by wave action and chemical weathering. Similar processes are present in the east on the current coastline.

However, aggradation at present is now in the form of a delta at Fredheim, and the beach is undergoing erosion rather than accumulation. On MT4 there are two distinctly different wave directions as the upper part has east-west ridges and the lower has the dominant north-south ridges. Between the two is a depression, which has undergone post depositional pro-nival

fluvial erosion. It seems possible that this depression originated as a lagoon, similar to the present day lagoon behind the delta. The delta also has a change in longshore drift and the direction of beach ridges is north-south, but coming from the west toward the east. Deltaic growth remained fairly constant spatially between 1977 and 1995, but rapidly increased between 1995 and 2009 especially along the coastline (Guegan et al., submitted). The increase in rate may be attributed to higher summer and MAAT causing glaciers and snow patches to undergo higher melt rates and thereby spring/summer runoff. Increased runoff produces a sediment flux due to higher volumetric rates of discharge entraining and transporting material within fluvial systems (Walker 1998). As seen in Finseth et al. (2012), the marine sediment in front of Fredheim is dominated by silts thereby supporting the theory of increased glacial flour transported by the rivers. It is slightly more difficult to evaluate the processes and landforms influencing the present erosion of the coast which has decreased in rate since the growth of the delta (Guegan et al., submitted).

It is quite likely that wave action was the main agent for eroding the coastline before delta growth began. However, automatic camera photos taken once per day between the 5 July 2012 and the 2 February 2013 (Appendix: Fredheim time-lapse) do not show waves reaching the cliff. But, as absence of evidence is not evidence of absence, it cannot be said for sure if waves do not reach the escarpment during high tide storms. They may in any case, be the main agent in producing accommodation space as waves assist in removal of sediment lost from the cliff. They appear to act as carriers of previously eroded soils. The main agent of coastal erosion appears to be from the thawing of permafrost and the freeze thaw action of the active layer. The highest erosion is evident where relict channels are present on the surface of the old alluvial plain, and where groundwater flow (active layer interflow) is concentrated (Finseth et al., 2012; Guegan et al., submitted). Fines are washed out of these areas causing sediments to become unstable due to reduced lateral support. Given that this theory comes solely through observation, it is not possible to calculate this at the present moment and needs further investigation.

Other important factors for further discussion are the presence of land and sea ice, especially the interaction between the ice foot and the coastal escarpment in combination with snow accumulation. Mechanisms pertaining to the dynamics associated with the tides may affect the erosion rate through variations in pressure on the coastal sediments. Studies suggest that sea ice dominates arctic waters leaving only a 3-4 month period of ice free conditions during the summer months (Lantuit et al. 2012). However, at Fredheim the ice free period since 1986 has been 5-6 months long lasting from July through November and sometimes into December (Norwegian Ice Service 2012). This is due to the warm Atlantic Waters that flow past the western edge of Svalbard and enter into the fjord systems causing significant

interannual variability in fjord water temperatures and sea ice content (Ådlandsvik and Loeng, 1991; Nilsen et al., 2008). There have even been years such as was the case in 2011/2012 and 2012/2013 where sea ice was not present at Fredheim at all. Through manual field measurements it has been shown the 2011/2012 year produced only 0.17m of erosion (Finseth et al. 2012), 0.16m less than the calculated average. As described by Hilaire-Gravel et al., (2010), sea ice can have protective, constructive or erosive effects on coastal development, though the predominant effect is to “severely decrease the potential for wave development and propagation and thereby limit wave action at the shoreline” (215). However, as discussed previously, waves do not appear to be a main erosive agent at Fredheim, and higher erosion rates seem to correspond with periods of sea ice cover. It is thought therefore that the presence of sea ice may contribute to the erosion of the coastal escarpment rather than protect it (Aré et al. 2008, Caline 2010). As sea ice data prior to 1986 is not available, it is difficult to assess how much sea ice was present during the periods of high erosion seen at Fredheim between 1977 and 1995. Sea ice and shorefast ice are generally thought to protect the shoreline by limiting wave-based erosion. However, during ablation tall fast ice can facilitate erosion by blocking outflow of proglacial water leading to outwashing of storm ridges (Rodzik and Zagorski 2009). Shorefast ice can also lead to abrasion, and plucking during break-up (Caline 2010). Of equal importance is the entrainment and export of sediments by sea ice. Evidence suggests that the changing sea ice regime may result in an increase in sediment entrainment as seen in Fredheim where the lack of sea ice allows subsurface shoreface sediments to be washed on top of the ice foot to later be transported away from the shoreline (Forbes et al., 2011). However sea ice interactions with the coastline are largely unexplored and need further investigation to assess the overall magnitude of their impact. It is of course probable that storminess was more inherent in the past and that the summer months with ice free periods were long enough to induce higher erosion rates than seen most recently.

The presence of the snow and ice foot also likely affect the temperature regime of the coastal permafrost as it will insulate the sediments and assist in proglacial fluvial erosion (Ballantyne, 1978; Christiansen 1998). The main wind direction is from the south east through Sassendalen and during winter months snow accumulates on top of the ice foot along the coastal cliff. The timing and duration of snow cover critically affect the surface conditions associated with the ground surface energy balance and thereby affect the intensity of freeze thaw action within the active layer (Ling and Zhang 2003). Delaying snow cover onset in the autumn results in a decrease in ground temperature and advancing the snow cover disappearance in spring leads to increased ground temperatures (Ling and Zhang 2003).

This in turn causes increased freeze thaw action thereby loosening cliff sediments to be easily washed away through nival waters.

#### **6.4 Implications for future coastal development**

Future development of Arctic coastlines is reliant on temporal changes. It is understood that climate change and sea-level rise from increase in freshwater contribution to the oceans, thermal expansion of the water, subsidence and land loss will affect sediment entrainment, transport and deposition in complex ways (Nicholls et al., 2007). As beach aggradation is dependent on sediment availability and accommodation space, acceleration in the rate of sea level rise may mean that the coastal morphology cannot keep up and coastline retreat will be imminent (Nicholls et al., 2007; Forbes et al., 2011). Higher sea level will increase erosion of coasts, leading to rapid retreat underlined by thawing permafrost, melting of ground ice, subsidence due to loss of ice, and warmer ground temperatures (Nicholls et al., 2007; Lantuit et al., 2012). However, at Fredheim and the other sites noted in Guegan et al., (submitted) ground ice is not a major contributor to sediment loss as the percentage of ground ice in Svalbard's unconsolidated coasts is negligible. Thawing permafrost is a major factor, as is increased snow accumulation at the coast. Increases in snow cover will warm the ground, insulating it over the winter and thereby increasing active layer depths. It is also apparent at Fredheim that sediment from inland is actually becoming more abundant and a delta is able to grow where before erosion was dominant. This may be a saving factor for the Fredheim coastline, if sediment availability produces natural barriers limiting coastal erosion due to sea ice and wave action (Ruz et al., 1992; Nichol, 2002). However, it is difficult to assess the full extent of the influence that sea ice has on coastlines.

One of the major changes in the Arctic will be decrease and even loss of sea ice. But, as Ogorodov et al., (2010) has pointed out, "warming events have not always led to an increase in wave energy or to acceleration of coastal erosion". This is apparent at Fredheim. As discussed, the open water season is quite long (5-6 months) and some years there is no sea ice at all. Yet, since 1995 coastal erosion rates have decreased. Evidently, decrease in sea ice and increased air temperatures do not suggest increased wind-wave activity. The acceleration of coastal erosion likely needs a combination of thermo-erosion, and wave-energy factors (Ogorodov et al., 2010). It is likely that increasing open water durations will increase the frequency of storm events in the arctic (Forbes et al., 2011). Yet, at Fredheim, the dominant wind direction does not favour large waves breaking on or directly in front of it. However, it is possible that dominant wind directions and fjord circulation patterns are altered due to changes in atmospheric circulation and warming sea temperatures. It is in any case clear that major changes in arctic coastlines are dependent upon climatic forcing and temporal changes.

## **6.5 Effects of coastal processes on cultural heritage mitigation**

In the past decades coastal erosion at Fredheim has been significant enough that the Governor of Svalbard has considered it necessary to move some of the buildings, Gammelhytta and the Outhouse, away from the coastline (Finseth et al., 2012). However it appears that erosion rates are decreasing and it may not be necessary to move the buildings any more, but rather that coastal protection may be a better option. In 1999 an ice floe rode up onto the beach, displacing sediments even onto MT1. Fortunately this did not happen at the location of any houses, but it did happen to crush two small fishing boats also cultural heritage. Therefore, even if coastal erosion slows down, it may be necessary to protect the coastline and buildings from ice ride/pile up as it represents a coastal hazard to infrastructure (Instanes et al., 2005). The areas which appear to undergo the most erosion at present are where relict fluvial channels are present and where large snow drifts accumulate in the winter. It may be of interest therefore to look into structures which can be built to avoid wash out of fines in the channels, and decreasing snow accumulation in the winter.

Moving the buildings may be of interest, however it is costly and by moving the buildings to a higher location it may be that the cultural heritage loses some of its character as it was strategically placed near the coastline for the purpose of ease of access to the sea, and hunting possibilities. Also, moving buildings closer to the slopes poses a different threat on the buildings as they will sit within a fen with high water content. It will be more likely for snow to build up around the buildings and drainage will be slow leaving the buildings sitting in water for much of the summer. There is still chance of active layer detachments on the slope, and active gelifluction will continue to creep downwards. It is therefore necessary to take all the different threats into consideration when reviewing mitigation strategies.

Therefore, to assess the total risk of geothreats on cultural heritage, the following (based off Petley, 1998) must be acknowledged:

- Probability that a specific event may happen at a known (regular/reoccurring) time of year or under specific circumstances (i.e. rate of coastal erosion)
- What the geomorphological hazard is including a description of the hazard and its geomorphic setting, magnitude, and probability of occurrence (i.e. causes of coastal erosion, spatial and temporal analysis)
- Vulnerability/evaluation of the cultural heritage at risk, i.e. type, structure, past use, current use, cultural value

The total risk of the cultural heritage therefore relates to the probability, frequency and magnitude of coastal erosion taking into consideration the expected loss of cultural value.



## Chapter 7 – Conclusions

This thesis has explored Holocene coastal development and used it alongside present day erosion and aggradational rates, and geomorphological processes as an analogue for possible future predictions concerning coastal evolution. The implementation of geomorphological maps has proved to be of significant value in understanding these processes (Sessford and Hormes, 2013). Furthermore, one can utilize data for mitigation strategies concerning cultural heritage threatened by coastal erosion.

Four study sites in Central Spitsbergen, Svalbard have been used to assess modern processes and erosion rates on unconsolidated sediment coasts (Guegan et al., submitted). The overall trend finds that erosion is active while the mechanisms behind erosion are complex and vary spatially even on extremely small regional scales in the order of 100s of metres. The average erosion rates for the four study sites range between 0 and 2 m/yr, with most segments eroding at rates between 0.3 and 0.4 m/yr. Spatial variation in coastal geomorphology, i.e. cliff morphology, cryology, and lithology, between these sites is one of the major factors influencing variations in erosion rate. However temporal variations i.e. storminess, sea ice, wind regime and temperatures largely impact future changes.

Present day coastal processes are used as a key to past shoreline development and when the past processes are seen from the context of the present, it is possible to outline possible future changes. Therefore, insight into the Holocene development of beaches through uplifted marine terraces has contributed to better understanding of these small scale variations. One of the field sites, Fredheim has been more thoroughly examined to delve into this topic.

Five uplifted marine terraces were assessed (Sessford and Hormes, unpublished) and through spatial and chronological analysis suggest that the highest terrace, MT5 is pre-LGM, and MT4 and MT3, underwent rapid uplift during the HTM between 11 235 and 9100 cal BP. Coastal development during this time was dominated by aggradation as fair weather beach berms indicating low storm activity. Uplift of MT2 and MT1 were completed during the cooling period before establishment of Neoglaciation between 7200 and 6800 cal BP, and 4200 and 3770 cal BP, respectively. During this cooler period, sea ice was more frequent and left imprints on the terraces through thrust deformations and hummocky beaches. A final 2 m uplift of the relict alluvial plain probably happened during the MWP (1200-950 cal BP). Coastal erosion and progradation of the Nøis river delta are modern (1912-2012). The following general conclusions concerning Svalbard coasts have been drawn:

- Svalbard has a number of coastlines made up of unconsolidated sediments which are currently undergoing erosion. The magnitude of erosion varies spatially and temporally, even on very small regional scales
- Thermal erosion is not a major threat to Svalbard coasts as there is a lack in ground ice. However increase in snow accumulation at the coasts assists in pro-nival fluvial erosion and thawing of permafrost.
- Future development of Arctic coastlines are mainly reliant on temporal changes
- Beach aggradation and erosion are dependent upon sediment availability, accommodation space, wind direction, frequency of storm events, and interactions between snow, ice foot, sea ice and permafrost.
- The effect of sea ice on coastal erosion is still a topic widely unexplored. The magnitude in which sea ice protects, constructs and erodes coastlines needs further analysis
- The need for more Quaternary mapping along Svalbard coasts is imminent

Having conducted spatial and temporal analysis of Holocene coastal development and combining it with modern erosion rates, research broadened to applied science in the field of coastal engineering to illustrate the benefits of collaboration between research disciplines. In so doing, various mitigation techniques for the cultural heritage at Fredheim have been reviewed resulting in suggestions to protect the coast rather than move the buildings or let nature run its course. It is recommended that mitigation strategies concerning cultural heritage need to combine knowledge of past processes in varying climatic settings to understand the probability of future events occurring. The total risk of the cultural heritage relates to the probability, frequency and magnitude of coastal erosion, taking into consideration the expected loss of cultural value.

## Chapter 8 – Future work

Much of the discussion pertaining to coastal processes is theoretical and does not have statistical data for backing. This study has been more of a reconnaissance of coastal processes in Svalbard in order to understand in which direction focus should be taken for future research.

Better age constraint of marine terraces and thereby shoreline development may be achieved through lake cores obtained from the small lakes located just south of Fredheim. It would be of interest to use cores as analogues for uplift both through sedimentation rates and macrofossil/microfossil dating. Cores would give a better understanding of uplift rates as well as insight into temperatures associated with the time. More detailed measurements of beach ridges would also benefit uplift rate reconstruction. By combining measurements with core data, it may be possible to link other uplifted marine terraces in Svalbard and thereby map uplift rates over the islands.

The influence and role of sea ice in coastal development has been greatly under examined. How does it influence coastal dynamics? There is a need to assess the role of fast ice throughout the year. This incorporates recording temperature changes in the shoreface before and after the departure of fast ice/ice foot. Studies should include the system as a whole, determining the impact on coastal erosion, resilience of nearshore permafrost, and distribution of the ice. This would require temperature and pressure logger installation in combination with remote sensing. Some work has begun on such issues in the Canadian Arctic (Stevens et al., 2010), but Svalbard is lacking in this field.

Investigations into permafrost growth and active layer development are lacking. It was thought that active layer detachment slides may be of interest to review changes in active layer thickness. If one could date the time of detachment, say through burial dating using cosmogenic nuclide techniques the active layer thickness could be determined and thereby give a proxy for permafrost development in Svalbard at low lying, coastal regions. It has been suggested that permafrost on Svalbard disappeared at low lying elevations during the LGM and that the onset of permafrost growth is to have begun between 2900-2650 cal. years BP (Jeppesen, 2001; Humlum et al., 2003). If such is the case, then active layer detachments could not have been released during the HTM. Instead, they should indicate more recent ages, and be associated with extreme events occurring during Neoglaciation or later. More data and assessment of such slides would be of interest to further permafrost studies in Svalbard.

As most cultural heritage on Svalbard is located near the coastline, all studies pertaining to changes in relative sea level, uplift rates, permafrost and coastal development are of interest to mitigation strategies for the protection of Svalbard's cultural memories. It is hoped that the results of this study may be used in the future as a stepping stone for the production of geological hazard risk assessment maps which may be used in the future to define tolerance limits for cultural heritage sites and thereby acted upon to preserve them in the most optimal manner. Cultural heritage must also therefore be rated using a defined system structured upon the technical condition of the artifacts, their past use and importance to society. Mitigation strategies propose a few possibilities; to move structures, to conduct archaeological investigations, to reinforce unstable regions or to document sites and let nature take its course. Decisions on which strategy to use will rely on more thorough scientific investigations relating to geo threats.

## Chapter 9 – References

- André, M. S., 1986, Dating Slope Deposits and Estimating Rates of Rock Wall Retreat in Northwest Spitsbergen by Lichenometry. *Geografiska Annaler. Series A, Physical Geography* 68, 1/2, 65-75.
- André, M. S., 1995, Holocene Climate Fluctuations and Geomorphic Impact of Extreme Events in Svalbard. *Geografiska Annaler. Series A, Physical Geography* 77, 4, 241-250.
- Anisimov, O. A., 2007, Potential feedback of thawing permafrost to the global climate system through methane emission. *Environmental Research Letters* 2, 045016
- Arlov, T. B., 1994, A Short History of Svalbard. Oslo, Norsk Polarinstitutt 95.
- Aré F. E., 1988, Thermal abrasion of sea coasts. *Polar Geography and Geology* 12, 1
- Aré, F., Reimnitz, E., Grigoriev, M., Hubberten, H. W., and Rachold, V., 2008, The Influence of Cryogenic Processes on the Erosional Arctic Shoreface. *Journal of Coastal Research* 24, 1, 110-121.
- Ådlandsvik, B. and Loeng, H., 1991, A study of the climatic system in the Barents Sea, *Polar Research* 10, 45-59.
- Ballantyne CK, 1978, The Hydrologic Significance of Nivation Features in Permafrost Areas. *Geografiska Annaler. Series A, Physical Geography* 60, 1/2, 51-54.
- Barton, N. and Choubey, V., 1977, The shear strength of rock joints in theory and practice. Rock Mechanics Meeting, Befo. Stockholm, Swedish Rock Mechanics Research Foundation: 95-117.
- Bednorz, E., 2011, Occurrence of winter air temperature extremes in Central Spitsbergen. *Theoretical and Applied Climatology* 106, 3, 547-556.
- Berner, K.S., Koç, N., Godtliebsen, F., and Divine, D., 2011, Holocene climate variability of the Norwegian Atlantic Current during high and low solar insolation forcing. *Paleoceanography* 26, 2, PA2220.
- Boulton, G. S., 1979, Glacial history of the Spitsbergen archipelago and the problem of a Barents Shelf ice sheet. *Boreas* 8, 31-57.
- Caline, F., 2010, Coastal-sea-ice action on a breakwater in a microtidal inlet in Svalbard [Doctor of Philosophy: Norwegian University of Science and Technology], 263 p.
- Corner, G.D., Kolka, V.V., Yevzerov, V.Y. and Møller, J.J., 2001, Postglacial relative sea level change and stratigraphy of raised coastal basins on Kola Peninsula, northwest Russia. *Global and Planetary Change* 31, 155-177.
- Christiansen, H. H., 1998, 'Little Ice Age' nivation activity in northeast Greenland. *The Holocene* 8, 6, 719-728.
- Dallmann, W. K., 1999, Lithostratigraphic lexicon of Svalbard: Review and recommendations for nomenclature use. Upper Palaeozoic to Quaternary bedrock, Tromsø, Norsk Polarinstitutt 318 p.

- D'Andrea, W., Vaillencourt, D.A., Balascio, N.L., Werner, A., Roof, S.R., Retelle, M., Bradley, R.S., 2012, Mid Little Ice Age and unprecedented recent warmth in an 1800 year lake sediment record from Svalbard. *Geology* DOI: 10.1130/G33365.1
- Divine, D., Isaksson, E., Martma, T., Meijer, H.A.J., Moore, J., Pohjola, V., van de Wal, R.S.W., Godtliebsen, F., 2011, Thousand years of winter surface air temperature variations in Svalbard and northern Norway reconstructed from ice-core data. *Polar Research* 30, 7379.
- Elberling, B., Christiansen, H. H., and Hansen, B. U., 2010, High nitrous oxide production from thawing permafrost. *Nature Geoscience Letters* 3, 332-335.
- Fairbanks, R.G., Mortlock, R.A., Chiu, T.-C., Cao, L., Kaplan, A., Guilderson, T.P., Fairbanks, T.W., Bloom, A.L., 2005, Marine Radiocarbon Calibration Curve Spanning 0 to 50,000 Years B.P. Based on Paired <sup>230</sup>Th/<sup>234</sup>U/<sup>238</sup>U and <sup>14</sup>C Dates on Pristine Corals. *Quaternary Science Reviews* 24.
- Feyling-Hanssen, R. W., 1965, Shoreline displacement in central Vestspitsbergen and a marine section from the Holocene of Talavere on Barentsøya in Spitsbergen. *Norsk Polarinstitut Skrifter* 93, 1-5.
- Feyling-Hanssen, R. W., and Olsson, I., 1960, Five radiocarbon datings of post glacial shorelines in central Spitsbergen. *Norsk Geografisk Tidsskrift* 86, 121-131.
- Finseth, J., Sessford, E.G., Hormes, A. 2012: Erosjonssikring av Fredheim; visualiseringsprosjekt; Evaluering av erosjonssikring av Fredheim. Svalbards Miljøvernfond, SINTEF Byggeforsk, Infrastruktur, SBF2012A0334, 43.
- Flyen, A. C., 2009, Coastal erosion: a threat to the cultural heritage of Svalbard?. Norwegian Institute for Cultural Heritage Research.
- Forbes, D.L. (editor). 2011, State of the Arctic Coast 2010 – Scientific Review and Outlook. International Arctic Science Committee, Land-Ocean Interactions in the Coastal Zone, Arctic Monitoring and Assessment Programme, International Permafrost Association. Helmholtz-Zentrum, Geesthacht, Germany, 178 p. <http://arcticcoasts.org>
- Forman, S. L., and Miller, G. H., 1984, Time-Dependent Soil Morphologies and Pedogenic Processes on Raised Beaches, Brøggerhalvøya, Spitsbergen, Svalbard Archipelago. *Arctic and Alpine Research* 16, 4, 381-394.
- Forman, S.L., Mann, D. & Miller, G.H., 1987, Late Weichselian and Holocene relative sea level history of Brøggerhalvøya, Spitsbergen, Svalbard Archipelago. *Quaternary Research* 27, 41–50.
- Girjatowicz, J. P., 2001, Studies on the formation and disintegration of grounded ice hummocks in sheltered areas of the southern Baltic coast. *Oceanological Studies* 30, 3-4, 3-16.
- Government of Norway., 2001, Svalbardmiljøloven. M. Miljøverndepartementet. Oslo, Government Administration Services, 7.
- Guegan, E.B.M., Sessford, E.G. & Schomacker, A. (submitted), Time-lapse aerial photography reveals significant coastal erosion on Svalbard, Norwegian high Arctic. *Geology*.

- Hald, M., Ebbesen, H., Forwick, M., Godtlielsen, F., Khomenko, L., Korsun, S., Ringstad Olsen, L., and Vorren, T. O., 2004, Holocene paleoceanography and glacial history of the West Spitsbergen area, Euro-Arctic margin. *Quaternary Science Reviews* 23, 20-22, 2075-2088.
- Hilaire-Gravel, D., Bell, T.J., and Forbes, D.L., 2010, Raised gravel beaches as proxy indicators of past sea-ice and wave conditions, Lowther Island, Canadian archipelago. *Arctic* 63, 2, 213-226.
- Hogan, K. A., Dowdeswell, J. A., Noormets, R., Evans, J., and Cofaigh, Ó. C., 2010, Evidence for full-glacial flow and retreat of the Late Weichselian Ice Sheet from the waters around Kong Karls Land, eastern Svalbard. *Quaternary Science Reviews* 29, 3563-3582.
- Hormes, A., Akçar, N., and Kubik, P. W., 2011, Cosmogenic radionuclide dating indicates ice-sheet configuration during MIS 2 on Nordaustlandet, Svalbard. *Boreas* 40, 636-649.
- Humlum, O., Instanes, A., and Sollid, J. L., 2003, Permafrost in Svalbard: a review of research history, climatic background and engineering challenges. *Polar Research* 22, 2, 191-215.
- Humlum, O., Elberling, B., Hormes, A., Fjordheim, K., Hansen, O., Heinemeier, J., 2005, Late-Holocene glacier growth on Svalbard, documented by subglacial relict vegetation and living soil microbes. *The Holocene* 15, 3, 419-430.
- Humlum, O., Solheim, J.E., and Stordahl, K., 2011, Identifying natural contributions to late Holocene climate change. *Global and Planetary Change* 79, 1-2, 145-156.
- Ingólfsson, Ó., 2011, Fingerprints of Quaternary glaciations on Svalbard: Geological Society. *Special Publications* 354, 15-31.
- Ingólfsson, Ó., and Landvik, J. Y., 2013, The Svalbard-Barents Sea ice-sheet - historical, current and future perspectives. *Quaternary Science Reviews* 64, 33-60.
- Instanes, A., Anisimov, O. A., Brigham, L., Goering, D., Khrustalev, L. N., Ladanyi, B., Larsen, J. O., Smith, O., Steverner, A., Weatherfield, B., and Weller, G., 2005, Infrastructure: Buildings, support systems, and industrial facilities, *in* Symon, C., Arris, L., and Heal, B., eds., *Arctic Climate Impact Assessment - Scientific Report*: New York, Cambridge University Press, 907-944.
- Jeppesen, J. W. (2001). Ice wedges and host sediments as palaeoclimatic indicators in central Spitsbergen, Svalbard. MSc thesis, The University Centre on Svalbard.
- Jessen, S. P., Rasmussen, T. L., Nielsen, T., and Solheim, A., 2010, A new Late Weichselian and Holocene marine chronology for the western Svalbard slope 30,000 0. cal BP. *Quaternary Science Reviews* 29, 1301-1312.
- Johannessen, L. J., 1997, Villa Fredheim: Longyearbyen, Governor of Svalbard, Environmental Section, in cooperation with the Svalbard Tourist Board and Svalbard Museum, 1-15.
- Kohler, J., Nordli, Ø., Brandt, O., Isaksson, E., Pohjola, V., Martma, T., and Faste Aas, H., 2011, Svalbard temperature and precipitation, late 19th century to present. Final report on ACIA-funded project.

- Krüger, J., Kjær, K.H., 1999, A data chart for field description and genetic interpretation of glacial diamicts and associated sediments - with examples from Greenland, Iceland and Denmark. *Boreas* 28, 386-402.
- Landvik, J. Y., Bolstad, M., Lycke, A. K., Mangerud, J., and Sejrup, H. P., 1992, Weichselian stratigraphy and paleoenvironments at Bellsund, western Svalbard. *Boreas* 21, 335-358.
- Landvik, J. Y., Mangerud, J., and Salvigsen, O., 1987, The Late Weichselian and Holocene shoreline displacement on the west-central coast of Svalbard. *Polar Research* 5, 29-44.
- Lantuit, H., and Pollard, W. H., 2005, Temporal stereophotogrammetric analysis of retrogressive thaw slumps on Herschel Island, Yukon Territory. *Natural Hazards and Earth System Sciences* 5, 413-423.
- Lantuit, H., 2008, The modification of arctic permafrost coastlines [Doctoral thesis: University of Potsdam], 120 p.
- Lantuit, H., and Pollard, W.H., 2008, Fifty years of coastal erosion and retrogressive thaw slump activity on Herschel Island, southern Beaufort Sea, Yukon Territory, Canada. *Geomorphology* 95(1/2), 84–102.
- Lantuit, H., Atkinson, D. E., Overduin, P. P., Grigoriev, M., Rachold, V., Grosse, G., and Hubberton, H., 2011, Coastal erosion dynamics on the permafrost-dominated Bykovsky Peninsula, north Siberia, 1951-2006. *Polar Research* 30, 7341, 1-21.
- Lantuit, H., Overduin, P. P., Couture, N., Wetterich, S., Are, F., Atkinson, D., Brown, J., Cherkashov, G., Drozdov, D., Forbes, D., Graves-Gaylord, A., Grigoriev, M., Hubberton, H. W., Jordan, J., Jorgenson, T., Ødegård, R. S., Ogorodov, S., Pollard, W., Rachold, V., Sedenko, S., Solomon, S., Steenhuisen, F., Streletskaia, I. and Vasiliev, A., 2012, The Arctic Coastal Dynamics database. A new classification scheme and statistics on arctic permafrost coastlines. *Estuaries and Coasts* 35 (2), 383-400, doi: 10.1007/s12237-010-9362-6
- Lauritzen, Ø., Salvigsen, O., Winsnes, T. S., and Andresen, A., 1989, Geological Map Svalbard 1:100 000, C8G Billefjorden. Oslo, Norsk Polarinstitut.
- Ling, F., and Zhang, T., 2003, Impact of the timing and duration of seasonal snow cover on the active layer and permafrost in the Alaskan Arctic. *Permafrost and Periglacial Processes* 14, 2, 141-150.
- Long, A. J., Strzelecki, M. C., Lloyd, J. M., and Bryant, C. L., 2012, Dating high Arctic Holocene relative sea level changes using juvenile articulated marine shells in raised beaches. *Quaternary Science Reviews* 48, 61-66.
- Luoto, T.P., Nevalainen, L., Kubischta, F., Kultti, S., Knudsen, K.L., Salonen, V.-P., 2011, Late Quaternary ecological turnover in High Arctic Lake Einstaken, Nordaustlandet, Svalbard (80° N). *Geografiska Annaler: Series A, Physical Geography* 93, 337-354.
- Mangerud, J., Bolstad, M., Elgersma, A., Helliksen, D., Landvik, J.Y., Lønne, I., Lycke, A.K., Salvigsen, O., Sandahl, T., Svendsen, J.I., 1992, The Last Glacial Maximum on Spitsbergen, Svalbard. *Quaternary Research* 38, 1-31.
- Mangerud, J., Bondevik, S., Gulliksen, S., Hufthammer, K.A., Hoisaeter, T., 2006, Marine 14C reservoir ages for 19th century whales and molluscs from the North Atlantic. *Quaternary Science Reviews* 25, 3228-3245.



- Mason, O.K., 2010, Beach Ridge Geomorphology at Cape Grinnell, northern Greenland: A Less Icy Arctic in the Mid-Holocene. *Geografisk Tidsskrift-Danish Journal of Geography* 110, 2: 337-355.
- Miller, G. H., Brigham-Grette, J., Alley, R. B., Anderson, L., Bauch, H. A., Douglas, M. S. V., Edwards, M. E., Elias, S. A., Finney, B. P., Fitzpatrick, J. J., Funder, S. V., Herbert, T. D., Hinzman, L. D., Kaufman, D. S., MacDonald, G. M., Polyak, L., Robock, A., Serreze, M. C., Smol, J. P., Spielhagen, R., White, J. W. C., Wolfe, A. P., and Wolff, E. W., 2010, Temperature and precipitation history of the Arctic. *Quaternary Science Reviews* 29, 15-16, 1679-1715.
- Møller, J.J., Yevzerov, V.Y., Kolka, V.V., and Corner, G.D., 2002, Holocene raised-beach ridges and sea-ice-pushed boulders on the Kola Peninsula, northeast Russia: indicators of climatic change. *The Holocene* 12, 2, 169-176
- Müller, J., Werner, K., Stein, R., Fahl, K., Moros, M., Jansen, E., 2012, Holocene cooling culminates in sea ice oscillations in Fram Strait. *Quaternary Science Reviews* 47, 1-14.
- Nichol, S. L., 2002, Morphology, Stratigraphy and Origin of Last Interglacial Beach Ridges at Bream Bay, New Zealand. *Journal of Coastal Research* 18, 1, 149-159.
- Nicholls, R.J., P.P. Wong, V.R. Burkett, J.O. Codignotto, J.E. Hay, R.F. McLean, S. Ragoonaden and C.D. Woodroffe, 2007, Coastal systems and low-lying areas. *Climate Change 2007: Impacts, Adaptation and Vulnerability. Contribution of Working Group II to the Fourth Assessment Report of the Intergovernmental Panel on Climate Change*, M.L. Parry, O.F. Canziani, J.P. Palutikof, P.J. van der Linden and C.E. Hanson, Eds., Cambridge University Press, Cambridge, UK, 315-356.
- Nichols, G., 1999, *Sedimentology and Stratigraphy*. Blackwell Publishing, Oxford.
- Nilsen, F., Cottier, F., Skogseth, R., and Mattsson, S., 2008, Fjord-shelf exchanges controlled by ice and brine production: The interannual variation of Atlantic Water in Isfjorden, Svalbard. *Continental Shelf Research* 28, 1838-1853.
- Norwegian Ice Service, 2012, Monthly average ice concentrations, Svalbard 1986 – 2012. Accessed 14.02.2012.
- Norwegian Meteorological Institute and Norwegian Broadcasting Corporation, 2013, Støwer, T.E., Eriksen, T.G., Eliassen, A. [www.yr.no](http://www.yr.no),
- Ogorodov, S. A., Belova, N. G., Kamalov, A. M., Noskov, A. I., Volobueva, N. N., Grigoriev, M. N., Wetterich, S., and Overduin, P. P., 2010, Storm surges as a forcing factor of coastal erosion in the western and eastern Russian Arctic. *Storm Surge Congress: Hamburg*.
- Petley, D. N., 1998, Geomorphological Mapping for Hazard Assessment in a Neotectonic Terrain. *The Geographical Journal* 164, 2, 183-201.
- Possnert, G., 1990, Radiocarbon dating by the accelerator technique. *Norwegian Archaeological Review* 23, 662-675.
- Prestvold, K., 2003, Isfjorden: A journey through the nature and cultural history of Svalbard: Longyearbyen, Governor of Svalbard. Environmental Section in cooperation with Svalbard Reiseliv AS, 26-29.
- Rachold, V., Are, F. E., Atkinson, D. E., Cherkashov, G., and Solomon, S. M., 2005, Arctic Coastal Dynamics (ACD): an introduction. *Geo-Marine Letters* 25, 2, 63-68.

- Reimer, P.J., Baillie, M.G.L., Bard, E., Bayliss, A., Beck, J.W., Blackwell, P.G., Bronk Ramsey, C., Buck, C.E., Burr, G.S., Edwards, R.L., Friedrich, M., Grootes, P.M., Guilderson, T.P., Hajdas, I., Heaton, T.J., Hogg, A.G., Hughen, K.A., Kaiser, K.F., Southon, J.R., Talamo, S., Turney, C.S.M., van der Plicht, J., Weyhenmeyer, C.E., 2009. INTCAL09 and Marine09 Radiocarbon age calibration curves, 0-50,000 years cal BP. *Radiocarbon* 51, 1111-1150.
- Rodzick, J., Zagórski, P., 2009, Shore ice and its influence on development of the shores of southwestern Spitsbergen. *International Journal of Oceanography and Hydrobiology* 38, 1, 163-180.
- Romanovsky, V. E., Smith, S. L., and Christiansen, H. H., 2010, Permafrost Thermal State in the Polar Northern Hemisphere during the International Polar Year 2007-2009: a Synthesis. *Permafrost and Periglacial Processes* 21, 2, 106-116.
- Ruz, M. H., Héquette, A., and Hill, P. R., 1992, A model of coastal evolution in a transgressed thermokarst topography, Canadian Beaufort Sea. *Marine Geology* 106, 251-278.
- Salvigsen, O. 1984, Occurrence of pumice on raised beaches and Holocene shoreline displacement in the inner Isfjorden area, Svalbard. *Polar Research* 2(1), 107-113.
- Salvigsen, O., Elgersma, A., Hjort, C., Lagerlund, E., Liestøl, O., and Svensson, N., 1990, Glacial history and shoreline displacement on Erdmannflya and Bohemanflya, Spitsbergen, Svalbard. *Polar Research* 8, 262-273.
- Salvigsen, O., and Slettemark, Ø., 1995, Past glaciation and sea levels on Bjørnøya, Svalbard. *Polar Research* 14, 2, 245-251.
- Salvigsen, O., 2002, Radiocarbon-dated *Mytilus edulis* and *Modiolus* from northern Svalbard: climatic implications. *Norsk Geografisk Tidsskrift* 56, 56-61.
- Schilder, G., 1984, Development and achievements of Dutch northern and arctic cartography in the sixteenth and seventeenth centuries. *Arctic* 37, 4, 493-514.
- Shakhova, N., Semiletov, I., Salyuk, A., Yusupov, V., Kosmach, D., and Gustafsson, O., 2010, Extensive Methane Venting to the Atmosphere from Sediments of the East Siberian Arctic Shelf. *Science* 327, 5970, 1246-1250.
- Solomon, S. M., 2005, Spatial and temporal variability of shoreline change in the Beaufort Mackenzie region, Northwest Territories, Canada. *Geo-Marine Letters* 25, 2-3, 127-137.
- Stevens, C. W., Moorman, B. J., and Solomon, S. M., 2010, Interannual changes in seasonal ground freezing and near-surface heat flow beneath bottom-fast ice in the near-shore zone, Mackenzie Delta, NWT, Canada. *Permafrost & Periglacial Processes* 21, 256-270.
- Svendsen, J. I., and Mangerud, J., 1997, Holocene glacial and climatic variations on Spitsbergen, Svalbard. *Holocene* 7, 1, 55-57.
- Tangen, H., and Justad, J., 2012, A survey on coastal erosion in Central Spitsbergen, Svalbard. SAMCot - Sustainable Arctic Marine and Coastal Technology. M. G. G. Bæverfjord, S. W. Danielsen and K. Heilemann. Trondheim, SINTEF: 61.
- Thieler, E.R., Himmelstoss, E.A., Zichichi, J.L., and Ergul, Ayhan., 2009, Digital Shoreline Analysis System (DSAS) version 4.0 — An ArcGIS extension for calculating shoreline change. U.S. Geological Survey Open-File Report 2008-1278. \*current version 4.3

- Ziaja, W., and Salvigsen, O., 1995, Holocene shoreline displacement in southernmost Spitsbergen. *Polar Research* 14, 3, 339-340.
- Velle, G., Kongshavn, K., Birks, H.J.B., 2011, Minimizing the edge-effect in environmental reconstructions by trimming the calibration set: Chironomid inferred temperatures from Spitsbergen. *The Holocene* 21, 417-430.
- Walker, H. J., 1998, Arctic Deltas. *Journal of Coastal Research* 14, 3, 719-738.
- Walter, K. M., Edwards, M. E., Grosse, G., Zimov, S. A., and Chapin III, F. S., 2007, Thermokarst lakes as a source of atmospheric CH<sub>4</sub> during the last deglaciation. *Science* 26, 633-636.
- Wangensteen, B., Eiken, T., Ødegård, R. S., and Sollid, J. L., 2007, Measuring coastal cliff retreat in the Kongsfjorden area, Svalbard, using terrestrial photogrammetry. *Polar Research* 26, 14-21.
- Werner, A., 1993, Holocene moraine chronology, Spitsbergen, Svalbard: lichenometric evidence for multiple neoglacial advances in the Arctic. *The Holocene* 3, 128-137.
- Wohlfarth, B., Lemdahl, G., Olsson, S., Persson, T., Snowball, I., Ising, J., Jones, V., 1995, Early Holocene environment on Bjørnøya (Svalbard) inferred from multidisciplinary lake sediment studies. *Polar Research* 14, 253-275.
- Woodroffe, C.D., and Murray-Wallace, C.V., 2012, Sea-level rise and coastal change: the past as a guide to the future. *Quaternary Science Reviews* 54, 4-11.

## Chapter 10 – Map descriptions of Fredheim and Skansbukta

Evangeline G. Sessford<sup>1,2</sup> and Anne Hormes<sup>2</sup>

<sup>1</sup>Department of Geosciences, the University in Oslo P.O. Box 1072 Blindern, 0316 Oslo

<sup>2</sup>Department of Geology, the University Centre in Svalbard P.O. Box 156, N-9171 Longyearbyen. [EvangelineS@unis.no](mailto:EvangelineS@unis.no) , [Anne.Hormes@unis.no](mailto:Anne.Hormes@unis.no)

### Introduction

Two Quaternary geological maps have been completed for cultural heritage sites from Inner Isfjorden. Fredheim has been conducted in 1:3000 for a 0.8 km<sup>2</sup> area and a 0.5 km<sup>2</sup> area at Skansbukta has been mapped in 1:2000 (Fredheim Quaternary Map, Skansbukta Quaternary Map: external disc [henceforth referred to as Map 1 and Map 2, respectively]).

The Quaternary maps serve as important stepping stones to evaluate landscape development of the area. In the frame of a project initiated by the Governor of Svalbard, we aim to establish a better understanding of interactions between Holocene climate changes and its impact on natural hazards including coastal erosion. A Holocene landscape analysis will be done in the frame of the Master thesis by Evangeline Sessford, based on the Quaternary map and additional data. The aim of this project is to conduct spatial and temporal terrestrial analysis for the field sites that will be used in the production of geological hazard risk assessment. The resulting observations of this study will provide the Governor of Svalbard with an assessment that can be used to define tolerance limits for Fredheim and Skansbukta and thereby acted upon to preserve the cultural heritage in the most optimal manner. A correlation of past natural hazard events and past climate variability might help to understand the occurrence of future hazardous events.

However, Quaternary mapping is of use to many research and industry fields. For example, often biologists require knowledge pertaining to sediment types and landforms to understand chemical compositions and impact on biological processes. Infrastructure development and protection are dependent upon sediment type and landforms for ground stability assessments.

The project objectives were to create detailed Quaternary geological maps of the cultural heritage sites. In Fredheim documented erosion rates along the coast have been reported with a high variability between 11 and 57 cm/year. The buildings in Fredheim are of vital interest for local tourism and history and the Governor has to evaluate measures in order to prevent the buildings from toppling down the coastal cliff in the next couple of decades. A Svalbard Miljøvernfond funded project aims to visualize different erosion protection

measures along the coastline of Fredheim. The mapping exercise in Skansbukta revealed gelifluction, debris flow and avalanche processes, but coastal erosion in this protected bay is negligible.

## Methods and sources of error

Both Quaternary maps were created using a combination of differential global positioning system (DGPS) measurements, aerial image analysis (Figure 1 and 2), digital terrain models (DTM) and field observations. Fieldwork at both sites was conducted in August 2011 and June 2012. Fredheim was also visited on a number of occasions intermittently between the two dates so as to gain an understanding of seasonal changes affecting landforms. During fieldwork it was possible to collect DGPS points, however real time processing was not functioning and thereby post-processing of data collection using Leica GeoOffice software was essential. At Fredheim, the ground control point (GCP) is located within one km of all points and measurements were satisfactory in their post processing. However, at Skansbukta the GCP is between 6 and 7 km away from all collected points and at times were unable to be measured during post-processing and remain as navigated points thereby producing larger errors. The majority of points that were unable to be processed are those at the top of the slope near to the cliffs, however sometimes the rover malfunctioned elsewhere, and thereby causing larger errors. Processed DGPS points, aerial images and DTM (Norwegian Polar Institute, 1990) were combined in ArcGIS 10 software for mapping purposes. Errors associated with the specific data sets are shown in Table 1. Personal photographs from fieldwork were examined during map creation to recall specific landforms for true representation. Maps are projected through UTM zone 33N using the WGS 1984 datum. Contours are extracted from the DTM which has a resolution of 20 m. This unfortunately produces contours which can only be used for approximate elevations due to the large scale maps.

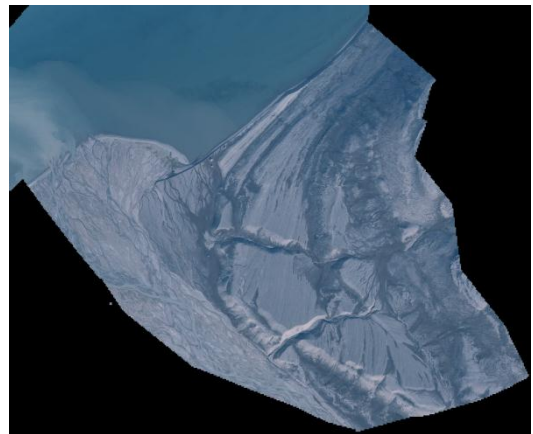


Figure 1: Aerial image 13824\_00048 of Fredheim (Norwegian Polar Institute, 2009)

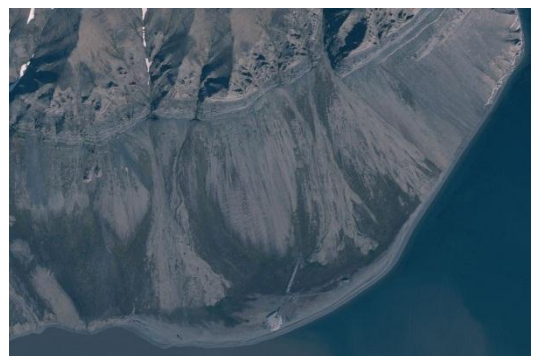


Figure 2: Aerial image 13822\_00081 of Skansbukta (Norwegian Polar Institute, 2009)

For all marine radiocarbon ages we report conventional dates and 68% (1 sigma standard

deviation). All marine radiocarbon dates including mollusks and foraminifera from marine sediments in isostatically uplifted marine terraces, were recalibrated to calendar ages using a reservoir age of  $440 \pm 52$  years corresponding to  $\Delta R$   $107 \pm 52$  years (Mangerud et al., 2006). The recalibration is based on two different recommendations using a marine reservoir effect of  $450 \pm 52$  (Mangerud in Mangerud et al. 2006) and  $438 \pm 52$  years (Bondevik and Gulliksen in Mangerud et al. 2006) for mollusks and foraminifera in Spitsbergen. The calibration is based on the Fairbanks '0107' calibration curve with the online calibration software (<http://radiocarbon.ldeo.columbia.edu/research/radcarbcal.htm>) as this curve uses only coral U/Th dates (Fairbanks et al., 2005).

## 10.2 Fredheim: Quaternary superficial deposits

### Glacial deposits and glacial history

The study area (Map 1, external disc; Figure 1) is known to have been glacially covered during the Last Glacial Maximum (LGM), based on studies of isostatically uplifted marine terraces (Salvigsen, 1984) and marine studies in Tempelfjorden (Forwick & Vorren, 2009). On the plateau east of Fredheim glacial erratic boulders and lateral meltwater channels have been found that would need further investigation, but that are assumed to date to LGM, therefore, the existence of till cover southeast of Fredheim has been confirmed.

It has been suggested on the *C9Q Adventdalen Geomorphological and Quaternary Geological Map* (Tolgensbakk et al. 2000) that there is glaciofluvial material along the edge of the pre-recent fluvial sediments and the gelifluction areas coming down from marine terraces, more or less where organic material is labeled on this map (Figure 3). This has not been described in this map as it was not found in any sections along the boundary between the Nøiselve and marine terraces. However, this does not rule out the possibility of glaciofluvial sediment being present under colluvium, gelifluction or organic material.

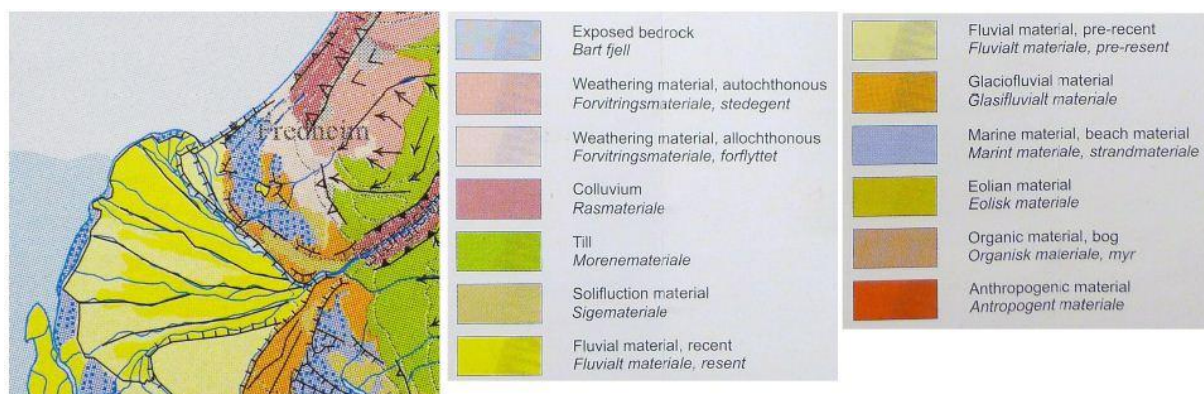


Figure 3: Excerpt from map C9Q, Adventdalen Geomorphological and Quaternary Geological Map indicating the glaciofluvial material identified at Fredheim, from Tolgensbakk et al. 2000.



## Marine deposits and Holocene emergence

The present day shore at Fredheim is made up of a beach and deltaic system with sediment deposition dominated by fluvial and wave (longshore drift) energy (Figure 4). It is considered a soft, weakly consolidated and easily erodible coast as described by Fairbridge (2004). The system acts as an analogue for past Holocene landform development. Beach sediments are clast dominated by mostly well rounded plates. The delta is made up of well-rounded clasts and sand that have been fluvially transported, less sorted than the beach deposits. The delta is prograding northward into Sassenfjorden and eastward along the shore due to longshore drift and is easily distinguishable due to the beach ridges formed during movement. It has grown 189,47m along the coastline at an average rate of 5,92m/yr between 1977 and 2009 (Guegan et al., submitted). Pits are formed on the delta and beach from sea ice and icebergs that have been thrust onshore and/or by the ice foot (henceforth referred to as shore ice if all three ice types are discussed) (Caline, 2010; Rodzik, 2009; Nichols, 1961). The ice foot as described by Caline (2010) is a fringe of ice attached to and along the shore and may be of varied widths. It is especially of interest in regards to its role in shore erosion and sediment transport as discussed further in (Guegan et al., submitted; Allard et al., 1998). The ablation of shore ice is unevenly distributed and causes the creation of ice tumuli overlain by gravel deposits that produce pitted beaches as ice thaws out (Rodzik, 2009; Nichols, 1961). Both pits and beach ridges appear on the present day shore. Within the delta there is a lagoon which is changing in shape, size and outflow location on a yearly basis (field observations and DGPS measurements, this study) and can be observed through aerial image analysis from photos taken in 1977, 1990, 1995 and 2009 (Norwegian Polar Institute, aerial image depository) (Guegan et al., submitted).



Figure 4: Fluvially dominated sedimentation affected by longshore drift and fjord circulation at Fredheim. (Aerial Image S90, Norsk Polarinstitut, 1990)

There are five uplifted marine terraces at Fredheim (MT1 – MT5) (Map excerpt 1). On the map these are numbered as five being the oldest and at the highest elevation while one is the lowest and youngest. Their relative age can be reconstructed based on their geomorphological relationship as the younger terraces cut older terraces. They are coloured blue and described in the legend as pre-recent marine beach material. The terraces are

covered with fairly well rounded, flat stones or round pebbles which have undergone periglacial frost cracking.

The uppermost terrace, MT5, lies between 70 and 80 m a.s.l. It is not very extensive and is visible only on the north side of the spring meltwater creek (henceforth referred to and unofficially named as Nordbekken) that flows from Fjordnibba, the mountain to the east of Fredheim, though not shown in the map. There are two faint beach ridges on its surface, running from north to south. It has not been possible to date MT5, but it is assumed to be older than the Last Glacial Maximum (LGM). This interpretation is based on three arguments:

1. Radiocarbon dates established from beach sediments on MT4 and MT3 indicate Early Holocene ages.
2. Marine terraces of comparable age along the west coast of Spitsbergen were dated to represent preserved pre-LGM marine landforms that were only covered with non-erosive glacier ice during LGM (Forman et al., 1987; Landvik et al., 2012, 2005)
3. The marine sediments of MT3 lie on top of a glaci-marine diamicton that is interpreted as LGM till. Therefore MT3 represents some of the oldest Holocene marine deposits and this supports our interpretation under point 2.

MT4 only extends to the south of Nordbekken and mostly to the south of Sørbekken (unofficially named) between 60-65 m a.s.l. This is likely because the steepness of the slope to the north did not allow for beach sedimentation and build-up to occur. Interestingly, while beach ridges on MT5 are trending north south, beach ridges on upper MT4 show east west trending beach ridges. It seems more plausible that the upper part of MT4 is actually part of MT5, due to this difference in beach ridge deposition; however, there is no large gradient change or steep slope dividing the two sections only a modern meltwater channel that may formerly have been a lagoon. MT4 has been radiocarbon dated to  $10767 \pm 193$  and  $11061 \pm 174$  cal BP ( $9\,927 \pm 60$  and  $10\,106 \pm 57$   $^{14}\text{C}$  years BP; Ua-44107, Ua-44108) with *Mya Truncata* shell fragments at point S, approximately 60 m a.s.l. at  $78^{\circ} 20' 57.2''$  N and  $16^{\circ} 56' 31.1''$  E. The shells were found along the gulley cut out by Sørbekken in loose sand/gravel at a depth of 86-83 cm below the surface (See: Sessford, Master thesis 2013 for a complete overview of dated material).

The largest and most extensive of the marine terraces is MT3 which lies between 30 and 55 m a.s.l. The terrace has been dated from *Mya Truncata* shell halves and fragments at 51 m a.s.l. along Sørbekken at  $78^{\circ} 20' 56.6''$  N and  $16^{\circ} 56' 13.6''$  E. Two samples, taken from depths between 240 and 267 cm below the surface return  $^{14}\text{C}$  dates of  $10636 \pm 170$  and  $10690 \pm 186$  cal BP ( $9842 \pm 60$  and  $9\,878 \pm 64$  years BP; Ua-44104, Ua-44105). Samples



were found in bimodal beach deposits directly above a sharp erosional boundary dividing it from glaciomarine diamicton containing red clay chunks and striated clasts. We interpret the glaciomarine diamicton as LGM till. The upper 55 cm of the terrace are bimodal beach sediments largely made up of pebbles, a third sample of shell fragments returned a date of  $10674 \pm 181$  cal BP ( $9867 \pm 63$   $^{14}\text{C}$  years BP; Ua-44106). Beach ridges on the surface are clear, numerous and relatively evenly spaced (Figure 5). MT3 is the first terrace with pitted beaches.

MT2 is a relatively narrow terrace with no distinct beach ridges. It is being overrun by gelifluction in the northeast and active layer detachments toward the south. The geomorphological expression of this terrace is the least clear of all marine terraces due to overprint by gelifluction processes, light vegetation and several ice pits on its surface.

The lowest of the terraces is MT1. Along with MT3, it is the most distinct terrace containing very clear beach ridges and some pitted areas in the northeast. In Figure 6, the ride up of the sea ice/iceberg can be seen in the middle of this lowermost terrace (Sysselmannen på Svalbard 2000). It is not exactly clear what type of ice has deformed

the sediments, but it appears to be either sea ice ride up or pile up. The ice floe was thrust onshore and destroyed two boats belonging to the cultural heritage site (Figure 6) (Bjerck, 1999).

## Fluvial deposits

Some of the most dominant features in the map are the fluvial sediments. There are two main types, recent and pre-recent (dark yellow and light yellow, respectively). The distinguishing factor between the two is whether or not water flows on an annual basis through the landform thereby entraining, transporting and depositing clasts and sediment. Therefore, in Nordbekken, Sørbekken and the alluvial fan at the mouth of Nordbekken recent fluvial sediments which are affected mostly by spring meltwater are mapped. The creeks



Figure 5: Beach ridges on MT3, note linearity and spacing. Image taken from the northeast of the map facing south west, Nordbekken can be seen in the bottom right corner of the photo. (Sessford, 2012)



Figure 6: Ice ride up/pile up from 1999 (Image from Sysselmannen på Svalbard, 2000)

usually run dry by September. Nøiselva and the delta are also considered recent sediments as they are reworked annually. The sediment in the channels as opposed to channel bars consists of fewer fines as those are washed out by repeated spring meltwater events. There is one region marked as recent fluvial sediments that lies between pre-recent alluvial sediments and does not have the river symbol within it and from first appearance looks to be a relict channel. Contrary to the relict channels, there are less fines and vegetation (Figure 7). The surface of this section appears to have recently been used for surface meltwater flow but has since been abandoned at its southern end. However, it has undergone significant (approximately 150 m) backcutting from spring meltwater flow at its northern end from the coastal escarpment (Figure 8).

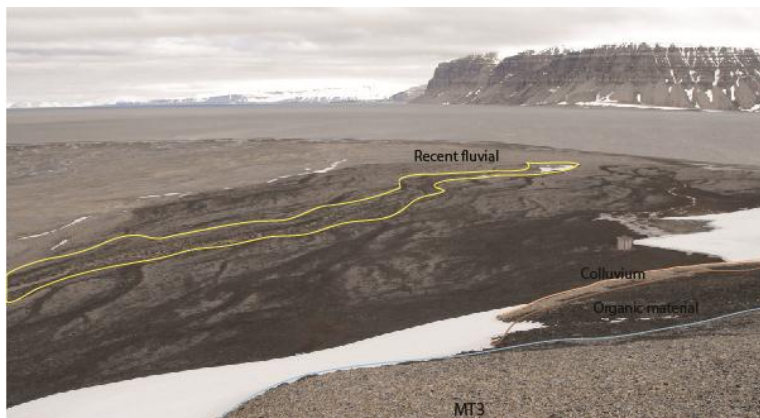


Figure 7: Pre-recent fluvial plain with recent fluvial sediments indicated in yellow. The limit between the pre-recent Nøis alluvial plain and the recent Sassen estuary is a sharp boundary seen clearly with vegetated river channels on the pre-recent delta (Sessford, June 2012).

Pre-recent sediments are those that are no longer undergoing sediment displacement due to surface flow of water. There are four distinct locations where pre-recent alluvial sediment is present, MT5, MT3, MT2 and between MT1 and the recent fluvial sediments of the Nøiselva. Those sediments which are on the terraces

override the beach sediments, making beach ridges indiscernible and distributing fines which are susceptible to ice segregation and frost cracking (French and Shur, 2010). It may well be that these pre-recent sediments are relict alluvial fans that were deposited shortly after the uplift of each terrace (Figure 9). Relict fluvial channels (coloured moss green) are easily discernible on the surface of pre-recent sediments due to the high vegetation content and their elongated, braided depressions. In regions close to organic material where standing water is present, and near the alluvial fan at the mouth of Nordbekken, some surface water flows along these channels (Figure 10). However, it always changes to water which flows within the active layer, above the permafrost table as what will henceforth be termed groundwater, and flows out as surface water when reaching both the coastally and fluvially eroded scarps (Figure 11).

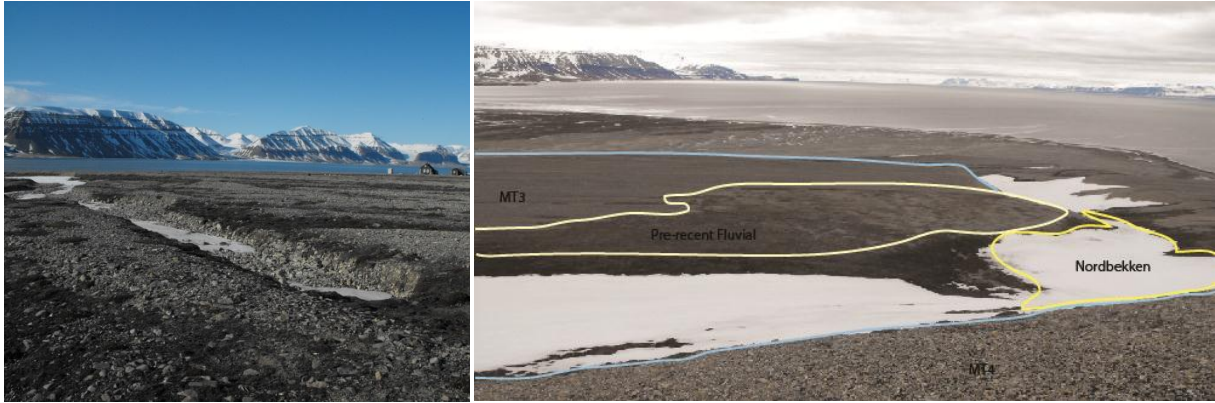


Figure 8 (left): Backcutting of relict channel due to spring meltwater flow (Sessford, June 2012)

Figure 9 (right): MT3 with beach ridges overlain by alluvial fan containing some vegetated relict channels (Sessford, June 2012)

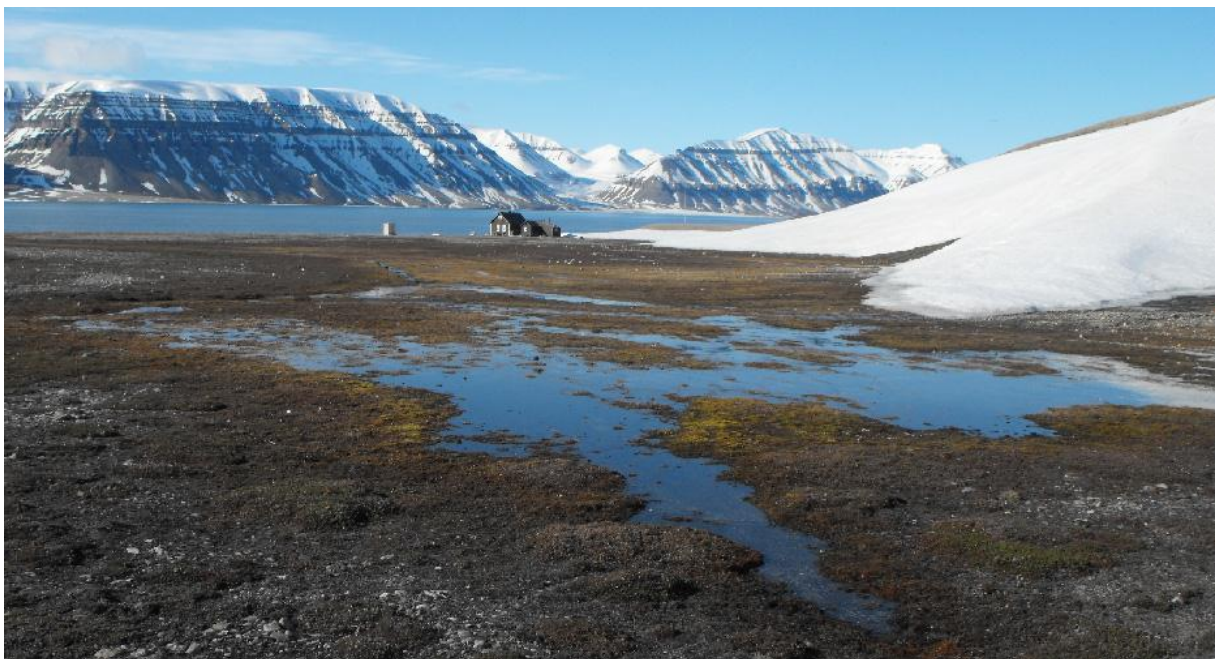


Figure 10: Organic material below Nordbekken alluvial fan and relict channels leading away from the fan toward the buildings and the fjord (Sessford, June 2012)



Figure 11 (left): Strong backcutting and erosion where relict channels meet the coastal escarpment due to concentrated groundwater flow (note groundwater at base of escarpment) (Sessford, August 2011)



## Slope deposits

Solifluction is a product of two mechanisms; gelifluction, thaw induced saturated flow of sediments, and creep, frost heave followed by thaw settlement (Matsumoto, 2002). It is a common feature found on Svalbard's slopes. The majority of movement at Fredheim is undergone in well saturated sediments containing excessive vegetation. Therefore, solifluction on the map has been labeled as gelifluction (light orange). The beach ridges on the marine terraces do not contain enough fines and are well drained and therefore less subject to gelifluction, even though the terraces have a slight gradient. The general trend at Fredheim is that gelifluction creeps downslope through two-sided freezing inducing plug-like flow and thereby dislocating the surface layer and creating lobes (Matsuoka, 2001). At Fredheim, lobes are found on steeper slope gradients, tend to be between 0,1 and 0,5 m in height, have a steep front lip and a slight depression toward the slope. The front lip may be either turf-banked (vegetated) or stone-banked (Matsuoka, 2001). However, in some places gelifluction accumulations can produce large gelifluction sheets or terraces such as above MT4 and MT5 where a large section of active layer made up of many smaller gelifluction lobes moves as 'one' piece forming a long, distinctive front lip (Matsuoka, 2001) (Figure 12).

On this map, colluvium refers to loose clasts and sediments that are originally a part of the beach terrace surfaces but are now on the sides of the slopes due to erosion (Figure 13).



Figure 12 (left): Examples of a gelifluction lobe where the line indicates the front lip (Sessford, June 2012)

Figure 13 (right): Non-vegetated area on the slope of MT3 consisting of colluvium. The shovel shows the boundary between the present day surface and colluvium. At this particular location (nearby to the radiocarbon sample), one can see cracking where the initialization of a possible slope failure may occur in the future. (Sessford, October 2011).

The dark pink parts of the map indicate active layer detachment slides (ALDS), some of which are labeled D#. Those that are labeled are more distinct in their appearance and their scarps have been measured to analyze past active layer thicknesses. ALDS's have three distinct parts to them, the detachment or slide scarp, the detached zone and the depositional zone. In most cases at Fredheim, the detached and depositional zones are difficult to discern due to post-detachment processes such as gelifluction and/or secondary detachments from

within the first. As detachment depths are only to the base of the active layer/top of the permafrost it is suggested in (Sessford, master thesis 2013) that scarp depths may be used as an indicator for past active layer thicknesses and thereby correlated with air temperatures to determine relative timing/frequency of ALDS detachment and probability of future events. ALDS D7 and D6 are interesting in that they appear to have been divided because of a small bedrock exposure.

## **Periglacial features**

All of the landforms and sediments at Fredheim have undergone periglacial processes in some form or manner. To the northeast of the map, slopes and some areas on the marine terraces containing exposed bedrock have undergone autochthonous weathering. It is hard to say how deep the weathering penetrates into the rock as no further investigations have been made in this study. More detail is given in the Bedrock section below.

Patterned ground is not very common in the area; however it is present on some of the pre-recent alluvial fans on the terraces. It has not been investigated as to whether or not ice wedges are associated with the patterned ground, but there is distinct cracking within the surface sediments.

## **Bedrock**

The presentation of bedrock geology in this map is limited due to the extensive Quaternary deposits draped over the surface. However, there are outcrops of the Gipshuken Fm. that have recently been exposed by the beach and within the tidal zone as a result of coastal erosion. This formation has been identified as part of the Gipsdalen Group and is of Sakmarian – Artinskian age (ca. 290 Ma) (Major, 1972; Cutbill and Challinor, 1965; Dallmann et al., 2001). The Gipshuken Fm. at Storgjelet and Sveltihel (locations in the near vicinity of Fredheim) is described as platform deposits of limestone/dolomite containing marly, shaley or sandy interbeds and thin gypsum layers (Major, 1972). This is representative of the upper section of the Fm. which has informally been named the Skansdalen Mb. by Dallmann, ed.(1999) who further describes the deposits as consisting of regularly bedded dolomites containing intercalated marly beds where bioturbation, algal mats and erosional surfaces are commonly found. The sediments represent cyclic deposits and are interpreted to have developed in a sabkha flat environment trending toward lagoonal deposition (Dallmann, 2001; Blomeier, 2009; Hüneke et al., 2001).

Higher up on Marine terrace MT3, the Gipshuken Fm. clearly crops out again in a similar manner to that at the present day coast and is likely analogous to it. The outcrop is escarpment-like, with many large well rounded boulders at the base of the cliff and appears

to have been heavily eroded by water both chemically and mechanically (Figure 14). However, it is clear that the rock has been exposed to the elements for much longer than the present day cliff as wind erosion has also made its mark by creating facets on exposed surfaces, and frost shatter has downsized boulders (Figure 15).

Bedrock exposure also occurs in those places marked as *Autochthonous bedrock weathering* on the map. These locations are mostly at higher elevations, but also in the steeper, northern region of the marine terraces. Blockfield-like exposures that are heavily frost-shattered, weathered and broken appear at the base of every slope between two marine terraces. On the northern part of MT3, only a thin veneer of beach sediments have been lain down and bedrock boulders heavily influenced by frost activity are present.



Figure 14 (left): Bedrock exposure on MT3, note well rounded-ness (Sessford, June 2012)

Figure 15 (right): Mechanical (wind) and chemically eroded boulders that have undergone frost shatter (Sessford, June 2012)

Between 90 and 100 m a.s.l. relatively large and distinct bedrock mounds are observed (Figure 16). These do not appear as outcrops but rather stand out as small hills and could easily be misinterpreted as marine terraces. However, there are no beach sediments on their surface but only weathered bedrock. They are divided laterally by small depressions

containing vegetation and undergoing gelifluction.

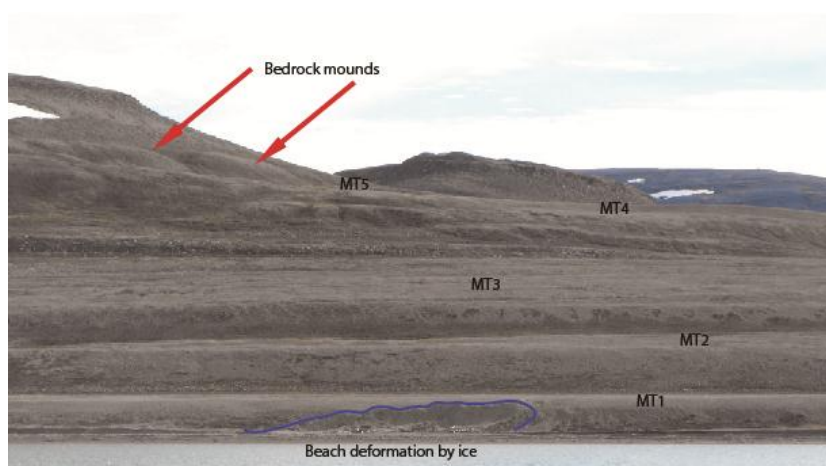


Figure 16: Terraces and bedrock mounds as indicated, the purple line delimits the beach deformation by sea ice (Sessford, August 2012)

## Anthropogenic structures and recent events

There are five buildings in Fredheim, four of which are cultural heritage buildings and protected by law. The structures were built by Hilmar Nøis and his kin and served as their main hunting station (Figure 17). The fifth building, south of the alluvial fan, is a recent structure built for tourists to relieve themselves. There are also remnants of two small fishing boats which stood in exactly the location at which the ice floe was thrust onto shore and unfortunately crushed them entirely. Two of the cultural heritage buildings, the Outhouse and Gammelhytta (Old Hut) have been moved south, away from the coastal escarpment due to the threat of coastal erosion and disappearing shoreline.



Figure 17: Buildings at Fredheim from left to right: Nødhytta (emergency hut), Outhouse, Villa, Gammelhytta (Old hut) (Sessford, May 2012)

## Organic material

Locations marked as organic material are areas in which standing water is present in the spring and early summer thereby allowing for high vegetation growth. There was an attempt to drill to the base of these bogs in the hopes of dating macrofossils as these regions are present on each terrace and could have been a good proxy for regional isostatic uplift. However, all dates turned up modern and therefore cannot indicate the onset of terrestrial plant growth due to uplift but rather due to other factors. Perhaps sediment or water availability was not extensive enough until modern times.

This study has placed one thermistor string as marked by a red dot within the active layer to observe freeze and thaw of the active layer in the pre-recent fluvial sediments. It was installed on October 1, 2011 and will run until April, 2013 (Figure 18). There has also been an automatic camera installed at the point marked with a **C** to observe sea ice changes and coastal erosion. It was installed on July 5, 2012 and will take one photo daily at 12:00 until uninstalled sometime in April 2013 (Figure 19).

Radiocarbon samples mentioned in the Marine deposits and Holocene emergence section were taken from the north side of Sørbekken gully in sections having become naturally exposed through slumping and colluvium deposition (Figure 20). The sediments were in permafrost that had been exposed and were quite saturated.



On the present day delta there are parts of a whale skeleton from a whale that has been beached within the last 20 years, as it lies on the section of delta which did not exist before 1990. A few bones from this skeleton have been displaced and moved up to the pre-recent fluvial material.



Figure 18 (left): Setting up the thermistor string (Hassberg, June 2012).

Figure 19 (right): Location of automatic camera and direction of photos taken by camera (Sessford, July 2012).



Figure 20 (left): Colluvium undergoing erosion through slumping; location of radiocarbon samples for MT3 (Sessford, June 2012).



### 10.3 Skansbukta: Quaternary superficial deposits

#### Marine material

All beach material at Skansbukta is considered to be recent i.e. there are no uplifted marine terraces located within the map that can be identified and dated. The well rounded, flat, flaggy beach clasts reach from sea level to approximately four metres a.s.l. The beach has a relatively steep coastline which has prograded since 1918 when the gypsum pier was constructed at the shore and can be seen in Figures 21 and 22. This is also shown by the way the cultural heritage items which have been left on the beach since 1918 have become partially covered by beach stones, and that the gypsum pier which used to reach the coastline is now approximately ten metres from the present day coastline (Figure 22). However, a recent study suggests that between 1990 and 2009 the overall trend, though minimal, is erosion of the Skansbukta coast (Guegan et al., submitted). The location of the coastline on the map has been measured using DGPS points of the high tide line on August 14, 2011. As indicated by tidal gauges in Ny-Ålesund, the morning high tide was 143 cm (Vannstand.no).

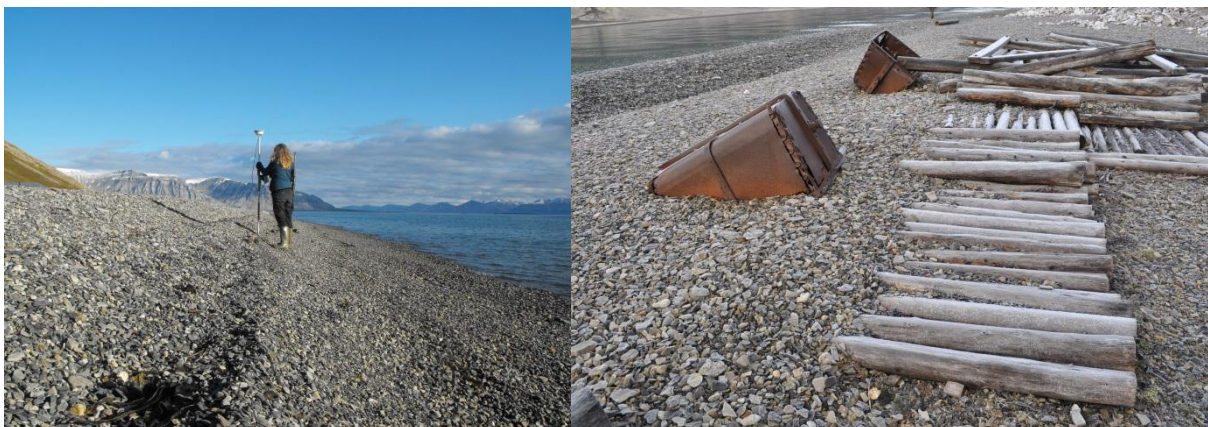


Figure 21 (left): Steep shoreface at Skansbukta (Sessford, August 2011)

Figure 22 (right): The beach at Skansbukta where stones overlying wooden structures and half burying mining buckets indicate progradation (Kelley, September 2011)

The darker blue coloured marine deposits with open circle markers indicate covered with lichen covered beach, and thereby distinguished from those without (Figures 23 and 24). Other than the presence of *Xanthoria elegans*, an orange lichen, there is no other distinguishing factor between this beach material and that of the recent beach. One interesting note is that there are no lichens close to the anhydrite pier. There is lichen-covered beach material dividing the vegetated colluvial and beach material from the recent beach material everywhere except at the southern parts of the beach. The distribution of the

lichen vegetation would suggest that where recent progradation has happened no lichen growth is possible.

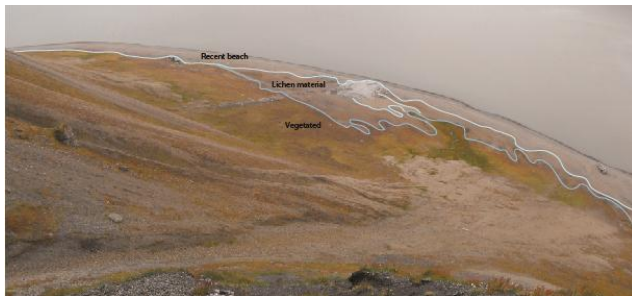


Figure 23: Approximate division of beach material at Skansbukta. Recent beach material is above the light blue line, vegetated material is below the dark blue line and lichen covered material is between the two (Sessford, August 2011).



Figure 24 (above): Seasonal pond, note steep gradient toward coast and lack of vegetation (Sessford, August 2011).



Figure 25 (above): Vegetated beach and colluvial sediments, note rock fall material lying on surface (Sessford, August 2011).

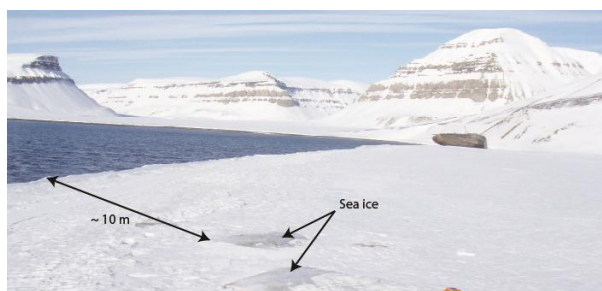


Figure 26 (above): Sea ice thrust on shore during winter (Sessford, April 2012).

The darker blue beach material containing vegetation symbols represents a combination of beach and colluvial material which is vegetated mainly by various types of moss (Figure 25). It also contains a significant amount of fines as can be observed by the presence of patterned ground as described within the periglacial features section. A smaller

feature which only appears in the northwest corner of the map is small seasonal ponds. These are small (between 10 and 30 cm deep) depressions in the lichen/vegetated beach deposits that do not contain any vegetation within them. They have a higher gradient slope on their southeast, towards the coast. They are marked as seasonal ponds because it is presumed that there is longer standing water/snow in them in the spring time and therefore vegetation is not growing in them. The last marine associated landform is beach hummocks shown as diagonal grey lines on the map. These are non-uniform mounds and depressions close to the present shoreline and within the recent marine material. It is presumed that the hummocks are formed from sea ice as it is thrust onto the shore during winter (Figures 26 and 27).

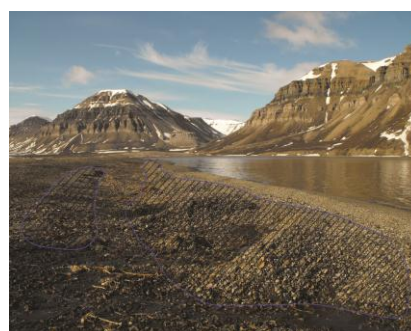


Figure 27 (left): Beach hummocks from the south side of Skansbukta (Sessford, June 2012).

## Slope deposits

The slopes at Skansbukta are made up of a number of different landforms the main components of which are rapid mass movement, rock fall, debris flow and snow avalanche deposits (Figure 28). Frost shattering within gully systems induces rock fall which collects at the base of the cliff in accumulation zones (Figure 29). At some point these accumulation zones are flushed out by an extreme event such as oversaturation and create debris flows. Debris flows are marked in red on the map and are characterized by very coarse, well compacted and stable angular clasts. They are deposited as elongated mounds or lobes and originate from chute like erosional gullies on the cliffs which are marked by gully edges on the map. These can be identified by their convex shape, lobe divisions, levees and steeper gradients in the upper regions, and spread out low gradient lower regions. It is likely that avalanche deposits co-exist with debris flow deposits but distinctions between the two is difficult on these particular deposits without direct observations (Eckerstorfer et al., 2012). Lobes represent different debris flow events and are marked out as lobe divisions (Figure 30). None of the lobes have been examined to gain understanding of event timing. However, it can be assumed that those on the surface are younger than those that are overridden because of their geomorphological relationship. Snow avalanche deposits and debris flows tend to originate from a confined area and spread out horizontally as they move downslope. Smaller, finer grained debris flows are present on the rapid mass movement deposits and are marked as black arrows. These seem to be more frequent and do not have long life preservation due to their small size and activity of rock fall and gelifluction which override them easily.



Figure 28 (above left): Skansbukta slopes from the bay, note the rapid mass movement deposit in the middle of two debris flow accumulations (Hassberg, June 2012)

Figure 29 (above centre): Rock fall accumulation at the base of gully below cliff and above debris flow run-out (Sessford, August 2011).

Figure 30 (above right): Elongated debris flow accumulations overriding each other with well-defined levees covering the snow avalanche deposits (Sessford, August 2011)

The rapid mass movement deposits are shown in pink on the map and are located below vertical cliff faces, as opposed to gullies. The main rapid mass movement deposit in the



middle of the map is made up of angular, blocky clasts of varying size but mainly in the pebble to small boulder range. Little to no gelifluction movement is indicative of active rock fall and rapid mass movement in the southeastern part of the accumulation. Whereas gelifluction in coarse material, shown as thin diagonal orange stripes is more active in the northwestern section of the map unit. You can also see in Figure 31, that there are some relict fan sections that are becoming covered by thin vegetation.



Figure 31 (above): Rapid mass movement deposit showing less active rock fall on the left where gelifluction is the more predominant slope movement, and the right side where rock fall is predominantly active (Sessford, September 2011).



Figure 32 (above): Gelifluction steps to the side and above mine entrance. Note how rock fall is caught on the surface of each step (Sessford, June 2012).

There are two types of gelifluction in Skansbukta. The first has already been mentioned and is only present on the rapid mass movement (Figure 31). The second is turf banked gelifluction lobes which are located in vegetated slopes and shown as a light orange colour on the map. Steps are between 0,1 and 0,5 m in height and have a front lip and a small depression on the slope side as described in the Fredheim map description. At Skansbukta, gelifluction lobes act as debris catchers during rock fall (Figure 32).

Rock fall debris extends out from the base of the slope to the dotted blue line overlying beach material. Most rock fall does not have a run out zone extending until the recent beach material likely because of two reasons. One, because rock size is generally not very large (with the exceptions of some boulders such as seen in Figure 33) and therefore does not contain enough kinetic energy to move a great distance, but mainly due to the presence of

vegetation, either on the slopes where there are gelifluction steps, or at the base of the slope which absorbs rock fall energy thereby slowing the rocks so that they come to a stop sooner (Figure 34) (Jones et al., 2000; Ritchie, 1963). It is quite probable that most rocks extending to the recent beach material have been moved there due to anthropogenic activity. Most of the rock fall is in fact quite small as seen in Figure 35, and there is much occurring in the spring or melting seasons which is caught on snow patch surfaces (Figure 35). It is also possible that much of the smaller debris is aeolian material.

The cliff base as distinguished by the solid black line with triangles and at the top of the slope has been measured using DGPS, therefore the position of this line represents the base of the cliff, and not the top. The base is at approximately 180 m a.s.l. and extends upwards approximately to 250 m a.s.l. although not necessarily entirely vertical.



Figure 33 (above left): Large rock fall boulder stopped in bog area (Sessford, August 2011).

Figure 34 (above centre): Rock fall debris come to stop on gelifluction steps, vegetation and cultural heritage material at mine entrance (Sessford, June 2012).

Figure 35 (above right): Small rock fall and aeolian debris caught on snow patch surface (Sessford, June 2012).

## Periglacial features and hydrology

Patterned ground in Skansbukta is not easily seen when standing directly on its surface but can be seen from above when standing on the slopes as shown in Figure 36. It is only present in the vegetated pre-recent beach deposits which likely have a large amount of fine grained aeolian sediments in them to allow for frost cracking. This is due to this area being less well drained and having finer sediments than the other beach areas. Patterned ground is not present in the organic material areas coloured in brown, as these are more bog like and have too much excess water for ice wedges to form (Figure 37). It is presumed that during the active mining times, most of the vegetated pre-recent beach area had an extensive amount of standing water in it during spring. The reason for this assumption comes from small drainage like channels within the path shown in Figure 38 and the presence of the bridge (now collapsed) for the trolley track (Figure 36).

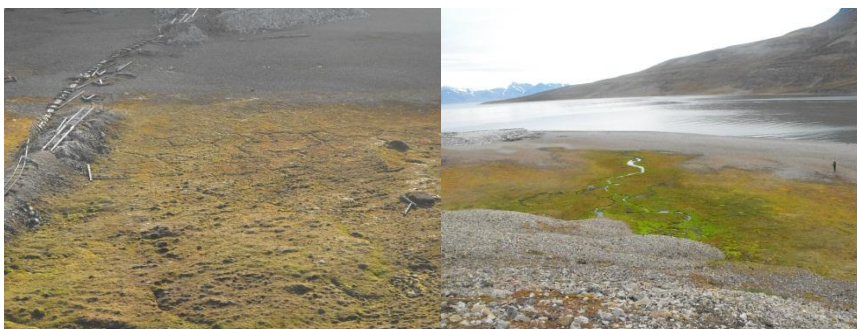


Figure 36 (far left): Patterned ground as seen from the slopes above the mine entrance (Sessford, August 2011).

Figure 37 (left): Bog north of cultural heritage zones and below debris flow accumulation (Sessford, August 2011).

Small fluvial channels labeled as intermittent rivers on the map originate from snow melt in the spring and throughout the summer if snow accumulation over the winter was excessive enough. Much snow accumulates above the cliff, within the gullies as well as on top of the



plateau. Water flows through the gullies and as small waterfalls over the cliffs above debris flow and snow avalanche accumulations (Figure 39). There is no water flow above the rapid mass movement deposits. Water continues to flow down to the sea as groundwater through the debris flow accumulations and resurfaces in the bogs to again flow as groundwater to the sea. Only in one place is groundwater outflow visible at the recent beach coastline.

**Figure 38: Man made path with small drainage opening (Sessford, July 2011).**

## **Bedrock**

The lowermost geologic unit of the towering cliff of Skansen is the Gipshuken Formation of Early Permian age. Anhydrite dominates the lowermost section but is overlain with intermittent layers of dolomite. Skansen has a very well exposed, 115 m thick, continuous section of finely-laminated algal dolomites above the anhydrite. These uppermost deposits are suggested by Lauritzen et al. (1989) to be sabkha deposits and terminate with caliche horizons, a sedimentary deposit of mainly hardened calcium carbonates evaporated from uprising ground water. The Kapp Starostin Formation rests conformably above the Gipshuken Formation, dates to the Late Permian and is lithologically composed of cherts, siltstones, siliceous sandstones and spiculitic shales (Lauritzen et al., 1989) (Figure 40). Its resistance to weathering produces a distinct marker boundary between it and the underlying Gipshuken Formation. The base of Kapp Starostin Formation is made up of the Vøringen Member, a bioclastic, coarse grained limestone containing brachiopod and bryozoan fauna, marking the large scale transgression of Late Artinskian-Early Kungurian age (Lauritzen et al., 1989). Bedding is almost horizontal; the dip is ca. 2° SW. The cliff base begins at an altitude of 232 m a.s.l. and rises straight up approximately 250 m a.s.l. It is split periodically by gullies often containing a buildup of allochthonous weathering material and seasonal flow of water.



Figure 39 (right): Waterfall over cliff from gulley (Sessford, August 2011).

Figure 40 (far right): Lowermost bedrock of the Gipshuken Fm. upper cliff exposures of the Kapp Starostin Fm., both showing autochthonous weathering (Sessford, August 2011).



Autochthonous bedrock weathering is present on all exposed bedrock surfaces. The photo (Figure 40) is taken from outside the map area in the southeast and looking back toward the cliffs above Skansbukta.

### **Anthropogenic structures**

Skansbukta is protected as a cultural heritage site by the governor of Svalbard (Sysselmannen.no). The cultural zones that are marked out in grey are structures from a number of different activities. Though originally constructed as a gypsum mining site, excavations were stopped when it was determined that the area is dominated by anhydrite and not gypsum (Prestvold, 2003). However, much of the mining infrastructure still remains along with more recent cultural items such as the hunting and fishing cabin which is also protected. Items included in the cultural heritage zones are the mine entrance, the trolley track leading from the mine to the loading bay, the loading bay, log piles and steel baskets, walking path from the cabin to toward the tracks, the cabin, the loading boat and log posts which used to serve as support for buildings (see Figures throughout description and Figures 41-43).



Figure 41 (above left): The loading boat (Sessford, August 2011).

Figure 42 (above centre): The hunting and fishing cabin (Sessford, August 2011).

Figure 43 (above right): All cultural heritage zones as seen from the slopes above (Sessford, August 2011).

## References

- Allard, M., Michaud, Y., Ruz, M.H. & Hequette, A. 1998: Ice foot, freeze-thaw of sediments, and platform erosion in a subarctic microtidal environment, Manitousuk Strait, northern Quebec, Canada. *Canadian Journal of Earth Sciences* 35(9), 965-979.
- Bjerck, H. 1999: Overvåkning av kulturmiljø på Svalbard: Målsetting, metode, lokaliteter og overvåkning. *Rapportserie. S. Miljøvern avdeling. Longyearbyen, Sysselmannen På Svalbard* 300, 63.
- Blomeier, D., Scheibner, C. & Forke, H. 2009: Facies arrangement and cyclostratigraphic architecture of a shallow-marine, warm-water carbonate platform: the Late Carboniferous Ny-Friesland Platform in eastern Spitsbergen (Pyrefjellet Beds, Wordiekammen Formation, Gipsdalen Group). *Facies* 55, 291-324.
- Caline, F. 2010: *Coastal-sea-ice action on a breakwater in a microtidal inlet in Svalbard*. Doctoral Thesis, Department of Civil and Transport Engineering. Trondheim, Norwegian University of Science and Technology, 263.
- Cutbill, J.L. & Challinor, A. 1965: Revision of the stratigraphical scheme for the Carboniferous and Permian rocks of Spitsbergen and Bjørnøya. *Geological Magazine* 102(5), 418-439.
- Dallmann, W.K., ed. 1999: *Lithostratigraphic Lexicon of Svalbard. Upper Palaeozoic to Quaternary bedrock. Review and recommendations for nomenclature use*. Committee on the Stratigraphy of Svalbard / Norsk Polarinstitutt. 320 pp.
- Dallmann, W.K., Kjærnet, T. & Nøttvedt, A. 2001: Geological map of Svalbard 1:100,000 Sheet C9G Adventdalen. *Norsk Polarinstitutt Temakart* 31/32.
- Eckerstorfer, M., Christiansen, H.H., Vogel, S. & Rubensdotter, L. 2012. Snow cornice dynamics as a control on plateau edge erosion in central Svalbard. *Earth Surface Processes and Landforms*, doi: 10.1002/esp.3292.
- Fairbridge, R.W. 2004: Classification of coasts. *Journal of Coastal Research* 20 (1), 155-165.
- Forman, S.L., Mann, D. & Miller, G.H., 1987. Late Weichselian and Holocene relative sea level history of Brøggerhalvøya, Spitsbergen, Svalbard Archipelago. *Quaternary Research* 27, 41–50.
- Forwick, M. & Vorren, T.O. 2009: Late Weichselian and Holocene sedimentary environments and ice rafting in Isfjorden, Spitsbergen. *Palaeogeography, Palaeoclimatology and Palaeoecology*, 280(1-2), 258-274.
- French, H. & Shur, Y. 2010: The principles of cryostratigraphy. *Earth-Science Reviews* 101(3-4), 190-206.
- Guegan, E.B.M., Sessford, E.G. & Schomacker, A. (submitted): Time-lapse aerial photography reveals significant coastal erosion on Svalbard, Norwegian high Arctic, *Geology*.



- Hüneke, H., M. Joachimski, Buggisch, W. & Lützner, H. 2001: Marine carbonate facies in response to climate and nutrient level: The upper carboniferous and Permian of central Spitsbergen (Svalbard). *Facies* 45(1), 93-135.
- Jakobsson, M., Macnab, R., Mayer, L., Anderson, R., Edwards, M., Hatzky, J., Schenke, H.-W., Johnson, P. 2008: An improved bathymetric portrayal of the Arctic Ocean: Implications for ocean modeling and geological, geophysical and oceanographic analyses. *Geophysical Research Letters* 35, L07602
- Jones, C. L., Higgins, J. D. & Andrew, R. D. 2000: *Colorado rockfall simulation program version 4.0 (for Windows)*. Colorado Department of Transportation, 127.
- Landvik, J., Brook, E.J., Gualtieri, L., Linge, H., Raisbeck, G., Salvigsen, O. & Yiou, F. 2012:  $^{10}\text{Be}$  exposure age constraints on the Late Weichselian ice sheet geometry and dynamics in inter ice-stream areas western Svalbard. *Boreas* in print.
- Landvik, J.Y., Ingólfsson, Ó., Mienert, J., Lehman, S.J., Solheim, A., Elverhøi, A. & Ottesen, D. 2005: Rethinking Late Weichselian ice-sheet dynamics in coastal NW Svalbard. *Boreas* 34, 7-24.
- Lauritzen, Ø., Salvigsen, O., Winsnes, T.S. & Andresen, A., 1989: Geological Map Svalbard 1:100 000, C8G Billefjorden, *Norsk Polarinstitutt Temakart* 5, Oslo.
- Major, H. & Nagy, J. 1972: Geology of the Adventdalen map area. *Norsk Polarinstitutt Skrifter* 138.
- Matsumoto, H. & Ishikawa, M. 2002: Gelifluction within a Solifluction Lobe in the Kärkevagge Valley, Swedish Lapland. *Geografiska Annaler, Series A, Physical Geography* 84 (3/4), 261-266.
- Matsuoka, N. 2001: Solifluction rates, processes and landforms: a global review. *Earth Science Reviews* 55, 107-134.
- Nichols, R.L. 1961: Characteristics of beaches formed in polar climates. *American Journal of Science* 259, 694-708.
- Prestvold, K. 2003: *Isfjorden: A journey through the nature and cultural history of Svalbard*. Governor of Svalbard, Environment Section, Longyearbyen.
- Ritchie, A.M. 1963: *The evaluation of rock fall and its control*. Highway Research Record, National Academy of Sciences – National Research Council, Washington, DC 17, 13-28.
- Rodzík, J. & Zagórski, P. 2009: Shore ice and its influence on development of the shores of southwestern Spitsbergen. *International Journal of Oceanography and Hydrobiology* 38(1), 183-180.
- Salvigsen, O. 1984: Occurrence of pumice on raised beaches and Holocene shoreline displacement in the inner Isfjorden area, Svalbard. *Polar Research* 2(1), 107-113.
- Statens Kartverk 2011: Vannstandsdata, Ny-Ålesund August 14, 2011.  
<http://vannstand.no/index.php/en/english-section/sea-level-data>. 26.10.2012

Sysselmannen På Svalbard 2000: *Fredheim, flytting*. Document number 00133.

Tolgensbakk, J., Sørbel, L. & Høgvard, K. 2000: Adventdalen geomorphological and Quaternary geological map, Svalbard 1:100,000, Spitsbergen sheet C9Q, *Norsk Polarinstitutt Temakart*. 32.

## **Chapter 11 – Holocene reconstruction and spatial analysis of coastal development in Svalbard**

Evangeline G. Sessford<sup>1, 2</sup> and Anne Hormes<sup>2</sup>

<sup>1</sup>Department of Geosciences, the University in Oslo P.O. Box 1072 Blindern, 0316 Oslo

<sup>2</sup>Department of Geology, the University Centre in Svalbard P.O. Box 156, N-9171 Longyearbyen. [EvangelineS@unis.no](mailto:EvangelineS@unis.no) , [Anne.Hormes@unis.no](mailto:Anne.Hormes@unis.no)

### **Abstract**

High geomorphic and climatic variability in Arctic coastlines makes evaluating future coastal erosion in a changing climate a challenge. Predictions must, among other things, incorporate modifications to sediment supply and accommodation space, changes in the permafrost regime, climate variability, including changing air and sea temperatures, precipitation, prevailing wind directions, and sea ice conditions. This study attempts to look back at the Holocene Thermal Maximum (HTM) and use geomorphological processes and climatic development in association with those of modern times as an analogue for future predictions concerning coastal erosion. Uplifted marine terraces hold a wealth of information unlocked through understanding of their elevations, spatial morphology, topography and chronology. Five terraces in Svalbard are assessed and spatial and chronological analysis suggest that the highest terrace, MT5, is pre-LGM and that MT4 and MT3 underwent rapid uplift during the HTM, shortly prior to  $11\,061 \pm 174$  cal BP and became fully terrestrial by 9100 cal BP. Uplift of MT2 and MT1 were completed during the cooling period following HTM with suggested emergence between 7200 and 6800 cal BP for MT2 and 4200 and 3770 cal BP for MT1. A final 2 m uplift of the relict alluvial plain probably happened during the MWP (1200-950 cal BP). Coastal erosion and progradation of the Nøis river delta are modern (1912-2012). Short standstills dominated by erosional processes likely occurred between each uplift event and producing the steep sections between each terrace. Interactions between sea ice, nivation, permafrost and wind and wave regimes are assessed to understand their implications on future coastal development in a warming climate.

### **Keywords**

Holocene, Svalbard, Coastal erosion, shoreline displacement

## Introduction

Coastal erosion in the arctic has recently come into focus for academics and a wider public due to increasing air and ocean temperatures and decreasing sea ice extent (ACIA, 2005). Questions relating to permafrost degradation, increasing erosion rates and impacts on existing and future infrastructure push forward the need to more fully understand the forcing mechanisms behind spatial and temporal changes affecting coastal development (Instanes et al., 2005; Nicholls et al., 2007; Aré et al., 2008; Lantuit and Pollard, 2008; Lantuit et al., 2011; Lantuit et al., 2012). Therefore, Holocene reconstruction relating landform development and climatic forcing with coastal dynamics is of increasing interest. Understanding the evolution of coastal development in connection with climate change, eustatic sea level rise, and isostasy is crucial to construct possible scenarios for arctic coastlines in the future.

According to Lantuit et al. (2012), in an investigation of 61 000 km of unconsolidated Arctic coasts, the present average erosion rate is 0.5 m/yr. Derived from a number of regional rates through the use of small and large scale aerial imagery, the variation is large, ranging from 0 m/yr in Svalbard to 1.15 m/yr in the American Beaufort Sea. It is likely that Svalbard coasts are comparatively stable, but it is doubtful that there is absolutely no change in coastal dynamics at all, but rather that they are complex and undergo high variability as indicated by Guegan et al., (submitted). Svalbard has been chosen for this study in order to try to capture the variations in coastal dynamics as landforms developed through the Holocene while undergoing climatic changes and isostatic uplift from the Last Glacial Maximum (LGM).

A combination of detailed geomorphological mapping of uplifted marine terraces and radiocarbon dating techniques has been used to reconstruct processes acting upon coastal development of shorelines throughout the Holocene. Processes including beach aggradation, coastal erosion, bedrock erosion, ice push and melt out and longshore drift are identified through mapping. Regression rates, erosion and aggradation rates are established through radiocarbon dating, aerial image analysis, and beach ridge morphology. By broadening the observation area, insight into inherent sediment sources is achieved. Incorporation of rates and age restraints has produced a shoreline displacement curve providing relative time constraints on uplift and thereby understanding of climatic influences on coastal processes in the past. Present day coastal processes are used as a key to past shoreline development and when the past processes are seen from the context of the present, it is possible to outline possible future changes.

We were able to not only collect data for the Holocene uplift and shoreline displacement, but also yearlong observations with a time lapse camera and available meteorological data.

Several published marine and lacustrine sediment cores give valuable information of the Holocene temperature reconstruction for Svalbard (Wohlfarth et al., 1995; Velle et al., 2001; Forman et al., 2004; Forwick and Vorren, 2007; and others). Tempelfjorden, in central Spitsbergen, has been studied in depth in regards to past ice dynamics, sediment deposition, timing of events and subsea landforms (Forwick et al., 2010).

## **Study area**

Direct observations and rates have been conducted through fieldwork and aerial image analysis of a single site, Fredheim. The study site is located on the southern coast of Tempelfjorden in central Spitsbergen (Figure 1). The area under investigation includes the present day coastline in connection with five palaeo-coastlines as delineated by uplifted marine terraces. The total area of interest is approximately 0.8km<sup>2</sup> and incorporates a number of influential landforms on coastal development, including a prograding delta, unconsolidated coastal cliff sediments, active layer inter flow of water through relict channels on a pre-recent alluvial plain, spring melt rivers, and large build-up of snow accumulations along the coastline which are often connected to the sea ice foot during winter.

Unlike most other Arctic regions which have a short open water season of 3-4 months (Lantuit et al., 2012), Sassenfjorden and much of western Spitsbergen have a longer season of approximately 5-6 months lasting from July through November and sometimes into December (Norwegian Ice Service, 2012). This is due to the warm Atlantic Waters that flow past the western edge of Svalbard and enter into the fjord systems, causing significant interannual variability in fjord water temperatures and sea ice content (Ådlandsvik and Loeng, 1991; Nilsen et al. 2008). There have even been years, such as was the case in 2011/2012 and 2012/2013 where sea ice was not present at Fredheim at all (Norwegian Ice Service 2012, personal observation). There was however, an ice foot during these years, as well as large snow drifts which built up along the coastal escarpment.

Fjord water circulation in front of Fredheim along the coast appears to be toward the west as seen from aerial images since 1977 (Figure 2). Dominant winter wind directions in Svalbard are from the southeast, though local winds may vary from this and wind data for the region is lacking. Svalbard climate has a high dynamic variability as indicated by the longest meteorological data record from the High Arctic which dates back to 1912. An overall warming trend is seen where the average MAAT measurements at Svalbard Airport rose from -6.7° C to -4.6° C for the periods 1961-1990 and 1981-2010 respectively (Førland et al., 2011).

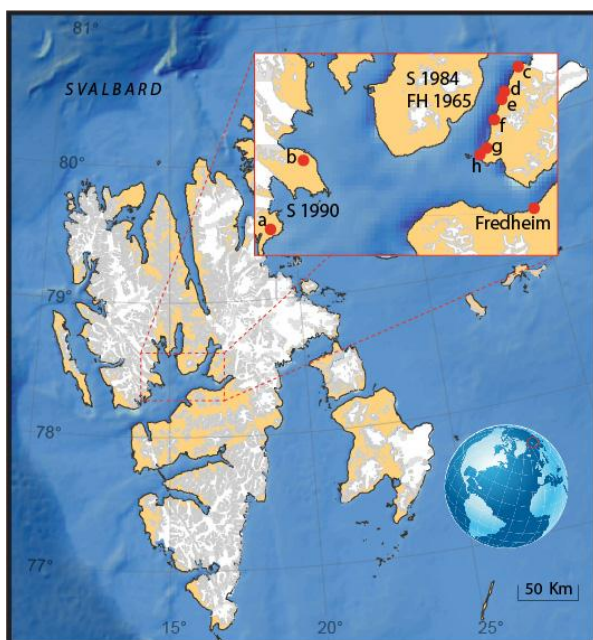


Figure1: Map of Svalbard with an inset of Inner Isfjorden indicating the field site, Fredheim as well as the locations for radiocarbon samples in Salvigsen, (1990) (S1990 a: Erdmannflya, b:Bohemannflya), in western Isfjorden, and , Salvigsen, (1984), and Feyling-Hanssen, (1965), on the eastern coast of Billefjorden, (S 1984) and (FH 1965) at (c:Teltfjellbekken, d: Ekholmvika, e: Kapp Ekholm, f: Phantomvika, g: Mytilusbekken, and h: Gåsodden).

Permafrost in Svalbard is approximately 100 m thick with an active layer thickness varying between 74 and 110 cm (Humlum et al., 2003; Christiansen et al., 2010), in valleys close to sea level, such as is the case in Fredheim. Permafrost temperatures at depth of zero annual amplitude vary between 2.3° and 5.6° C, however, a significant warming in the order of 0.04° - 0.07° C yr<sup>-1</sup> has been observed in Svalbard permafrost (Christiansen et al., 2010). Results from the International Permafrost Association: Third European Conference on Permafrost (EUCOP III) show that Svalbard has the warmest permafrost so far north in the northern hemisphere (Christiansen and Etzelmüller, 2010).

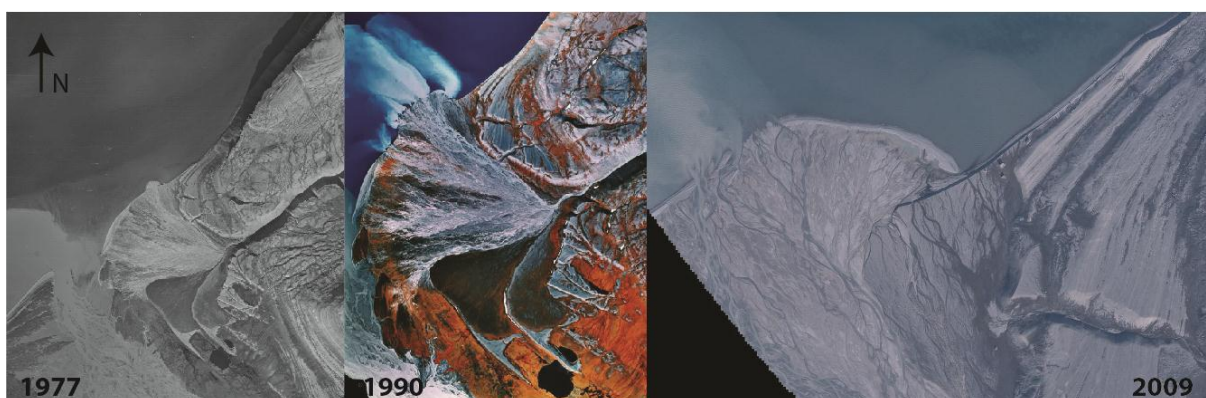


Figure 2: Aerial images of Fredheim from 1977, 1990, and 2009 indicating fjord surface circulation toward the west. Note deltaic growth toward the east. (Images adapted from Norwegian Polar Institute).

## Methods

Relative chronology of landform development at Fredheim has been conducted through spatial investigation. Landforms and sediments have been mapped and identified through field observations in August 2011 and June 2012, and supported by analysis of a 2009 panchromatic orthorectified aerial image (Norwegian Polar Institute). Field work consisted of differential GPS measurements, sediment logging, and observations of geomorphological processes. Leica GeoOffice software was used to post process DGPS points and later combined with the aerial image in ArcGIS to visualize the Quaternary map (Map 1, external disc). Absolute chronology has been established through collection of *Mya truncata* shell halves and fragments found in marine terraces and dated by radiocarbon techniques.

We measured detailed sedimentological logs in the marine terraces MT4 and MT3. Sedimentological descriptions are used to interpret the depositional environments (Nichols, 1999). Mollusk samples were collected 75 cm and 100 cm below the terrace surface (64.25 and 64 m a.s.l., respectively) in MT4. On MT3 mollusk samples were collected at 50 cm and 2.57 m below surface (50.5 and 48.40 m a.s.l.).

Both mollusk fragments and paired shells were identified before chemical preparation following techniques of Feyling-Hanssen, (1965). The radiocarbon analyses were determined with the Uppsala EN-tandem accelerator (Possnert, 1990). Radiocarbon ages are reported in Table 1, as conventional dates with 1 standard deviation and as calibrated ages. In the text all radiocarbon ages are calibrated given as cal BP (before present: 1950 AD). The radiocarbon dates were calibrated to calendar ages using a reservoir age of  $440 \pm 52$  years. This is based on two different recommendations using a marine reservoir effect of  $450 \pm 52$  (Mangerud in Mangerud et al. 2006) and  $438 \pm 52$  years (Bondevik and Gulliksen in Mangerud et al. 2006) for mollusks and foraminifera in Spitsbergen. The calibration is based on the Fairbanks '0107' calibration curve with the online calibration software (<http://radiocarbon.ldeo.columbia.edu/research/radcarbcal.htm>) (Fairbanks et al., 2005) as this curve uses only coral U/Th dates. All terrestrial material was calibrated with Calib 6.0 and INTCAL09 (Reimer et al., 2009).

The shoreline displacement curves are inferred from re-calibrated radiocarbon dates in western Isfjorden (Salvigsen, 1990), and inner Isfjorden (more specifically, the east coast of Billefjorden) (Feyling-Hanssen, 1965; Salvigsen, 1984) in central Spitsbergen (Figure 1 and Table 1). Radiocarbon dates and sedimentological analysis from this study (Map 1 and Figures 3 and 4), in combination with recalibrated dates and published curves produce the shoreline displacement curve for Fredheim (Figure 5).

## Results

### Spatial observations and mapping

The relative chronology of Fredheim is established through mapping of the Holocene landforms and sediments. By analyzing how landforms have developed in relation to each other, the relative order of events is determined. The Quaternary map is the result of field and aerial image investigation. Five uplifted marine terraces have been identified. Pre-recent alluvial fans have been deposited subsequently to beach development and therefore overlying beach ridges on top of each terrace. Hummocky sections of beach are identified as well as beach deformation by ice. Landscape development can be interpreted based on the Quaternary map alongside shoreline displacement and sedimentary logs combined with radiocarbon dates.

Table 1: Radiocarbon ages referred to in the text and used in the inferred shoreline displacement curve.

Reference	Location	Material	ID	m.a.s.l	14C yrs	1 Sigma	cal yrs BP	±
Feyling-Hanssen (1965)	Teltfjellbekken	<i>Mya truncata</i> No.358	Ua-132	56,0	9965	160	11174	130
Feyling-Hanssen (1965)	Phantomvika	<i>Mya truncata</i> No.349	Ua -128	50,7	10105	150	11032	294
Feyling-Hanssen (1965)	Ekholm vika	<i>Astarte</i> No. 350	Ua-124	42,0	9435	200	10117	339
Feyling-Hanssen (1965)	Ekholm vika	<i>Astarte</i>	U-203	9,7	4500	90	4553	204
Feyling-Hanssen (1965)	Mytilusbekken	<i>Mytilus</i> No. 343	Ua-126	5,2	3935	100	3770	196
Salvigsen (1984)	Kapp Ekholm	<i>Larix occidentalis</i> driftwood	unknown	65,0	10030	140	11633	423
Salvigsen (1984)	Gåsodden	<i>Mytilus edulis</i>	T-4628	18,1	6440	80	6841	167
Salvigsen (1990)	Erdmannflya	Shell fragments	T-6287	47,0	10160	110	11113	225
Salvigsen (1990)	Bohemannflya	<i>Hiatella arctica</i>	Lu-2364	20,0	9950	90	10808	235
This study	Fredheim	<i>Mya truncata</i> fragments	Ua-44108	64,3	10106	57	11061	174
This study	Fredheim	<i>Mya truncata</i> fragments	Ua-44107	64,0	9927	60	10767	193
This study	Fredheim	<i>Mya truncata</i> half	Ua-44106	50,5	9867	63	10674	181
This study	Fredheim	<i>Mya truncata</i> fragments	Ua-44105	48,4	9878	64	10690	186
This study	Fredheim	<i>Mya truncata</i> fragments	Ua-44104	48,4	9842	60	10636	170

### Sediment description MT4 (Figure 3)

#### Unit 1

The lowermost unit is a horizontally bedded and imbricated deposit with rounded and subrounded pebbles. It is less sorted than units 3 and 4 and is therefore interpreted as a storm beach.

#### Unit 2

A gradual, undulating boundary separates the storm beach deposit from a 10 cm thick sand layer that changes height over the profile. This sand layer with *Mya truncata* shell fragments represents a sublittoral environment and indicates a sea level rise with a still suppressed site. It contains shell fragments of *Mya truncata* (MT4 shell-1, Ua-44107) and was deposited



between 10960 and 10574 cal BP. This age overlaps with 1 standard deviation with the ages that we yielded from terrace MT3. The other dated shell fragments indicate only a slightly older age of terrace MT4 which was dated to be between 11235 and 10887 cal BP (MT4 shell-2, Ua-44108). These age overlaps can be interpreted to represent rapid isostatic uplift and or reworking of older shell fragments by coastal processes.

#### Unit 3 and 4

The uppermost unit consists of imbricated subrounded and rounded pebbles and represents a littoral environment during uplift of the site. The upper 20 cm of pebbles are frost shattered and carbonate precipitation penetrates to the same depth (Unit 4). We did not observe any carbonate precipitation on MT3 and this observation might be used as an additional argument that terrace MT4 has undergone longer weathering processes than MT3 and must therefore be relatively older.

#### **Sediment description of MT3 (Figure 4)**

##### Unit 1

The lowermost unit 1 of terrace MT3 is very compact, unsorted, massive yellowish silty clay with smaller and bigger clasts. The clasts are subrounded and subangular and one clast showing very clear striations was found. Therefore, this unit is interpreted as a glaciomarine mud. Another indicator for the glacial origin of this unit is a rip-up clast of reddish clay that is incorporated within the diamict.

##### Unit 2

This unit is composed of subrounded/rounded gravel and sand. A bullet shaped boulder was found at the bottom of this deposit that might have been reworked from the underlying glacial till. Half a shell and fragments of *Mya truncata* were found close to the lowermost boundary of the unit (MT3 shell-1, UA-44104; MT3 shell-2, Ua-44105, respectively). The coarse sand and pebbles are horizontally bedded and interpreted as beach deposit. According to the radiocarbon ages the beach deposition started between 10876 and 10466 cal BP (Table 1). The erosive boundary of the beach deposit on top of the diamicton indicates a rather rapid sea level rise at the site parallel to a rapid isostatic uplift causing a littoral environment of the area.

### Unit 3

A gradual boundary separates this medium to coarse sand containing pebbles of local carbonate lithologies and quartzite, from the beach deposit below. We suggest that the gradual boundary can be interpreted as a transgressive phase.

### Unit 4

The beach deposits of Unit 4 are very loose and continued to cover the lower part during logging; therefore, the boundary of Unit 4 to Unit 3 could not be described. The top unit of the logging site shows horizontally bedded, well rounded pebbles and sand. The radiocarbon ages of the *Mya truncata* fragments (MT3 shell5, Ua-44106; 10855 – 10493 cal BP) that were found in this beach deposit overlap with one standard deviation with the beach deposit of Unit 2.

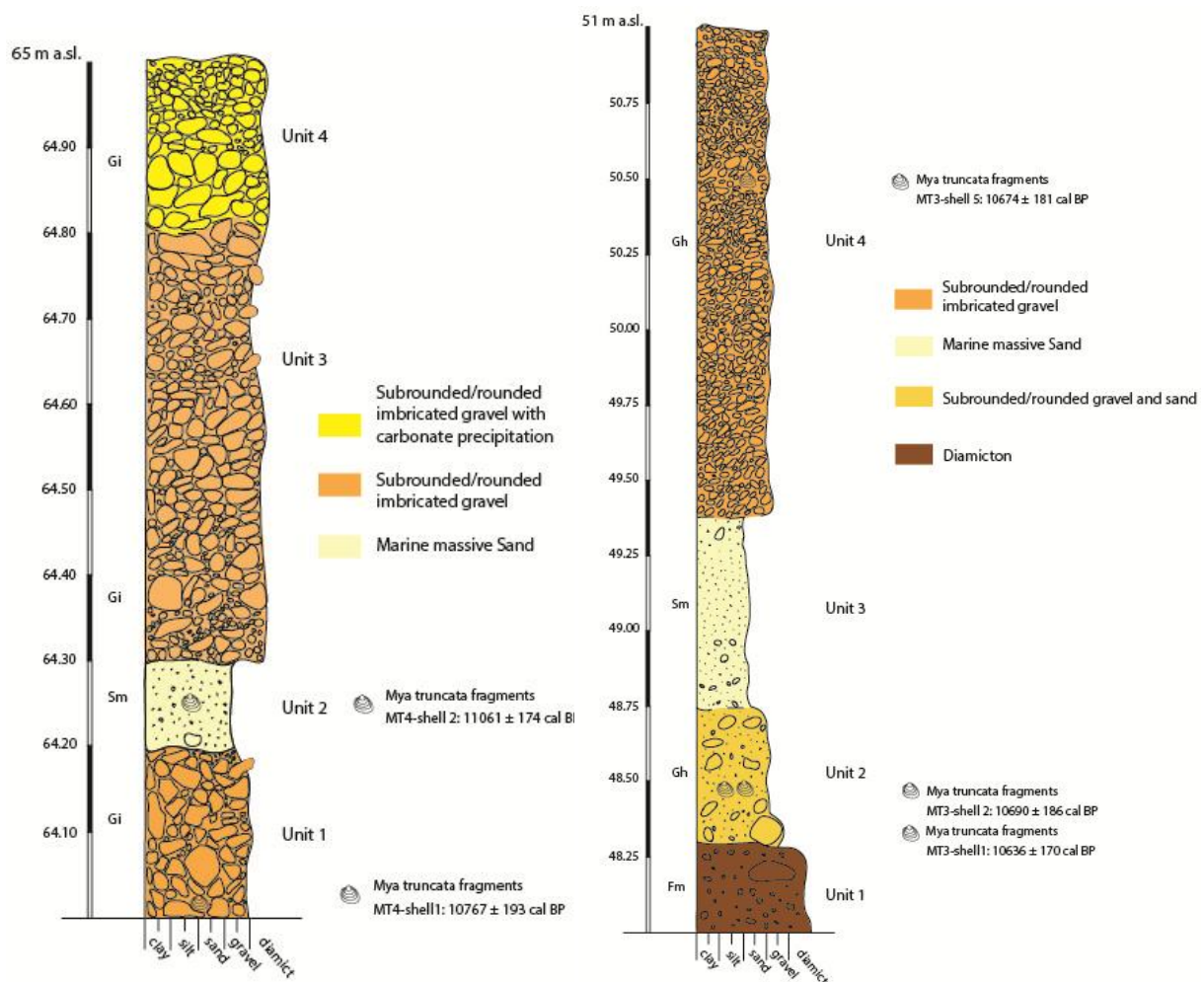


Figure 3 (above left): Sedimentological log of MT4 indicating radiocarbon sample depths and changes in depositional environment.

Figure 4 (above right): Sedimentological log of MT3 with radiocarbon sample depths and indications of a transgression between Unit 1 and Unit 2.

## Shoreline Displacement

Results from sedimentological descriptions and radiocarbon dates produce the shoreline displacement curve for Fredheim shown in Figure 5. Uplift onset of MT4, began by  $11\,061 \pm 174$  cal BP as indicated by radiocarbon ages, and final uplift of MT1 was completed by 3770 cal BP as suggested by radiocarbon ages and curves from Feyling-Hanssen, (1965), and Salvigsen, (1984). A small transgression is interpreted during uplift of MT3 as indicated by the gradual boundary between units 2 and 3.

## Discussion

### Interpretation of landform development

Relative chronology and interpretation will begin with the oldest landforms and events and end with the most recent known event. Deglaciation of Sassendalen began approximately 11 300/11

200 cal BP (Forwick et al. 2010) and glacier retreat was enough to allow marine flooding over all of Fredheim by  $11\,061 \pm 174$  cal BP, as delineated by the oldest date recovered from MT4. MT5 however, remains higher than early Holocene maximum flooding surface (local marine limit) of Inner Isfjorden according to Salvigsen (1984), and appears undisturbed by glaciation as clear beach ridges can be seen on its surface. It is therefore suggested that MT5 is older than LGM. It is well known in Svalbard that many marine terraces situated in inter-ice-stream areas and or beneath cold based ice have been preserved having little to no surface disturbances (Forman and Miller 1984, Landvik et al. 2005). Feyling-Hanssen (1965) discussed an 84.5m terrace in inner Isfjorden which produced an age of  $24\,945 \pm 734$  cal BP from radiocarbon dating on *Mya truncata* and *Hiattella arctica* fragments. However, this is interpreted to have been contaminated and likely represents a minimum age. As MT5 lies above MT4 between 70 and 80m a.s.l. it seems highly probably that this is also the case at Fredheim.

Upper MT4 uplifted sometime prior to lower MT4 where *Mya truncata* fragments were sampled at 64 and 64.25 m a.s.l. and returned ages of  $11\,061 \pm 174$  cal BP and  $10\,767 \pm 193$  cal BP respectively. The glacial diamicton present below samples on MT3 and noted in

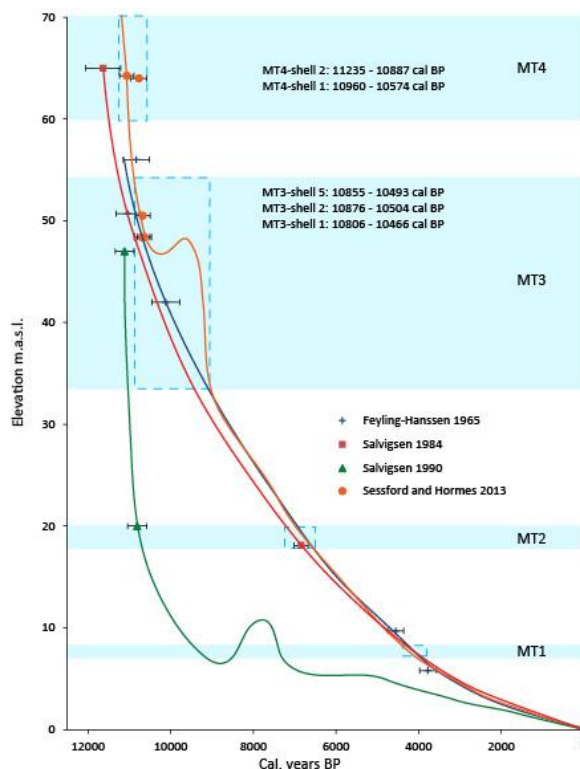


Figure 5: Inferred shoreline displacement curves as indicated by recalibrated radiocarbon dates from Feyling-Hanssen, (1965), Salvigsen, (1984), and Salvigsen, (1990). Results from this study, for Fredheim, are shown in relation to the others. The blue dashed boxes indicated the time frame elevation change used in emergence rate calculations. The transgression noted in the Sessford and Hormes curve is indicated by the sedimentological observations on MT3

Figure 4, where striated boulders, rip up clay, and bullet shaped clasts are present, suggests glacial proximal flooding and transgressional period. The lack of fines between the glacial diamicton and littoral deposits suggests that deep water was not present for long. MT3 emerged quite rapidly as is noted by the erosional boundary between the glacial diamicton and beach sediments, and lack of fines. Radiocarbon ages for MT3 suggest beach deposition started shortly prior to 10636 and  $10690 \pm 186$  cal BP (Table 1).

Subsequent terraces MT2 and MT1 have not been dated as no material suitable for dating was found during fieldwork, however as their elevations are similar to those of Feyling-Hanssen (1965) and Salvigsen (1984) it is assumed that uplift of marine terraces was completed by 3574 cal BP (bound by the youngest date from Feyling Hanssen, 1965) and that there was a standstill in uplift after MT3 became terrestrial. MT2 and MT1 likely uplifted sometime between 7200 and 3574 cal BP. Between 3200 cal BP and during the Medieval Warm Period (MWP), when shorelines were approximately 2 m higher than at present (Salvigsen, 1984), a large alluvial plain formed (Map 1). A final period of uplift of the pre-recent alluvial plain, on which the buildings at Fredheim have been built, likely occurred sometime during the MWP between 1200 and 950 cal BP, as indicated by the shoreline displacement curve by Salvigsen, (1984).

Since uplift of the pre-recent alluvial plain, both erosion and aggradation have been taking place at the coast. Aerial images show that between 1977 and 2009, the average rate of erosion has been 0.33 m/yr (Guegan et al., submitted). However, Guegan et al. (submitted) acknowledge that erosion rates have decreased from 0.4 m/yr (1977-1995) to 0.23 m/yr (1995-2009) due to the growth of the modern delta which has had an average growth rate of 3.6 m/yr since 1977. Average delta growth rate has remained stable over the study time period; however, a major shift in growth direction from north to east occurred in the mid-90s, thereby influencing the rate of erosion on the coastal escarpment at Fredheim (Figure 2).

Each of the marine terraces has alluvial fans overriding beach ridges suggesting deposition took place after uplift (Map 1, at Nordbekken). It is difficult to ascertain the time difference between uplift and deposition. It is possible that “Nordbekken” (unofficial name) was present during uplift and that changes in base level occurred relatively soon after uplift as down cutting through the unconsolidated beach and diamicton would not have been difficult. In May 2012, each of the fens (marked in brown as organic material in Map 1) was drilled in the attempt to date onset of biological growth. As each of the fens is located on a different terrace, the hope was to provide time constraints for when marine terraces became terrestrial and vegetation growth was possible. This, alongside the radiocarbon ages would then have

provided a clearer picture of uplift rate and development of alluvial fans. However, all dates were returned as modern.



Figure 6: Hummocky beach on MT3, note the rounded boulders from mechanical weathering through wave action, and holes from chemical weathering (Sessford, June 2012).



Figure 7: Modern beach reach as delineated by the solid line, and hummocks outlined by the dashed line (Sessford, June, 2012).

Palaeo beaches as shown by the uplifted marine terraces were deposited relatively rapidly, sedimentation was dominated by sand and pebbles and wave action through longshore drift was eminent. The beach ridges and pitted beaches show a distinct difference in accommodation space availability and/or processes acting upon beach material. In the north on MT3, toward the bedrock exposures and higher slope gradients there is no space for beach ridges to form; instead they spread out toward the south where space is available. Hummocks and pits are instead present closer to the exposed bedrock which has been affected by chemical and mechanical

weathering by water, though subsequently affected by periglacial and Aeolian processes (Figure 6). When observing the present day beach, hummocks and pits appear where the ice foot sits during the winter (Figure 7). Hummocks on MT2 and MT1 vary from those on MT3 and the present day beach by having a different morphological character in that many have higher ridges up-slope, have a curved backscarp and tend to run parallel to the shore (Figure 8). Pits on these terraces tend to be behind the ridges (upslope) and are elongated along the palaeo shore. A similar landform to the hummocks on MT2 and MT1 is found on the modern shore where an ice floe had been pushed up on shore during an extreme event in 1999 (Figure 9).





Figure 8 (left): Ice thrust ridge on MT3 during deposition of MT2 and cooler times within the Holocene (Sessford, June 2012).

Figure 9 (right): Modern ice thrust ridge (marked as deformation by ice in Map 1) (Sessford, June, 2012).

## Uplift and climate

It has long been acknowledged that uplifted marine terraces, (also known as raised beaches) are of primary importance in regards to glacial reconstruction and are considered isostatic fingerprints of past ice volume expansions (Birkenmajer, 1960; Feyling-Hanssen, 1965; Boulton, 1979; Forman and Miller, 1984; Salvigsen, 1984; Landvik et al., 1987; Salvigsen et al., 1990; Landvik et al., 1992; Ziaja and Salvigsen, 1995; Salvigsen et al., 2005; Ingolfsson, 2011; Long et al., 2012; Ingolfsson and Landvik, 2013). Here, we use the displacement of marine terraces, their sedimentologic architecture and their geomorphology to reconstruct further processes acting upon the former coastline of Fredheim.

Vertical shoreline displacement combined with radiocarbon dating of whale bones, shells and driftwood can be used for reconstruction of the timing of deglaciation, the rate of isostatic uplift and for spatial and temporal comparison between shorelines (Ziaja and Salvigsen 1995). The Holocene shoreline displacement curves shown in Figure 5, are inferred through recalibrated dates from Salvigsen, (1984), Salvigsen, (1990), and Feyling-Hanssen (1965). Combined, the curves give inner Isfjorden a displacement from 65 m a.s.l. to 5.8 m a.s.l. between 11,633 and 3770 cal BP suggesting an isostatic rebound of 55.3 m during the early and mid-Holocene (Feyling-Hanssen, 1965; Salvigsen, 1984). The inferred emergence as suggested by Salvigsen, (1990), is presented to indicate differences in emergence isobases as indicated by Ingolfsson and Landvik (2013). Dates retrieved from this study have been used alongside sedimentary analysis to indicate inferred emergence at Fredheim. Onset of emergence is suggested to have begun by 11235 cal BP as indicated by the standard error of the highest/oldest recovered date. This coincides well with Forwick et al., (2010) who propose that Sassenfjorden was ice free by 11 300/11 200 cal BP.

The surface topography of marine terraces i.e. beach ridge amplitude and wavelength, and shore gradient, serve as indicators of processes acting upon the shoreline during emergence and thereby record vertical and horizontal movement of the shoreline. Due to isostatic uplift the resulting beach plains will slope so that forelands prograde and older beach ridges will be more elevated than those that are younger (Feyling-Hanssen 1965). The slope gradient therefore depends upon the rate of emergence and progradation of the shoreline, resulting in rapid ( $\sim >100$  cm/century scale) or slow ( $\sim 10 - 100$  cm/century scale) displacement (inferred from Feyling-Hanssen and Olsson 1960). At Fredheim, MT4 displays the most rapid uplift as inferred by the distance between the highest and lowest elevations of each terrace in combination with age constraints in Figure 5, showing progradation of approximately 151 cm/century between 11 235 and 10 574 cal BP. MT3 suggests an emergence rate of 114 cm/century (between 10 855 and 9100 cal BP. In comparison MT1 and MT2 appear to have undergone much slower progradation of only 50 cm/century between 7200 and 6800 cal BP, and 23 cm/century between 4200 and 3770 cal BP, respectively. Emergence rates are supported by those of Salvigsen, (1984) where average uplift rate between 10 000 and 8000 cal BP is 190 cm/century and slowed down to 45 cm/century between 8000 and 4000 cal BP. Uplift rates coincide with deglaciation observations by Forwick et al., (2010) which suggest step wise retreat of the Sassendalen glacier, where glacial proximal conditions were present during the mid-Holocene and isostatic rebound would have been less substantial. It is likely that rebound also occurred in a step wise fashion as indicated by the steep slopes between each terrace which may indicate periods of erosion. Forwick et al., (2010) propose that general glacier growth in the area occurred between 4 and 5 cal ka BP which coincides well with decrease in uplift rate of MT1. To further access the climatic time frame of uplift, the processes associated with beach formation should be reviewed. One can associate changes in climatic forcing with the development of the shoreline by observing changes in beach ridge formation, hummocky/pitted areas and extent of bedrock chemically and mechanically weathered by waves. This is a branch of study which has only briefly been touched upon (Møller et al., 2002; Nichol, 2002).

### **Geomorphic processes and climate**

Site specific factors such as exposure, wind direction, fjord circulation, coastal plain gradient and sediment supply affect the formation of beach building and erosion processes (Møller et al., 2002). Beach ridges are formed along the top of the forelands due to dominant longshore beach drift, often producing storm ridges (Feyling-Hanssen 1965) or fair weather berm ridges (Mason, 2010). A fair weather beach might be characterized by low amplitude ( $<0.5$ m) beach crests with wavelengths of approximately 5m and are flat crested (Mason, 2010; Long et al. 2012). Møller et al., (2002) identifies ridges having a steep seaward scarp and a marked

landward swale to be indicative of erosional stormy events in comparison to a gentle seaward slope associated with fair weather. Although beach ridges were not measured directly at Fredheim, one can see in Figure 10, from MT3 that beach ridges are relatively flat crested, have approximate amplitude of 30-50 cm and wavelengths approximately 5-6 m. The same trend is exemplified on MT4 and MT1. Ridges on MT2 are however, difficult to



Figure 10: Fair weather beach ridges on MT3. The Black backpack dimensions are approximately 60 by 20 cm (Sessford, June 2012).

assess due to periglacial processes of gelifluction and active layer detachment sliding.

Modern surface water circulation in front of Fredheim is along the coast toward the west as indicated by aerial images since 1977. However, the delta is prograding eastward and wave generated beach ridges grow

parallel with progradation. Wave activity at Fredheim is virtually limited to local wind waves as fetch distance is minimal due to its location with the fjord system and the now present Nøis delta protecting the shoreline. However, this is not the case when winds are from the northeast through Tempelfjorden where fetch distance is in the order of 14 km. Nonetheless, by broadening the observation area, insight into dominant wind direction during the Holocene is toward the southeast and beach ridges formed from sediment supplied from deltaic systems coming from Nøisdalen (Figure 2 and Map 1). Similar processes are described in Mason, (2010). Ridges infer a long term easterly direction of littoral sediment transport. The main variation in wind direction appears to have occurred after development of upper MT4 where beach ridges had formed in an east-west trend, and switched to a north-south trend for the remainder of the Holocene. Modern beach ridges to the west of Fredheim and at the western edge of the Nøis delta follow this pattern, and it is only directly in front of Fredheim that local winds seems to have the most impact on beach development.

Beach ridges in Arctic environments are often disrupted as hummocks/pits (Nichols, 1961; Urdea, 2007; Hilaire-Gravel et al., 2010). There appears to be three different processes forming hummocks at Fredheim; ice melt out (ice foot, sea ice, permafrost, buried glacier ice, icebergs), build up of sediments around boulders, ice thrust deformation ridges and swales. Hummocks forming on the modern beach are found where the ice foot sits during the winter suggesting that as the ice is present sediment is deposited around the ice pieces and when melt out occurs hummocks are left from the spaces between ice where sediment has been lodged, and pits where the ice has melted away (Nichols, 1961; Urdea, 2007; Rodzik and



Zagórski, 2009; Hilaire-Gravel et al., 2010). However, as MT3 was developed during the HTM it seems unlikely that sea ice would be present due to higher sea surface and air temperatures (Miller et al., 2010) suggesting that the hummocks are likely a result of lack of accommodation space or that this area as suggested by the bedrock boulders was likely undergoing erosion, rather than aggradation. It is also possible that the hummocks are created because of large boulders falling onto the shoreline through erosion of the bedrock. Sediments would then not build smoothly as ridges, but around the boulders in hummocks. Similar processes are present in the east on the modern coastline. However, on MT2 and MT1 where accommodation space is not lacking and large boulders are not present, there are also hummocky and pitted beach areas. An increase in ice rafted debris in the area at 7930 cal BP is attributed to enhanced sea ice formation (Baeten et al., 2010). Therefore, it is possible that these hummocks have more to do with ice. These hummocks have a slightly different morphological character in that many have higher ridges up-slope, have a curved backscarp and tend to run parallel to the shore (Figure 8). These terraces were likely a product of uplift during cooler times prior to or during Neoglaciation and it is possible that they formed from ice berg ride up or pushing due to strong winds (Møller et al., 2002; Urdea, 2007). They are also found just on the steep erosional edge of MT3 suggesting that during the formation of MT2 beach ice was thrust all the way up the escarpment onto MT3. A modern example of ice ride up can be seen (Figure 9) where an ice floe had been pushed up on shore, over the modern beach and disrupting sediments on MT1 during an extreme event in 1999. It is unclear whether this was caused by ice ride up, thrusting or by high winds during a major storm event.

### **Modern processes**

Studies suggest that the Arctic has undergone a decline of temperatures throughout the last 2000 years but is now entering into a warmer phase which may imitate climatic periods throughout the Holocene (Divine et al., 2011; D' Andrea et al., 2012). Development of Holocene beaches and the present day beach have very similar features. During the Early Holocene and the HTM, accommodation space was not lacking. The retreat of LGM glaciers left space and sediments for re-working. Since the LIA the erosion of the area in front of Fredheim has also provided space for accumulation of sediments and the progradation of the Nøis River delta (Guegan et al., submitted). Increased warming on Svalbard has produced more sediment transported through the river systems to be deposited at the coastline. However, temperatures are not presently as warm as during the HTM, but more similar to that of the cooling period prior to Neoglaciation, where cooler temperatures favoured sea ice formation and strong winds (Baeten et al., 2010; Müller et al., 2012). This can be seen through the parallel formation of both beach ridges and hummocky areas due to longshore

drift, sea ice thrust on shore, and the presence of the ice foot. As development of the modern delta has progressed, coastal erosion rates have been decreasing and the majority of erosion has taken place where pre-recent fluvial channels are located and large snow drifts accumulate along the escarpment (Guegan et al., submitted). It seems likely that pro-nival fluvial erosion has increased since the LIA (Christiansen 1998). The return of modern ages from the fens situated on the terraces is an indicator of this. If larger snow drifts are able to accumulate due to higher precipitation and favourable wind conditions, it is likely that aeolian material is also being transported and deposited in the same locations. The combination of excess fines and more water from snow drifts provides suitable conditions for plant growth that may not have been possible in warmer times during the HTM. Larger snow drifts on the coast will also affect the temperature regime of coastal permafrost by insulating the sediments. The timing and duration of snow cover critically affects the surface conditions associated with the ground surface energy balance and thereby affects the intensity of freeze thaw action within the active layer (Ling and Zhang 2003). Delaying snow cover onset in the autumn results in a decrease in ground temperature and advancing the snow cover disappearance in spring leads to increased ground temperatures (Ling and Zhang 2003). This in turn causes increased freeze thaw action thereby loosening cliff sediments to be easily washed away through nival waters.

Investigations into permafrost growth and active layer development are lacking. It was thought that active layer detachment slides may be of interest to review changes in active layer thickness. If one could date the time of detachment, say through burial dating using cosmogenic nuclide techniques the active layer thickness could be determined and thereby give a proxy for permafrost development in Svalbard at low lying, coastal regions. It has been suggested that permafrost on Svalbard disappeared at low lying elevations during the LGM and that the onset of permafrost growth is to have begun between 2900-2650 cal BP (Jeppesen, 2001; Humlum et al., 2003). If such is the case, then active layer detachments could not have been released during the HTM. Instead, they should indicate more recent ages, and be associated with extreme events occurring after Neoglaciation and possibly during the MWP.

### **Future predictions on coastal processes**

Understanding the evolution of coastal development in connection with climate change, eustatic sea level rise, and isostasy is crucial to construct possible scenarios for arctic coastlines in the future (from intro)

Open water proxies suggest that the HTM coalesced with increased mass of warm Atlantic and Pacific water moving northward (Miller et al., 2010). This, along with increased summer

insolation, decreased perennial sea-ice cover and the northward advance of the Polar front were major contributing factors to rise in sea surface temperatures (Hald et al., 2004; Jessen et al., 2010; Miller et al., 2010; Berner et al., 2011). Miller et al., 2010, (p. 1703), suggest that, "quantitative estimates of HTM summer temperature anomalies around Svalbard range from 1 to 3° Celsius... and sea-surface temperatures were as much as 4-5 ° Celsius". Bednorz, (2011), describes a 1.65° Celsius increase in mean winter temperature per decade since 1975/1976 and that negative extremes are becoming less frequent. Such negative extremes are generally associated with high sea ice concentrations in mid-late winter; something which Sassenfjorden have not seen in recent years. On the other hand, positive extremes are increasing, though not yet at a significant rate, and tend to coincide with low pressure troughs over the Fram Strait, bringing warm air masses from the south (Bednorz, 2011). It seems, therefore that Svalbard is consistently showing signs of warming.

Future development of Arctic coastlines is reliant on temporal changes. It is understood that climate change and sea-level rise from increase in freshwater contribution to the oceans, thermal expansion of the water, subsidence and land loss will affect sediment entrainment, transport and deposition in complex ways (Nicholls et al., 2007). As beach aggradation is dependent on sediment availability and accommodation space, acceleration in the rate of sea level rise may mean that the coastal morphology cannot keep up and coastline retreat will be imminent (Nicholls et al., 2007; Forbes et al., 2011). Higher sea level will increase erosion of coasts, leading to rapid retreat underlined by thawing permafrost, melting of ground ice, subsidence due to loss of ice, and warmer ground temperatures (Nicholls et al., 2007; Lantuit et al., 2012). Thawing permafrost is a major factor, as is increased snow accumulation at the coast. Increases in snow cover will warm the ground, insulating it over the winter and thereby increasing active layer depths. It is also apparent at Fredheim that sediment from inland is actually becoming more abundant and a delta is able to grow where recently erosion was dominant. This may be a saving factor for the Fredheim coastline, if sediment availability produces natural barriers limiting coastal erosion due to sea ice and wave action (Ruz et al., 1992; Nichol, 2002). However, it is difficult to assess the full extent of the influence that sea ice has on coastlines.

One of the major changes in the arctic will be decrease and even loss of sea ice. But, as Ogorodov et al., (2010) has pointed out, "warming events have not always led to an increase in wave energy or to acceleration of coastal erosion". This is apparent at Fredheim both during the HTM and at present. The open water season is quite long (5-6 months) and some years there is no sea ice at all. Yet, since 1995 coastal erosion rates have decreased. Evidently, decrease in sea ice and increased air temperatures do not necessarily suggest increased wind-wave activity. The acceleration of coastal erosion likely needs a combination

of thermo-erosion, and wave-energy factors (Ogorodov et al., 2010, Lantuit et al., 2012). It is likely that increasing open water durations will increase the frequency of storm events in the arctic (Forbes et al., 2011). In Svalbard the dominant winter wind direction is from the SSE to the NNW (Humlum, 2002) and therefore not in favour of large waves breaking on the shore at Fredheim during the winter when there is a lack of sea ice. As all of the beach ridges at Fredheim are considered fair weather beaches, it can be assumed that large storms are likely occurring during the winter when the sea ice foot is able to protect the coast from wave action, as no storm beaches are observed. On that note, detailed investigations regarding predominant wind directions elsewhere than where main settlements are located are lacking. However, it is possible that dominant wind directions and fjord circulation patterns will alter due to changes in atmospheric circulation and warming sea temperatures. It is in any case clear that major changes in arctic coastlines are dependent upon climatic forcing and temporal changes.

More detailed examination of beach ridge amplitude and wavelength will give better insight into the physiographic conditions present at the time of deposition. This includes conditions suitable for sea ice formation, frequent storm events, and shifts in frequency and intensity of the wind regime. Better age constraint of marine terraces and thereby shoreline development may be achieved through lake cores obtained from the small lakes located just south of Fredheim. It would be of interest to use cores as analogues for uplift both through sedimentation rates and macrofossil/microfossil dating. Cores would give a better understanding of uplift rates as well as insight into temperatures associated with time of deposition.

## **Conclusion**

Spatial and chronological analysis suggests that MT5 is pre-LGM and MT4 and MT3 underwent rapid uplift during the HTM starting shortly prior to 11 061 cal BP and becoming fully terrestrial by 9100 cal BP. Uplift of MT2 and MT1 were completed during the cooling period following HTM and maybe into Neoglaciation with suggested emergence between 7200 and 6800 cal BP for MT2 and 4200 and 3770 cal BP for MT1. The last uplift of the relict alluvial plain probably happened during the MWP (1200-950 cal BP). Present coastal erosion and progradation of the Nøis river delta are modern (1912-2012).

Uplift likely occurred in a stepwise fashion, following the same pattern as glacier retreat. Therefore, standstills likely occurred between each uplift event thereby producing the steep slopes on the edge of each terrace.

The uplifted marine terraces are interpreted as having formed during predominantly calm periods where sediment accumulation was rapid. The steep slopes dividing each major uplift event are thought to represent short-lived periods of beach erosion, due to step-like glacier retreat and which have more recently undergone periglacial processes (gelifluction and active layer detachment sliding). However, further studies are needed to assess these erosional periods in greater detail.

Hummocky and pitted beach sections on MT3 are interpreted to have been developed due to lack of accommodation space and the presence of boulders disrupting clear beach formation. However, on MT2 and MT1 these sections may have been more influenced by ice-push as they were deposited during cooler times and are predominantly in areas where accommodation space was not lacking.

Due to the recent erosional period during modern times present accommodation space has been created. Now as Svalbard is entering a warm period, growth rate of the Nøis river delta has increased, replicating the same processes that have been exhibited throughout the Holocene. It shows both beach ridge accumulation as well as hummocky/pitted areas where sea ice has been thrust on land by wind.

## **Acknowledgments**

Sincere thanks are expressed toward Henrik Rasmussen for guidance in shoreline displacement analysis, figures, and assistance in editorial work. Thanks are also directed toward Bernd Etzelmüller for assistance in structuring the manuscript.

## References

- ACIA, 2005. Arctic Climate Impact Assessment., Cambridge, U.K., p. 1042.
- Ådlandsvik B and Loeng H, (1991) A study of the climatic system in the Barents Sea. *Polar Research* 10, 45-59.
- Are F, Reimnitz E, Grigoriev M, Hubberten HW and Rachold V, (2008) The Influence of Cryogenic Processes on the Erosional Arctic Shoreface. *Journal of Coastal Research* 24, 1: 110-121.
- Baeten NL, Forwick M, Vogt C and Vorren TO, (2010) Late Weichselian and Holocene sedimentary environments and ice rafting in Isfjorden, Spitsbergen. *Geological Society of London, Special Publications* 344, 207-223.
- Bednorz E, (2011) Occurrence of winter air temperature extremes in Central Spitsbergen. *Theoretical and Applied Climatology* 106, 3: 547-556.
- Berner KS, Koç N, Godtliobsen F and Divine D, (2011) Holocene climate variability of the Norwegian Atlantic Current during high and low solar insolation forcing. *Paleoceanography* 26, 2: PA2220.
- Birkenmajer K. (1960) Raised marine features of the Hornsund area, Vestspitsbergen. *Studia Geologia Polon.*, 5: 1—95.
- Christiansen HH, (1998) 'Little Ice Age' nivation activity in northeast Greenland. *The Holocene* 8, 6: 719-728.
- Christiansen HH and Etzelmüller B, (2010) Report from the international permafrost association: Third european conference on permafrost (EUCOP III) in Longyearbyen, Svalbard. *Permafrost and Periglacial Processes* 21, 4: 366-369.
- Christiansen HH, Etzelmüller B, Isaksen K, et al., (2010) The thermal state of permafrost in the nordic area during the international polar year 2007–2009. *Permafrost and Periglacial Processes* 21, 2: 156-181.
- Fairbanks, R.G., Mortlock, R.A., Chiu, T.-C., Cao, L., Kaplan, A., Guilderson, T.P., Fairbanks, T.W., Bloom, A.L., 2005. Marine Radiocarbon Calibration Curve Spanning 0 to 50,000 Years B.P. Based on Paired <sup>230</sup>Th/<sup>234</sup>U/<sup>238</sup>U and <sup>14</sup>C Dates on Pristine Corals. *Quaternary Science Reviews* 24.
- Feyling-Hanssen RW and Olsson I, (1960) Five radiocarbon datings of post glacial shorelines in central Spitsbergen. *Norsk Geografisk Tidsskrift* 86, 121-131.
- Feyling-Hanssen RW, (1965) Shoreline displacement in central Vestspitsbergen and a marine section from the Holocene of Talavere on Barentsøya in Spitsbergen. *Norsk Polarinstitutt Skrifter* 93, 1-5.
- Finseth, J., Sessford, E.G., Hormes, A. 2012: Erosjonssikring av Fredheim;visualiseringsprosjekt; Evaluering av erosjonssikring av Fredheim. SvalbardsMiljøvernfond, SINTEF Byggforsk, Infrastruktur, SBF2012A0334, 43.
- Forbes, D.L. (editor). (2011) State of the Arctic Coast 2010 – Scientific Review and Outlook. International Arctic Science Committee, Land-Ocean Interactions in the Coastal Zone, Arctic Monitoring and Assessment Programme, International Permafrost Association. Helmholtz-Zentrum, Geesthacht, Germany, 178 p. <http://arcticcoasts.org>

- Forman SL and Miller GH, (1984) Time-Dependent Soil Morphologies and Pedogenic Processes on Raised Beaches, Brøggerhalvöya, Spitsbergen, Svalbard Archipelago. *Arctic and Alpine Research* 16, 4: 381-394.
- Forman SL, Lubinski DJ, Ingólfsson Ó, et al., (2004) A review of postglacial emergence on Svalbard, Franz Josef Land and Novaya Zemlya, northern Eurasia. *Quaternary Science Reviews* 23, 11-13: 1391-1434.
- Forwick M and Vorren TO, (2007) Holocene mass-transport activity and climate in outer Isfjorden, Spitsbergen: marine and subsurface evidence. *The Holocene* 17, 6: 707-716.
- Forwick M, Vorren TO, Hald M, et al., (2010) Spatial and temporal influence of glaciers and rivers on the sedimentary environment in Sassenfjorden and Tempelfjorden, Spitsbergen. *Geological Society of London, special publications* 344, 163-193.
- Førland EJ, Benestad R, Hanssen-Bauer I, Haugen JE and Skaugen TE, (2011) Temperature and precipitation development at Svalbard 1900-2100. *Advances in Meteorology* 2011, Article ID 893790: 1-14.
- Guegan EBM, Sessford EG, and Schomacker A. (submitted) Time-lapse aerial photography reveals significant coastal erosion on Svalbard, Norwegian high Arctic, *Geology*.
- Hald M, Ebbesen H, Forwick M, et al., (2004) Holocene paleoceanography and glacial history of the West Spitsbergen area, Euro-Arctic margin. *Quaternary Science Reviews* 23, 20-22: 2075-2088.
- Hilaire-Gravel D, Bell TJ and Forbes DL, (2010) Raised gravel beaches as proxy indicators of past sea-ice and wave conditions, Lowther Island, Canadian archipelago. *Arctic* 63, 2: 213-226.
- Humlum O, (2002) Modelling late 20th-century precipitation in Nordenskiöld Land, Svalbard, by geomorphic means. *Norsk Geografisk Tidsskrift* 56, 96-103.
- Humlum O, Instanes A and Sollid JL, (2003) Permafrost in Svalbard: a review of research history, climatic background and engineering challenges. *Polar Research* 22, 2: 191-215.
- Humlum O. (2005) Holocene permafrost aggradation in Svalbard. *Geological Society London, Special Publications* 242: 119-129.
- Ingólfsson Ó, (2011) Fingerprints of Quaternary glaciations on Svalbard. *Geological Society, Special Publications* 354, 15-3
- Ingólfsson Ó and Landvik JY, (2013) The Svalbard-Barents Sea ice-sheet - historical, current and future perspectives. *Quaternary Science Reviews* 64, 33-60.
- Instanes, A., Anisimov, O., Brigham, L., Goering, D., Khrustalev, L.N., Ladanyi, B. and Larsen, J.O., 2005. Chapter 16: Infrastructure: Buildings, support systems, and Industrial facilities. *Arctic Climate Impact Assessment*.
- Jeppesen, J. W. (2001). Ice wedges and host sediments as palaeoclimatic indicators in central Spitsbergen, Svalbard. MSc thesis, The University Centre on Svalbard.
- Jessen SP, Rasmussen TL, Nielsen T and Solheim A, (2010) A new Late Weichselian and Holocene marine chronology for the western Svalbard slope 30,000-0. cal years BP. *Quaternary Science Reviews* 29, 1301-1312.



- Landvik JY, Ingólfsson Ó, Mienert J, et al., (2005) Rethinking Late Weichselian ice-sheet dynamics in coastal NW Svalbard. *Boreas* 34, 7-24.
- Lantuit H and Pollard WH, (2008) Fifty years of coastal erosion and retrogressive thaw slump activity on Herschel Island, southern Beaufort Sea, Yukon Territory, Canada. *Geomorphology*, 95(1/2): 84–102.
- Lantuit H, Atkinson DE, Overduin PP, et al., (2011) Coastal erosion dynamics on the permafrost-dominated Bykovsky Peninsula, north Siberia, 1951-2006. *Polar Research* 30, 7341: 1-21.
- Lantuit H, Overduin PP, Couture N, et al., (2012) The Arctic Coastal Dynamics database. A new classification scheme and statistics on arctic permafrost coastlines, *Estuaries and Coasts* 35, 2: 383-400.
- Ling F and Zhang T, (2003) Impact of the timing and duration of seasonal snow cover on the active layer and permafrost in the Alaskan Arctic. *Permafrost and Periglacial Processes* 14, 2: 141-150.
- Long AJ, Strzelecki MC, Lloyd JM and Bryant CL, (2012) Dating high Arctic Holocene relative sea level changes using juvenile articulated marine shells in raised beaches. *Quaternary Science Reviews* 48, 61-66.
- Mangerud J, Bondevik S, Gulliksen S, Hufthammer KA, Hoisaeter T, (2006) Marine <sup>14</sup>C reservoir ages for 19th century whales and molluscs from the North Atlantic. *Quaternary Science Reviews* 25, 3228-3245.
- Miller GH, Brigham-Grette J, Alley RB, et al., (2010) Temperature and precipitation history of the Arctic. *Quaternary Science Reviews* 29, 15-16: 1679-1715.
- Møller JJ, Yevzerov VY, Kolka VV, and Corner GD, (2002) Holocene raised-beach ridges and sea-ice-pushed boulders on the Kola Peninsula, northeast Russia: indicators of climatic change. *The Holocene*, v. 12, no. 2, p. 169-176
- Müller J, Werner K, Stein R, et al., (2012) Holocene cooling culminates in sea ice oscillations in Fram Strait. *Quaternary Science Reviews* 47, 1-14.
- Nichol SL, (2002) Morphology, Stratigraphy and Origin of Last Interglacial Beach Ridges at Bream Bay, New Zealand. *Journal of Coastal Research* 18, 1: 149-159.
- Nicholls RJ, Wong PP, Burkett VR, et al., (2007) Coastal systems and low-lying areas. *Climate Change 2007: Impacts, Adaptation and Vulnerability. Contribution of Working Group II to the Fourth Assessment Report of the Intergovernmental Panel on Climate Change*, M.L. Parry, O.F. Canziani, J.P. Palutikof, P.J. van der Linden and C.E. Hanson, Eds., Cambridge University Press, Cambridge, UK, 315-356.
- Nilsen F, Cottier F, Skogseth R and Mattsson S, (2008) Fjord-shelf exchanges controlled by ice and brine production: The interannual variation of Atlantic Water in Isfjorden, Svalbard. *Continental Shelf Research* 28, 1838-1853.
- Norwegian Ice Service, 2012. Monthly average ice concentrations, Svalbard 1986 – 2012. Accessed 14.02.2012.
- Ogorodov SA, Belova N G, Kamalov A M, et al., (2010) Storm surges as a forcing factor of coastal erosion in the western and eastern Russian Arctic, *Storm Surge Congress: Hamburg*.

- Possnert, G., 1990. Radiocarbon dating by the accelerator technique. *Norwegian Archaeological Review* 23, 662-675.
- Reimer, P.J., Baillie, M.G.L., Bard, E., Bayliss, A., Beck, J.W., Blackwell, P.G., Bronk Ramsey, C., Buck, C.E., Burr, G.S., Edwards, R.L., Friedrich, M., Grootes, P.M., Guilderson, T.P., Hajdas, I., Heaton, T.J., Hogg, A.G., Hughen, K.A., Kaiser, K.F., Southon, J.R., Talamo, S., Turney, C.S.M., van der Plicht, J., Weyhenmeyer, C.E., 2009. INTCAL09 and Marine09 Radiocarbon age calibration curves, 0-50,000 years cal BP. *Radiocarbon* 51, 1111-1150.
- Rodzik J, Zagórski, P., (2009) Shore ice and its influence on development of the shores of southwestern Spitsbergen. *International Journal of Oceanography and Hydrobiology* 38, 1: 163-180.
- Ruz MH, Héquette A and Hill PR, (1992) A model of coastal evolution in a transgressed thermokarst topography, Canadian Beaufort Sea. *Marine Geology* 106, 251-278.
- Salvigsen, O., 1984. Occurrence of pumice on raised beaches and Holocene shoreline displacement in the inner Isfjorden area, Svalbard. *Polar Research* 2, 107-113.
- Salvigsen, O., Elgersma, A., Hjort, C., Lagerlund, E., Liestol, O., Svensson, N.-O., 1990. Glacial history and shoreline displacement on Erdmannflya and Bohemanflya, Spitsbergen, Svalbard. *Polar Research* 8, 261–273.
- Stuiver, M., Kra, R., 1986. Calibration Issue. *Radiocarbon* 28, 805-1030.
- Urdea P, (2007) About some geomorphological aspects of the polar beaches. *Revista de geomorfologie* 9, 5-16.
- Velle G, Kongshavn K and Birks HJB, (2011) Minimizing the edge-effect in environmental reconstructions by trimming the calibration set: Chironomid-inferred temperatures from Spitsbergen. *The Holocene* 21, 3: 417-430.
- Wohlfarth B, Lemdahl G, Olsson S, et al., (1995) Early Holocene environment on Bjørnøya (Svalbard) inferred from multidisciplinary lake sediment studies. *Polar Research* 14, 2: 253-275.

## **Chapter 12 – Time-lapse aerial photography reveals significant coastal erosion on Svalbard, Norwegian high Arctic**

Emilie B.M. Guegan<sup>1</sup>, Evangeline G. Sessford<sup>2</sup>, and Anders Schomacker<sup>3</sup>

<sup>1</sup>Sustainable Arctic Marine and Coastal Technology (SAMCoT), Centre for Research-based Innovations (CRI), Norwegian University of Science and Technology (NTNU), Trondheim, Norway; Emilie.Guegan@ntnu.no

<sup>2</sup>Department of Arctic Geology, the University Center in Svalbard, and Department of Geosciences, University of Oslo, NORWAY; EvangelineS@unis.no

<sup>3</sup>Department of Geology, Norwegian University of Science and Technology (NTNU), Trondheim, NORWAY; Anders.Schomacker@ntnu.no

### **Abstract**

The new Digital Shoreline Analysis System tool (DSAS) was used to quantify coastal erosion rates for unconsolidated coasts on Svalbard at four different sites in Isfjorden; Vestpynten, Fredheim, Skansbukta and Svea. The study sites present varying geomorphology, sediments and exposure to environmental forces and were chosen to illustrate disparities in erosional response. This investigation based on aerial photographs from 1969 to 2012 reveals that coastal erosion is occurring on Svalbard with rates varying between 0 to 2 m/yr. These results differ from previously published data indicating insignificant erosion for Svalbard coastlines. Highest erosion rates indicating both temporal and spatial variation have been identified at Vestpynten. At Fredheim the coastal bluff clearly indicates erosion rates up to 0.73 m/yr, in combination with the progradation of a deltaic system. Svea and Skansbukta sites, however, have been almost stable over the 40 year study period with annual erosion rates between 0 and 0.2 m/yr.

### **Introduction**

Climate change in the Arctic leads to increasing temperatures, precipitation and increasing storm frequency and concomitant changes in coastal erosion rates and is predicted to increase (Instanes et al., 2005). Arctic coasts vary greatly in morphology and geological history but are characterized by the presence of both onshore and offshore permafrost and a relatively short (3 to 4 months) period of open water (Lantuit et al., 2012). However, in the central fjord regions of Svalbard where warm Atlantic waters affect the thermal regime of sea surface temperatures, open water is generally present for 5-6 months a year and recently (i.e. 2011-2013 at Fredheim) for the entire year (Nilsen et al., 2008; Norwegian Ice Service,

2012; Sessford and Hormes, (in prep). Sea ice and shorefast ice generally protect the shoreline by limiting wave-based erosion. However, during ablation tall fast ice can facilitate erosion by blocking outflow of pronival water leading to outwashing of storm ridges (Rodzik and Zagorski, 2009). Shorefast ice can also lead to abrasion, and plucking during break-up (Caline, 2010). In most cases throughout the Arctic, the presence of massive ground ice is a major contributor to high erosion rates (Lantuit and Pollard, 2008; Lantuit et al., 2012) through thermal erosion and slumping of cliffs due to thawing permafrost. Coastal erosion rates in the Arctic are known to be greater than in more temperate environments and are mainly due to the presence of permafrost and ground ice which contributes to coastal erosion through thermal mechanical erosion (Aré, 1988). Temporal variability in erosion rates is governed by climatic forcing and thereby storminess and the presence of sea ice whereas spatial variability concerns cliff morphology, cryology and lithology (Aré, 1988; Lantuit et al., 2012). During their investigation of 61 000 km of Arctic coasts, Lantuit et al. (2012) reported an average erosion rate of 0.5 m/yr. This average is derived from a number of regional rates of which Svalbard is the lowest and the American Beaufort Sea the highest, returning 0 m/yr and 1.15 m/yr, respectively (Lantuit et al., 2012). These rates are comparable to others around the Arctic such as 0.59 m/yr on the Bykovsky Peninsula in the Russian Laptev Sea during the 1951 – 2006 period (Lantuit et al., 2012), 0.6 m/yr for the Beaufort Mackenzie region of Canada between 1972 and 2000 (Solomon, 2005), on Herschel Island in the Canadian Beaufort Sea 0.61 m/yr and 0.45 m/yr were calculated by Lantuit and Pollard (2008) for the 1952 - 1970 and 1970 - 2000 periods, respectively, and 0.31 m/yr for the 1949 – 1976 period near Barrow Alaska on the American Chuckchi Sea (Harper, 1978).

High erosion rates present great engineering challenges for any coastal infrastructure and understanding contemporary erosion rates is important to strengthen models simulating warmer scenarios and reduced sea ice and thereby the influence of increased wave action on Arctic coasts (Instanes et al., 2005; Richter-Menge et al., 2006; Stroeve et al., 2008).

This study presents erosion rates for four of Svalbard's unconsolidated coastlines. Svalbard is an archipelago located between 74° and 81° N with relatively mild mean annual air temperatures considering its high latitude, of -6° C to -8° C (Hanssen-Bauer et al., 1990) (Figure 1).

Svalbard coastlines are dominated by bedrock (67% after Etzelmuller et al, 2002), and tidewater glacier margins. Our study focuses on the unconsolidated sediment coasts, using four study sites. Svea and Vestpynten are close to modern infrastructure whereas Fredheim and Skansbukta are proximal to cultural heritage buildings. Understanding the general behavior of unconsolidated coastlines is therefore of primary importance and necessary

background data for any further investigations in Arctic coastal settings dominated by unconsolidated material.

## Setting

The four investigation sites are situated in central Spitsbergen along the two major fjords of Spitsbergen, Isfjorden and Van Mijenfjorden (Error! Reference source not found.).

Vestpynten investigation site is situated 5 km west of Svalbard's main settlement, Longyearbyen, along Adventfjorden. It is made up of a 900 m long section of unconsolidated bluffs and low gradient beaches. The soil in Vestpynten is stratified and well graded beach sediments with particle size between gravel and silt (Figure DR1; supplementary material).

For this site aerial photographs from 1971 (1:7000; panchromatic), 1977 (1:6000; panchromatic), 1995 (1:6000; Colored Infrared Photography (CIR)), 2008 (Ground Sample Distance (GSD) 10 cm; RGB) and 2011(GSD 10 cm; RGB) were analyzed. The sediments are very dry without any indication of ice lenses. Maximum bluff height is 6 m but is

approximately 4 m on average. The sea ice is very sparse at this site and have been absent for many years.



Figure 1: Location of the study sites on Svalbard. LYR indicates the main settlement, Longyearbyen. 1: Vestpynten, 2: Fredheim, 3: Skansbukta, 4: Svea.

Fredheim is located on the coast of Sassenfjorden in the inner part of Isfjorden. The total length of coastal cliff measured in this study at Fredheim is 290 m and average height is 2 m. It is made up of unconsolidated fluvial deposits. The dominating composition is sand and gravel (Finseth et al., 2012). Between approximately 150-300 m west of the measured start of coastal cliff section is the main outlet for the Nøis River and the rapidly prograding delta. Bedrock has

recently become exposed in the foreshore (Figure DR1; supplementary material). Erosion rates of 25 and 57 cm/year for the coastal escarpment have been suggested by two preliminary studies (Johannessen, 1997; Flyen, 2009). Waves do not generally break against the cliff as it is in the backshore zone, though may be possible during large storm events at high tide (observations from time-lapse images taken between 05.07.2012 and 02.02.2013, Sessford and Hormes, in prep). Sea ice is usually present from December through May,

though is not always the case as noted previously. However, whether sea ice is present or not, an ice foot formed by a combination of ice drift (ice bergs) and water spray from waves attaches to the cliff throughout the winter and snow fans build up on its surface.

Skansbukta in Isfjorden is one of the most sheltered bays in Svalbard. Surrounded by mountains on three sides, it is mainly open to south-easterly winds. The 990 m coastal section of unconsolidated beach material does not consist of a cliff, only a steep shoreface. Therefore, the coastline is delimited by the high tide water line (Figure DR1; supplementary material). Beach deposits are made up of smooth plate like to round pebbles and boulders. The majority of boulders are found in the southern reaches of the beach where it is in closer cliffs of Skansen. Sea ice (though not always fast ice) within the bay and ice foot along the shore is common during winter months.

The Svea study site is located between Kapp Amsterdam and Damesbukta, 5 km south-west of Sveagruva, a Norwegian mining settlement in Van Mijenfjorden. The dominant coastal landform at the site is a sub-vertical bluff, up to 6 m high, of varied sediments including poorly sorted gravels, clayey diamicton and a well sorted silty clay (Kristensen et al. 2009) (Figure DR1; supplementary material). This bluff is exposed NW toward the 60 km long Van Mijenfjorden where high local waves can be generated. According to Lothe and Finseth (2012), the dominant wind direction is 240° which is also the dominant wave direction, with a 1-year wave height of 1.35 m. The studied section consists of the 350 m long bluff easily identified in the aerial photographs. Only aerial photographs from 1969 (1:5000; panchromatic) and 2009 (GSD 20; RGB) were analysed for this site. In comparison with the other sites, Svea has a different permafrost history where steep thermal gradients indicate a contemporary aggradation of permafrost (Gregersen et al., 1988).

## **Measurements of coastal erosion**

Coastline positions were delineated on aerial photographs from 1969 to 2012 provided by the Norwegian polar Institute. Aerial photographs from 1998, 2006, and 2009, were orthorectified and served as a base to georeference remaining datasets in ArcGIS.

Coastlines were mapped on the aerial photographs for each year. Wherever possible, coastal bluffs or cliffs were used as markers for mapping the coastline as this provided better accuracy in terms of identification on the aerial photographs and is not subject to error due to tidal variations.

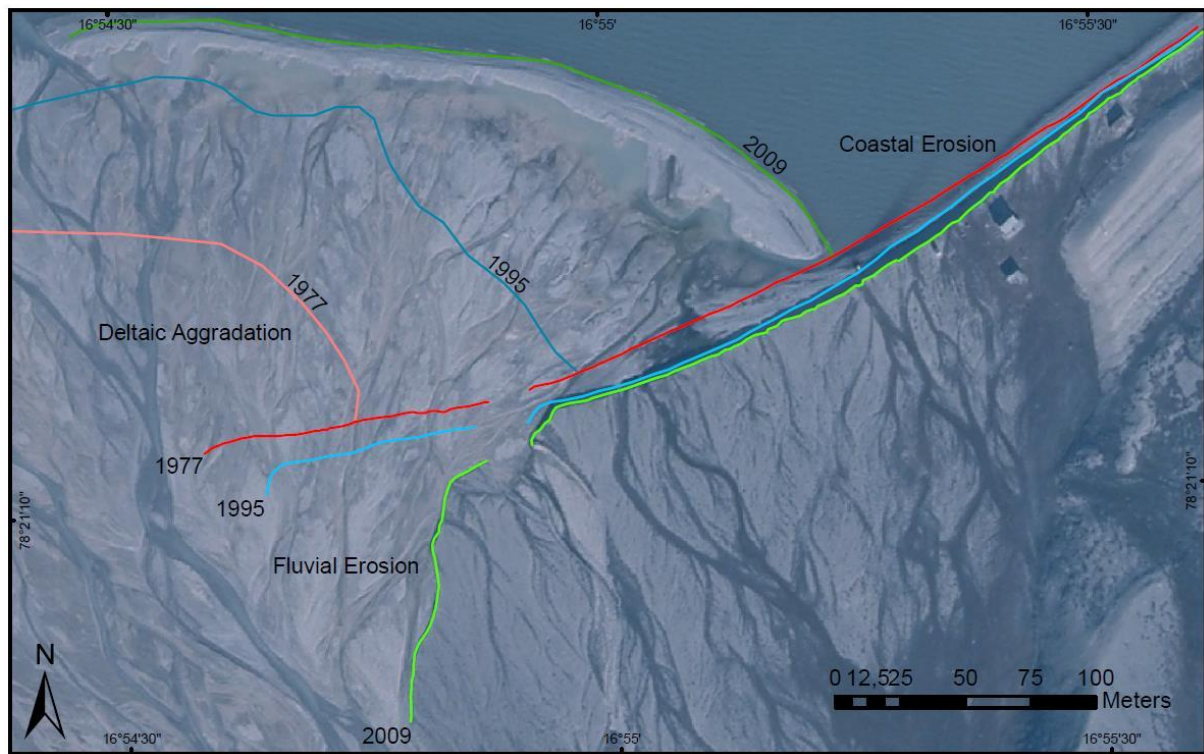


Figure 2: Coastal erosion and aggradation of the river delta from Sassendalen at Fredheim in 1977, 1995 and 2009. The limits of deltaic aggradation and fluvial erosion were measured by Digital Shoreline Analysis System tool (DSAS) and plotted in ArcGIS on the reference aerial photograph from 2009 (Norwegian Polar Institute).

Using the United States Geological Survey (USGS) design tool DSAS (Digital Shoreline Analysis System; Thieler et al., 2009), transects perpendicular to the oldest coastlines were constructed at every site. Transects were spaced at 10 m intervals, and the distance between each coastline was measured for each transect. The coastal erosion rates were obtained by dividing the retreating distance by the number of years between each photo survey.

## Results

Figure 3 presents the annual erosion rates for each site and at each studied time increment. Summary statistics were evaluated for each site and coastal segments for each period and for the entire combined dataset (Table DR1; online supporting material).

At Vestpynten the coast has been divided in five segments based on the spatial and temporal variation of erosion rates, where segment 1 is the westernmost and 5 is the easternmost. While most of the segments show erosion of the coast, segment 1 shows an accretion rate of 0.75 m/yr between 1971 and 1995. Segment 2 (between 140 and 300 m) is stable over the 40 year period; the coastline position has not changed. Segment 3 (between 300 and 500 m) presents an average annual erosion rate of 0.18 m/yr but up to 0.75 m/yr for



some parts between 1971 and 1995, and has afterwards, been stable since 1995, i.e. no

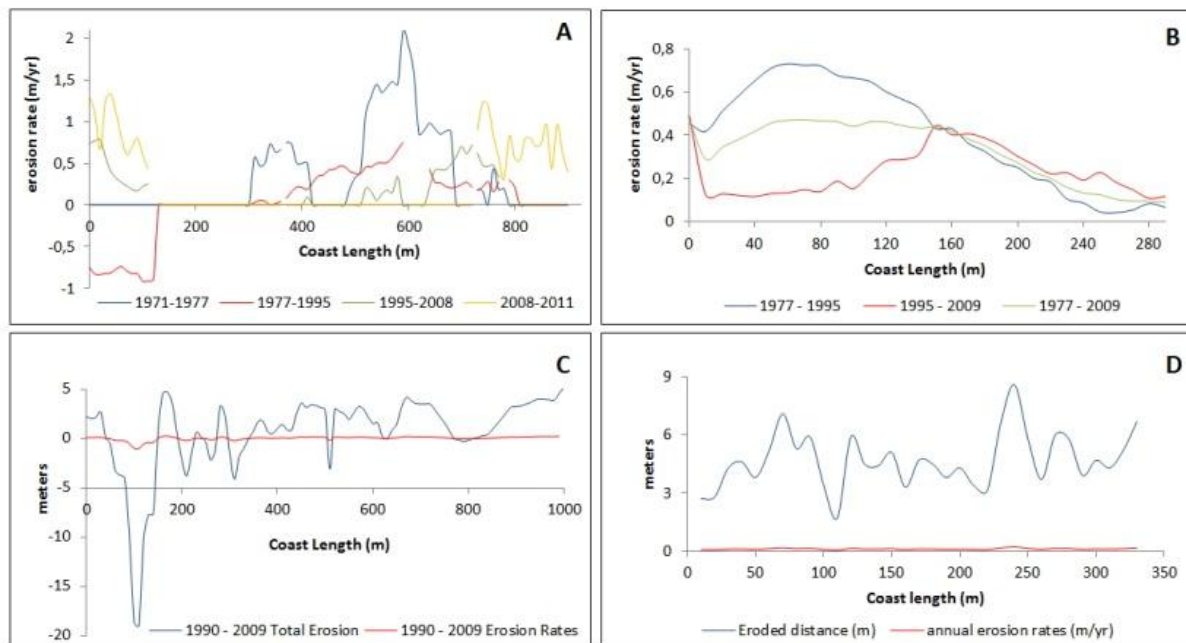


Figure 3: Erosion rates for A) Vestpynten and B) Fredheim and total erosion distance for C) Skansbukta and D) Svea

erosion has been recorded from 1995 to 2011. Segment 4 (between 500 and 810 m) shows the most constant erosion rate during the study period with an average annual erosion rate of 0.4 m/yr, but with maximum rates reaching 2.1 m/yr between 1971 and 1977. Segment 5, at the eastern end of the section, has been stable from 1971 to 2008, without any visible erosion, but undergoes severe erosion since 2008 with annual erosion rates of 0.69 m/yr over the last three years, but as high as 0.96 m/yr at some places, now threatening the access road to Bjørndalen (Figure DR1; supplementary document). At Vestpynten, the erosion is highly variable in time and space. Most importantly it appears that erosion is currently active at this site.

The average rate of erosion at Fredheim between 1977 and 2009 is 0.33 m/yr where the maximum erosion rate is 0.47 m/yr and the minimum is 0.1 m/yr. However, when the time periods are divided between 1977-1995 and 1995-2009, it can be seen that erosion rates prior to 1995 were much higher (Table DR1, online supporting material). The largest erosion rates occurred before 1995 and the most stable location along the cliff is at 150 m where erosion rate has remained stable at 0.43 m/yr over the entire observation period (Figure 3). Erosion appears highest directly in front of the prograding delta which has grown 189 m at an average rate of 5.9 m/yr along the coast and overtaken approximately 120 m of cliff section that had the highest erosion between 1977 and 1995. The highest erosion rates appear to move eastward with the front of the delta. The first transect, at 0 metres along the coastline can be considered an outlier as high erosion in the 1995-2009 period is due to increased

fluvial erosion as the Nøis River changed its course. The total area of sediment loss is 3085 m<sup>2</sup> as extrapolated from aerial images and coastal cliff retreat (Figure 2). Total volume of sediment loss is approximately 6170 m<sup>3</sup> when multiplied by the average cliff height of 2 m.

Only two series of aerial images from 1990 and 2009 are available from Skansbukta. The average erosion rate is 0.04 m/yr. However, this is due to aggradation in many sections of the 990 m long coastline. In the innermost section, total aggradation has been up to 18.7 m whereas erosional areas are more modest with the maximum total erosion distance of only 5 m. If taking the length of coastline into consideration the dominant process has been erosion as aggradation is limited to a few transects. Total aggradational and erosional surface areas amount to 1107 m<sup>2</sup> and 1603 m<sup>2</sup> respectively. Total volume is not calculated as the beach interface is not a cliff and elevations cannot be determined accurately from the available aerial imagery.

Despite the long time interval between the two aerial photographs, the coastal changes in Svea are small. The maximum erosion is 4.7 m over 42 years, corresponding to a maximum annual erosion rate of 0.11 m/yr (Table DR1, supplementary material). Erosion is not significantly active in Svea, and despite the high bluff of unconsolidated till, the coastal segment has been stable over the last 42 years.

## **Discussion and conclusions**

Our study reveals that Svalbard's unconsolidated coasts undergo active erosion. The average erosion rates for the four study sites range between 0 and 2 m/yr, with most segments eroding at rates between 0.3 and 0.4 m/yr. This is clearly lower than the most spectacular erosion rates reported from other Arctic coasts, e.g. 6 m/yr in Russia; 2.5 m/yr in the Beaufort Sea; and, 5 m/yr in Tuktoyaktuk, Canada (Reimnitz et al., 1985; Are, 1988). The erosion rates of Svalbard's unconsolidated coasts reported here are of the same order of magnitude as the average erosion rates of Arctic coastlines determined by Lantuit et al. (2012) of 0.5 m/yr and the erosion rates of 0.31 m/yr at the Chuckchi Sea coast (Harper, 1978). Understanding variables associated with the erosional response of Arctic coasts remains challenging as many diverse parameters both within the soils and through environmental forces acting upon it have to be integrated. Thick snow banks in front of the Vestpynten and Svea bluffs could increase the effect of the coastal permafrost thermal regime, which would be degrading in the first case and aggrading in Svea. The active and complex erosion in Vestpynten is of great concern for nearby infrastructure (Figure DR1, online supporting material). Since 2008, the easternmost segment of the bluff is eroding at rates equivalent to 1 m/yr. The transition from a stable steady state to active erosion can potentially be explained by a decline in sea ice extent, an increase in summer sea surface

temperature, sea level rise, and an increase in storm power and wave action (Jones et al., 2009).

At Fredheim, there are two main changes since 1977; a prograding delta has accelerated in growth rate, and the coastal erosion rate has decreased. Figure 2 clearly indicates that deltaic growth remained fairly spatially constant between 1977 and 1995, but rapidly increased between 1995 and 2009 especially along the coastline. Increased runoff and discharge produces a higher sediment flux thereby entraining and transporting larger amounts of material within fluvial systems (Walker, 1998). Due to high coastal erosion rates between 1977 and 1995, accommodation space along the coast of the fjord has increased and has space enough for deposition. Fjord circulation patterns, longshore drift and accommodation space have caused the delta to grow eastwards, rather than outwards into the fjord. As the delta has grown it appears to have naturally protected the coast and erosion rates have decreased. Natural protection seems to be in accordance with Harper's (1978) supposition that offshore bars and borrow pits are related to the spatial variation of erosion.

However, erosion has continued to affect the coastal cliff at Fredheim even though it appears to be unaffected by waves (though storms during high tide events were unobserved and so cannot be ruled out). Other factors must contribute to coastal erosion. The first factor to take into account is sea ice which has been present most winters since 1977, though less frequently as of recent years (Sessford and Hormes, in prep). Through manual field measurements it has been shown that the erosion in 2011/2012, a winter season with shore ice and open water, was 0.17 m (Finseth and Sessford, 2012). It is proposed that the presence of shore ice may contribute to erosion, rather than protect the coastal escarpment. Skansbukta also has an ice foot during winter and the beach is made up of flat stones and pebbles. For erosion to take place, strong waves and or ice plucking is needed to transport stones away from the shore. As the bay is relatively well protected, it seems more likely that sediment is plucked away during melt-out in the spring.

The analysis and observation collected during this study have increased the baseline knowledge of coastal erosion rates in Svalbard. They have supported that coastal erosion is active in Svalbard unconsolidated coasts, and while the mechanisms behind erosion are very complex and not yet fully understood, the engineering design for protection structures of historical buildings or construction of new coastal infrastructure need to consider this current ongoing site specific erosion.

## **Acknowledgements**

This paper results from a collaboration between two Norwegian projects and institutions; The Sustainable Arctic Marine and Coastal Technology (SAMCoT) based at NTNU and financed by the Norwegian Research Council and their Industry partners alongside master student studies based at UNIS, Svalbard, financed by Svalbard Science Forum. Special thanks are addressed to Harald Faste Aas, from the Norwegian Polar Institute for helping us with the work done on aerial photographs. The authors also gratefully acknowledge useful comments on the manuscript from Dr. Anne Hormes. Support and assistance has been provided by numerous colleagues, notably Prof. Lars Grande.

## References cited

- Aré F. E., 1988. Thermal abrasion of sea coasts, *Polar Geography and Geology*, v. 12, iss. 1, 158 p.
- Caline, F., 2010. Coastal-sea-ice action on a breakwater in a microtidal inlet in Svalbard. Norwegian University of Science and Technology, [Ph.D. thesis]: The University Center of Svalbard, 233 p.
- Etzelmüller, B., Ødegård, R.S. and Sollid, J.L., 2002. The spatial distribution of coast types on Svalbard, in *Arctic Coastal Dynamics: Report of the 3 rd. International Workshop*, University of Oslo, Oslo (Norway) 2-5. Edited by Volker Rachold, Jerry Brown, Steven Solomon and Johan Ludvig Sollid. p. 33-41.
- Finseth, J., Sessford, E.G., Hormes, A., 2012. Erosjonssikring av Fredheim; visualiseringsprosjekt; Evaluering av erosjonssikring av Fredheim. Svalbards Miljøvernfond, SINTEF Byggforsk, Infrastruktur, SBF2012A0334, 43.
- Flyen, A. C., 2009. Coastal erosion: a threat to the cultural heritage of Svalbard? *Polar Research in Tromsø*. J. Holmén. Oslo, Norwegian Institute for Cultural Heritage Research: p. 13-14.
- French, H., Shur, Y., 2010. The principles of cryostratigraphy. *Earth-Science Reviews*, 101(3-4), p. 190-206.
- Gregersen, O. & Eidsmoen, T., 1988. Permafrost Conditions in the Shore Area at Svalbard: Fifth International Conference on Permafrost in Trondheim, Norway, August 1988, v. 2, p. 933-936.
- Harper, J.R., 1978. Coastal erosion rates along the Chucki Sea coast near Barrow, Alaska. *Arctic* v. 31, p. 428–433.
- Hanssen-Bauer, I., Kristensen Solas, M. and Steffensen, E.L., 1990. The climate of Spitsbergen, 39/90, The Norwegian Meteorological Institute, Oslo.
- Instanes, A., Anisimov, O., Brigham, L., Goering, D., Khrustalev, L.N., Ladanyi, B. and Larsen, J.O., 2005. Chapter 16: Infrastructure: Buildings, support systems, and Industrial facilities. *Arctic Climate Impact Assessment*.
- Johannessen, L. J., 1997. Villa Fredheim. Longyearbyen, Governor of Svalbard, Environmental Section, in cooperation with the Svalbard Tourist Board and Svalbard Museum: p. 1-15.
- Jones, B.M., Arp, C.D., Jorgenson, M.T., Hinkel, K.M., Schmutz, J.A., and Flint, P.L. 2009b. Increase in the rate and uniformity of coastline erosion in Arctic Alaska. *Geophysical Research Letters*, 36, L03503, doi: 10.1029/2008GL036205.
- Kohler, J., Nordli, Ø., Brandt, O., Isaksson, E., Pohjola, V., Martma, T., Faste Aas, H., 2011. Svalbard temperature and precipitation, late 19th century to the present, Final report on ACIA-funded project.

- Kristensen, L., Benn, D.I., Hormes, A., Ottesen, D., 2009. Mud aprons in front of Svalbard surge moraines: Evidence of subglacial deforming layers or proglacial glaciotectonics? *Geomorphology* 111, p. 206-221.
- Lantuit, H., Overduin, P. P., Couture, N., Wetterich, S., Are, F., Atkinson, D., Brown, J., Cherkashov, G., Drozdov, D., Forbes, D., Graves-Gaylord, A., Grigoriev, M., Hubberten, H. W., Jordan, J., Jorgenson, T., Ødegård, R. S., Ogorodov, S., Pollard, W., Rachold, V., Sedenko, S., Solomon, S., Steenhuisen, F., Streletskaia, I. and Vasiliev, A., 2012: The Arctic Coastal Dynamics database. A new classification scheme and statistics on arctic permafrost coastlines, *Estuaries and Coasts*, v.35 (2), p. 383-400, doi: 10.1007/s12237-010-9362-6
- Lantuit, H and Pollard, W.H, 2008: Fifty years of coastal erosion and retrogressive thaw slump activity on Herschel Island, southern Beaufort Sea, Yukon Territory, Canada. *Geomorphology*, v. 95(1/2), p. 84–102.
- Lauritzen, Ø., Salvigsen, O., Winsnes, T.S., Andresen, A., 1989: Geological Map Svalbard 1:100 000, C8G Billefjorden, Norsk Polarinstitut, Oslo.
- Lothe, A. and Finseth, J., 2012: Coastal Structures at Svalbard – Lessons learned from structures in the past. Report number: SAMCoT\_WPx\_2011\_01
- Mars, J.C., Houseknecht, D.W., 2007. Quantitative remote sensing study indicated doubling of coastal erosion rate in past 50 yrs along a segment of the Arctic coast of Alaska. *Geology* v. 35, p. 583-586.
- Nilsen, F., Cottier, F., Skogseth, R., and Mattsson, S., 2008, Fjord-shelf exchanges controlled by ice and brine production: The interannual variation of Atlantic Water in Isfjorden, Svalbard: *Continental Shelf Research*, v. 28, p. 1838-1853.
- Norwegian Ice Service, 2012. Monthly average ice concentrations, Svalbard 1986 – 2012. Accessed 14.02.2012
- Nordli, Ø., 2010. The Svalbard Airport temperature series. *Bulletin of Geography – physical geography series*, v.3, p. 6-26.
- Remnitz, E., Graves, S.M., and Barnes, P.W., 1985: Beaufort Sea coastal erosion, shoreline evolution, and sedimentflux. U.S. Geological Survey Open-File Report 85-380. 67 p.
- Richter-Menge, J., Overland, J., Proshutinsky, A., Romanovsky, V., Bengtsson, L., Brigham L., Dyurgerov, M., Gascard, J.C., Gerland, S., Graversen, R., Haas, C., Karcher, M., Kuhry, P., Maslanik, J., Melling, H., Maslowski, W., Morison, J., Perovich, D., Przybylak, R., Rachold, V., Rigor, I., Shiklomanov, A., Stroeve, J., Walker, D., and Walsh, J., 2006 . State of the Arctic Report, NOAA OAR Special Report, NOAA/OAR/PMEL, Seattle, WA, 36 p.
- Rodzik, J. and Zagorski, P., 2009: Shore ice and its influence on development of the shores of south-western Spitsbergen. *Oceanological and Hydrobiological Studies* 38 (Supplement 1): p. 163-180.
- Sessford, E.G. and Hormes, A., in prep: Holocene reconstruction and spatial analysis of coastal development in Svalbard.

- Solomon, S.M., 2005: Spatial and temporal variability of shoreline change in the Beaufort Mackenzie region, Northwest Territories, Canada. *Geo-Marine Letters* v. 25 (2–3), p 127–137.
- Stroeve, J., Serreze, M., Drobot, S., Gearheard, S., Holland, M., Maslanik, J., Meier, W. and Scambos, T., 2008: Arctic Sea Ice Extent Plummets in 2007, *Eos Trans. AGU*, v. 89(2), p. 13–14, doi:[10.1029/2008EO020001](https://doi.org/10.1029/2008EO020001).
- Thieler, E.R., Himmelstoss, E.A., Zichichi, J.L., and Ergul, Ayhan., 2009. Digital Shoreline Analysis System (DSAS) version 4.0 — An ArcGIS extension for calculating shoreline change: U.S. Geological Survey Open-File Report 2008-1278. \*current version 4.3
- Walker, J.H., 1998: Arctic deltas, Coastal Education and Research Foundation, Inc., v. 14(3), p. 719-738.
- Zajaczkowski, M., W. Szchucinski, et al., 2004: Recent changes in sediment accumulation rates in Adventfjorden, Svalbard. *Oceanologia*, v.46(2), p.217-231. <http://sharki.oslo.dnmi.no/eklima> (July 2012).



## **Chapter 13 – Erosjonssikring av Fredheim; visualiseringsprosjekt (Erosion protection at Fredheim; visualization project)**

Jomar Finseth<sup>1</sup>, Evangeline G. Sessford<sup>2, 3</sup> and Anne Hormes<sup>3</sup>

<sup>1</sup>SINTEF Byggforsk, Infrastruktur, P.O. Box 4760 Sluppen, 7465 Trondheim.  
[Jomar.Finseth@sintef.no](mailto:Jomar.Finseth@sintef.no)

<sup>2</sup>Department of Geosciences, the University in Oslo P.O. Box 1072 Blindern, 0316 Oslo

<sup>3</sup>Department of Geology, the University Centre in Svalbard P.O. Box 156, N-9171 Longyearbyen. [EvangelineS@unis.no](mailto:EvangelineS@unis.no) , [Anne.Hormes@unis.no](mailto:Anne.Hormes@unis.no)

### **Introduction**

This report is added to the thesis to illustrate the applicability of coastal research to cultural heritage mitigation strategies and coastal protection. It is presented in its original format as submitted by SINTEF to Svalbard Miljøvernfond and therefore does not follow the same formatting scheme as the previous sections of this thesis.

Rapportnummer - Åpen

# Rapport

## Erosjonssikring av Fredheim; visualiseringsprosjekt

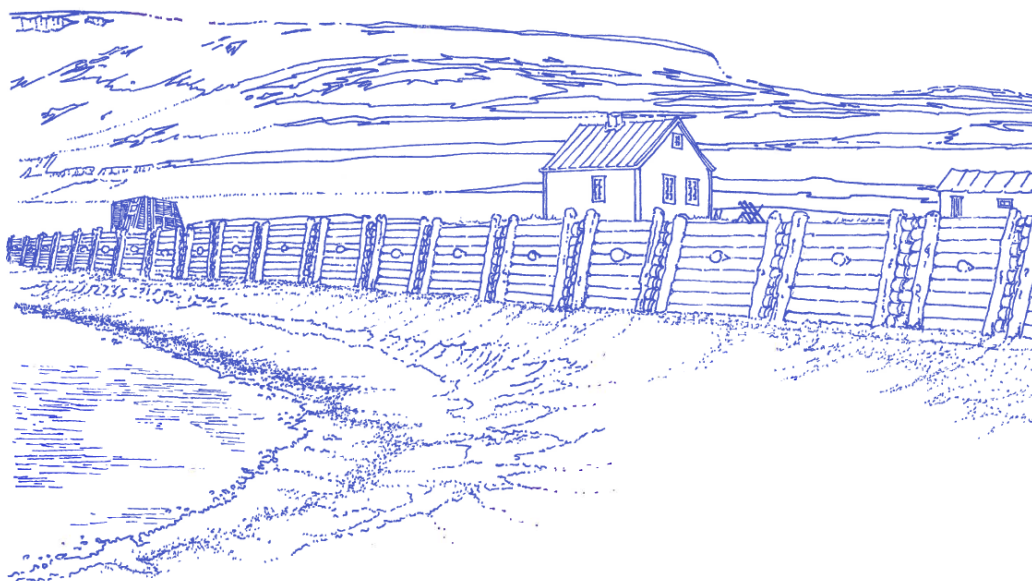
Evaluering av erosjonssikring av Fredheim

### Forfattere

Jomar Finseth, SINTEF

Evangeline Sessford, UiO, UNIS

Anne Hormes, UNIS



Fredheim fra sør-vest, med erosjonssikring

**SINTEF Byggforsk**

Infrastruktur

2012-11-30

**SINTEF Byggforsk**

Postadresse:  
Postboks 4760 Sluppen  
7465 Trondheim

Sentralbord: 73593000  
Telefaks: 73595340

byggforsk@sintef.no  
<http://www.sintef.no/Byggforsk/>  
Foretaksregister:  
NO 948007029 MVA

# Rapport

## Erosjonssikring av Fredheim; visualiseringsprosjekt

Evaluering av erosjonssikring av Fredheim

EMNEORD:

Arktisk

Erosjonssikring

Svalbard

Kulturminne

VERSJON

FORFATTER

Jomar Finseth, SINTEF

DATO

2012-11-30

OPPDRAGSGIVER(E)

Svalbard Miljøvernfond

OPPDRAGSGIVERS REF.

Trine Krystad

PROSJEKTNR

ANTALL SIDER:

46

### SAMMENDRAG

#### Sammendrag

Denne rapporten er en mulighetsstudie og en visualisering vedrørende erosjonsbeskyttelse av Fredheim. Fredheim er et av Svalbards mest kjente og besøkte kulturminner og ligger i utløpet av Sassendalen nordre side, ved innløpet til Tempelfjorden. Kulturminnet består av et knippe bygninger der to av dem, Danielbu og Fredheim er bygget henholdsvis i 1911/1912 av Daniel Nøis og 1924 av Hilmar Nøis. Mange års målinger og undersøkelser utført av forskjellige forskere og institusjoner viser at kystlinjen i front av husene på Fredheim trekker seg bakover på grunn av erosjon, med store variasjoner i erosjonsrater fra år til år. Gjennom finansiering fra Svalbard Miljøvernfond har SINTEF Byggforsk sammen med UNIS sett på ulike muligheter for erosjonsbeskyttelse som et alternativ for å bevare husene og husenes geografiske plassering. Studien omfatter i tillegg en geologisk oversikt basert på feltarbeid i området. Resultatene fra prosjektet er delvis beskrevet i tekst, men er i hovedsak presentert som bilder og skisser.

UTARBEIDET AV

Jomar Finseth

KONTROLLERT AV

Maj Gøril Glåmen Bæverfjord

GODKJENT AV

Arnstein Watn

SIGNATUR



SIGNATUR



SIGNATUR



RAPPORTNR

ISBN

978-82-14-05419-4

GRADERING

Åpen

GRADERING DENNE SIDE

Åpen

# Historikk

---

VERSJON	DATO	VERSJONSBEKRIVELSE
1	2012-12-04	Sluttrapport

# Innholdsfortegnelse

1 .....	Bakgrunn	107
2 .....	Innledning	108
3 .....	Prosjekt-team	108
4 .....	Grunnleggende undersøkelser	109
4.1	Detaljert beskrivelse av undersøkelsesmetoder	109
5 .....	Funn	111
5.1	Resultat undersøkelser	111
5.2	Mulige fremtidige byggematerialer	114
5.3	Erosjonsrater	115
6 .....	Geologi	116
6.1	Bedrock Geology of Fredheim	116
6.2	Methods	117
6.3	Site Descriptions	120
6.4	Bedrock Sample Descriptions	123
6.4.1	Sedimentological Structure	123
6.4.2	Q-system Rock Quality	123
6.5	Unconsolidated Sediments	124
6.5.1	Terrestrial	124
6.6	Marine	127
6.7	Hazards	128
6.8	Summary of Geology	129
6.9	Discussion	129
7 .....	Erosjonssikring av Fredheim	131
7.1	Byggeteknikk	132
7.2	Presentasjon av mulige løsninger for erosjonssikring av Fredheim	134
7.2.1	"Barentsburg"	134
7.2.2	"Coles Bay"	137
7.2.3	"Pyramiden"	140
7.2.4	Tradisjonell erosjonssikring	142
8 .....	Diskusjon og konklusjon	144
9 .....	Referanser	146

**BILAG/VEDLEGG**

---

[Skriv inn ønsket bilag/vedlegg]

---

## Bakgrunn

Svalbard med dets plassering der UNIS i sterk grad kan bistå med lokal fagkunnskap og gode logistiske løsninger, gir et naturlig valg av feltlaboratorium. I et samarbeid med både avdeling for Arktisk Teknologi og avdeling for Arktisk Geologi på UNIS har det både i 2011 og 2012 vært gjennomført en rekke undersøkelser av interessante kystområder for å finne gode feltlaboratorier med hensikt å studere fenomenet kysterosjon. Fredheim har vært en av de mer interessante stedene når det gjelder erosjon og har inngått i SINTEF sine ekskursionsjoner i 2011-12. I samtaler med miljøvernavdelingen hos Sysselmannen har SINTEF fått forståelsen at det er bekymring knyttet til Fredheim, se Figur 1, nettopp i forhold til at kystlinjene nærmer seg husene fra år til år. Med dette som bakteppe søkte SINTEF, sammen med UNIS, om midler fra Svalbards Miljøvernfond for å presentere løsninger der Fredheim kan sikres uten at husene nødvendigvis må flyttes. SINTEF fikk tilslag på søknaden ved tildelingen våren 2012.



Figur 1 Fredheim sett fra sør-vest.

SAMCoT er et Senter for Forskningsbasert Innovasjon (SFI) finansiert gjennom Norges Forskningsråd og flere nasjonale og internasjonale industribedrifter. Målet med senteret er innovasjon og utvikling rundt marin og kystnær arktisk teknologi. Senterets hovedpartnere er NTNU, SINTEF og UNIS, der NTNU har ansvar for ledelse. Gjennom dette prosjektet som går over 5 (8) år skal SINTEF gjennomføre forskning og utvikling knyttet til blant annet kysterosjon. Fredheim er en av de stedene hvor SINTEF vil gjennomføre erosjonsmålinger de neste år.



## Innledning

Svalbard Miljøvernfond har i to prosjekter de siste to årene gitt SINTEF mulighet til å studere utfordringer knyttet til kystnære konstruksjoner på Svalbard. I 2011 presenterte SINTEF rapporten *"Bygging i strandsonen på Svalbard – Hva forteller fortidens kaier oss om fremtidens anlegg"*, som er en studie og rapport på byggeskikk, materialbruk og tilstand for Spitsbergens kaianlegg. I 2012 fikk SINTEF finansiering for prosjektet: *"Erosjonssikring av Fredheim"*, et prosjekt der målet er å presentere et forslag for fremtidig erosjonssikring av Fredheim..

Målet med dette prosjektet er å se på muligheter for å sikre Fredheim i forhold til kysterosjon som hvert år flytter kanten strandlinjen nærmere husene. Det er i årene 2010-2012 gjennomført en større studie som omfatter mange forhold vedrørende å forstå de naturlige prosessene i området og mange av disse data er brukt i denne undersøkelsen. Feltarbeid sommeren 2012 er gjennomført med henblikk på å få kompletterende data som i hovedsak benyttes for dette prosjektet; en mulighetsstudie og visualisering for gjennomføring av sikringstiltak på en slik måte at Fredheims særpreg opprettholdes i årene fremover.

Resultatene og forslagene i denne rapporten er ikke av dimensjonerende art. Det vil si at det ikke er gjennomført kvalitetssikrede kalkulasjoner i forhold til om løsningene kan benyttes slik de er presentert. SINTEF har utført denne studien som en visualiseringsstudie, men det ligger allikevel en erfaringsbasert vurdering til grunn for alle forslag i forhold til gjennomførbarhet. Hvis noen av de forslagene som presenteres i denne rapporten blir brukt i den sammenheng de er foreslått må konstruksjonen med dreninger m.m. dimensjoneres før erosjonssikringstiltaket gjennomføres.

## Prosjekt-team

Prosjektteamet i dette prosjektet har vært tverrfaglig sammensatt. I utgangspunktet skulle studien dekke følgende områder:

- Geoteknikk/permafrost /erosjonssikring
- Geologi/ landskapsutvikling under klimaendring
- Landskapsarkitektur
- Bølger/bølgebeklastning på kyst

Med bakgrunn i ny kunnskap om erosjonsprosessene og de geologiske forholdene på Fredheim under prosjektperioden, samt ved at prosjektleder har valgt å legge større fokus på selve visualiseringen og presentasjon av flere opsjoner, så har prosjektteamet en noe annen sammensetning enn først presentert i søknaden. Den største endringen er knyttet til at studier rundt bølger og bølgekrefter på kysten ved Fredheim er tatt ut, noe som gjenspeiles spesielt i kapittel 4 og 5. Følgende personer har i større eller mindre grad deltatt i prosjektet:

- |                       |                      |   |
|-----------------------|----------------------|---|
| • Jomar Finseth       | Prosjektleder        | SINTEF Byggforsk                        |
| • Anne Holmes         | Geologi/veiledning   | UNIS                                    |
| • Evangeline Sessford | Geologi/feltnålinger | UNIS                                    |
| • Bridget Thodesen    | Landskapsarkitektur  | SINTEF Byggforsk                        |
| • Ingvild Sæbu Vatn   | Landskapsarkitektur  | LPO Arkitekter i Nord, Longyearbyen     |
| • Håkon Tangen        | Feltnålinger         | SINTEF Byggforsk (sommerjobb 2011)      |
| • Joar Justad         | Feltnålinger         | SINTEF Byggforsk (sommerjobb 2011/2012) |

## Grunnleggende undersøkelser

I og med at Fredheim har vært et interessant område for arbeidspakken på arktisk kystteknologi i SAMCoT-prosjektet, knyttet til studier av erosjonsrater og -prosesser, så har SINTEF utført en rekke undersøkelser de to siste årene. Det som presenteres i denne rapporten er kun relevant informasjon som har vært nødvendig i forhold til de løsninger som er presentert.

Beskrivelser av geologien i dette området er presentert som en stor del av rapporten. På dette området har teamet samlet mye informasjon og det er spesielt student Evangeline Sessford og førsteamanuensis Anne Holmes fra UNIS som har gjennomført et omfattende feltarbeid og bidratt på dette området. Sessford vil til neste år levere Masteroppgave på temaet geologi og geologiske avsetninger i området rundt Fredheim, med forsvar av graden i mai 2013, og har vært innleid ressurs i dette prosjektet. På denne måten har prosjektet vært tilført ressurser og resultater av høy verdi og kvalitet uten at det i vesentlig grad har vært belastet økonomien i prosjektet.

Undersøkelser og funn knyttet til geologi er i hovedsak presentert i eget kapittel, men har u diskutabel relevans og verdi for de vurderingene som er gjort i dette prosjektet.

Følgende undersøkelser er gjennomført i felt av SINTEF og UNIS, av betydning for dette prosjektet, sommeren 2011 og 2012:

- Geodesi-målinger av kystlinje (Differensiell GPS: DGPS)
- Avstandsmålinger mellom kystlinje og hus (manuell)
- Høyder
- Fjellkvalitet
- Visuell beskrivelse av "fjell i dagen"
- Enkle jordanalyser fra prøver på land, samt sjøbunnssedimenter
- Vurdering av mulige "geo-farer" (for eksempel ras og erosjon)
- Meteorologiske data

I tillegg til de målinger og undersøkelser som er utført av SINTEF og UNIS vedrørende erosjonsmålinger, inneholder rapporten data fra tidligere målinger funnet i følgende publiseringer:

*Flyen, A. C. (2009). Coastal erosion . a threat to the cultural heritage of Svalbard? Polar Research in Tromsø. J. Holmén. Oslo, Norwegian Institute for Cultural Heritage Research: 13-14.*

*Johannessen, L. J. (1997). Villa Fredheim. Longyearbyen, Governor of Svalbard, Environmental Section, in cooperation with the Svalbard Tourist Board and Svalbard Museum: 1-15.*

## Detaljert beskrivelse av undersøkelsesmetoder

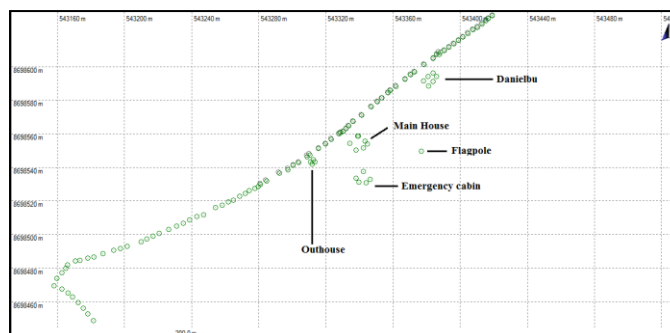
Av de undersøkelser som er gjennomført så er de fleste nærmere beskrevet i kapittel 0. Utover dette kan det være nødvendig å forklare følgende metoder nærmere:

### DGPS

DGPS-systemet (Differensiell GPS) er en utvidelse av GPS-systemet. Denne metoden bruker to eller flere GPS-mottakere for å hente inn posisjoner gitt fra satellittnavigasjonssystemene GPS og GLONASS. Hensikten med metoden er å plassere den ene mottakeren på ett kjent landbasert

referansepunkt med kjente koordinat (statisk mottaker) samtidig som den andre mottakeren brukes til målinger. Satellittene vil kontinuerlig gi den statiske mottakeren en varierende posisjon som avviker fra den kjente posisjonen, der størrelsen på avviket henger sammen med antall satellitter tilgjengelig, altså satellittenes posisjon i satellittbanene og terrenget mottakeren anvendes i.

Dette posisjonsavviket vil være det samme for alle mottakerne anvendt i samme tidsintervall. Hensikten er derfor å bruke avvikene beregnet av den statiske mottakeren til å korrigere posisjonene målt med andre mottakere i samme tidsperiode. Avviket kan implementeres direkte til mottakeren



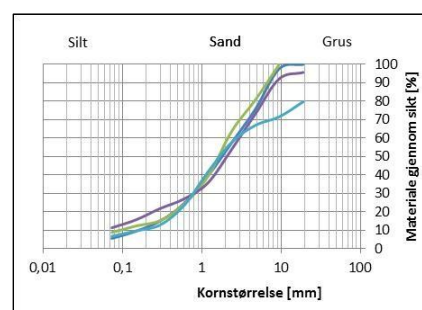
Figur 2 Typisk plott etter DGPS undersøkelse.

ved hjelp av radio, internett eller GSM nettet (RTK, Real Time Kinematic), eller

ved etter-prosessering av data hentet fra mottakerne. Etter-prosessering er metoden brukt i dette prosjektet. En vanlig GPS kan ha omtrent 5 - 10 m avvik, avhengig av hvor mange satellitter som er tilgjengelig. Nøyaktighet av DGPS er i stort grad avhengig av innmålte statiske mottakerposisjoner og på Svalbard er disse posisjonene målt opp av Norsk Polar Institutt. Ved bruk av disse innmålte posisjonene så er det mulig å oppnå en nøyaktighet på  $\pm 10$  cm.

## Enkle jordanalyser fra prøver på land, samt sjøbunnsedimenter

Både i 2011 og 2012 er det samlet inn et relativt stort antall prøver av jorden nær sjøen og i sjøen ved Fredheim. Disse jordprøvene har blitt analysert i geoteknisk laboratorier både på UNIS og SINTEF for å finne sammensetningen knyttet til størrelse av korn. Denne metoden kalles kornfordelingsanalyse og kan gjennomføres enten med våt eller tørket jord. I hovedsak gjennomføres en sikteanalyse med et sett sikter sammensatt etter en standard. Dette vil gi en beskrivelse av kornfordeling i området stein til fin sand. Hvis sikteanalysen viser at store deler av prøven inneholder silt og leire så må det i tillegg gjennomføres en hydrometeranalyse der fordelingen av jord i denne størrelsen (mindre enn 0,063 mm) bestemmes gjennom måling av densitet med sedimentering av jordpartikler i vannbad.



Figur 3 Typisk plott fra kornfordelingsanalyse; velgradert sand.

Sammensetningen vedrørende mengde av de forskjellige kornstørrelsene presenteres i et plott og vil fortelle en del om jordens egenskaper. I dette tilfellet er det spesielt viktig å se på jordens egenskaper i front av erodert skråning, samt vurderinger av egnetheten til jorda i området i forbindelse med bygging der nettopp de lokale jordmassene utgjør hoveddelen av byggematerialene.

Tabell 1 Beskrivelse av jord knyttet til kornfordeling (ISO 14688-1).

Material	Diameter (mm)		
Grus	2,0	< d <	64
Sand	0,063	< d <	2,0
Silt/leire		d <	0,063

## Funn

Dette kapittelet omhandler de funn som vil ha betydning i forhold til risikoen vedrørende mulig ødeleggelse av husene på Fredheim som konsekvens av erosjon. Det er i tillegg gjort andre funn i denne undersøkelsen som kan være en risiko i forhold til ødeleggelse av husene, dette er presentert i 0.

### 1.1 Resultat undersøkelser

Dette kapittelet omhandler funnene som har betydning i forhold til risikoen for ødeleggelse av husene på Fredheim som konsekvens av erosjon. Det er i tillegg gjort andre funn i denne undersøkelsen som kan indikere en risiko i forhold til ødeleggelse av husene, dette er presentert i kapittel 0.

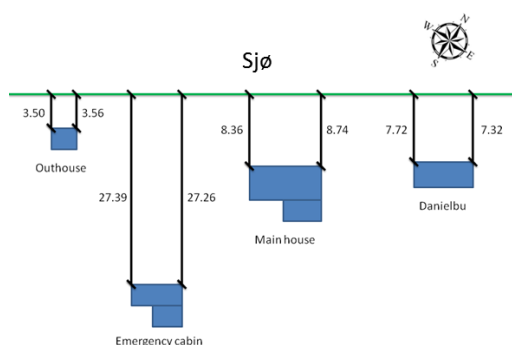
Tabell 2 Resultat fra målinger utført ved Fredheim i perioden 1987-2012. Målingene i meter er i hovedsak utført med målebånd mellom det nord-østre hjørnet på de enkelte bygg og erosjonskanten.

År (periode)	1987 (Manuell)	1990 (Manuell)	1993 (Manuell)	1996 (Manuell)	1998 (Manuell)	2010 (DGPS)	2011 (Manuell)	2012 (Manuell)
Kilde	(Bjerck 1999)	(Bjerck 1999)	(Bjerck 1999)	(Bjerck 1999)	(Bjerck 1999)	Tangen, Justad 2012)	Tangen, Justad 2012)	(Tangen, Justad et al. 2012)
Uthus	5.61	4.64	3.5	2.55	2.28	0.95 <sup>2)</sup>	3.62	3.56
Nødhytte	Ingen data	Ingen data	Ingen data	Ingen data	Ingen data	Ingen data	27.63	27.26
Hovedhus	17.7	16.64	15.88	Ingen data	15.38	9.24	8.46	8.74 <sup>3)</sup>
Danielbu	6.46	5.83	4.9	4.55	4.63 <sup>1)</sup>	8.102 <sup>1)</sup>	7.47	7.32

<sup>1)</sup> Målefeil i manuelle målinger på Danielbu i 1998

<sup>2)</sup> Uthus og Danielbu er flyttet i denne perioden.

<sup>3)</sup> Målefeil i manuelle målinger på hovedhus i 2012



Figur 4 Forenklet skisse av bygningene på Fredheim. Målene er oppgitt i meter og er utført i 14. juni 2012 (Tangen og Justad et al. 2012).

Tabell 3 Erosjonsrater presentert i cm basert på malinger vist i tabell 2.

	1987 - 1990	1990 - 1993	1993 - 1996	1996 - 1998	1998 - 2010	2010 - 2011	2011 - 2012
Uthus	97	114	95	27	133 <sup>1)</sup>	-	6
Nødhytte	-	-	-	-	-	-	37
Hovedhus	106	76		50	614	78	11
Danielbu	63	93	35		253 <sup>1)</sup>	63	15

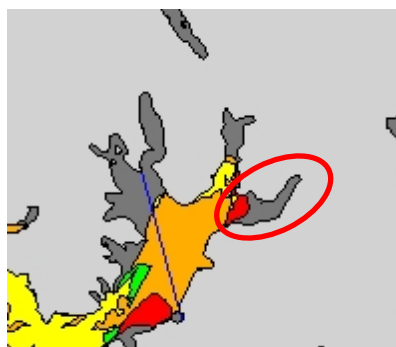
<sup>1)</sup>Uthus og Danielbu er flyttet i perioden. Dette forklarer lave erosjonsrater for disse to bygninger i forhold til erosjonsrate for hovedhus

Som tabellen over viser er det små variasjoner i erosjonsrater mellom erosjonskanten og det enkelte hus. Dette kan i hovedsak adresseres erosjonsmekanismene ved Fredheim. Det er tidligere hevdet at erosjonen i veldig sterk grad er knyttet til bølgeerosjon, men funn presentert i kapittel 0 viser at dette sannsynligvis ikke er tilfelle. Bølger er en medvirkende faktor, men i hovedsak gjelder dette som transportør av allerede eroderte masser. Hovedårsaken for erosjon kommer fra smelting og utrasing av permafrost jord der vannførende kanaler fra bakenforliggende områder er den største driveren. I disse kanalene er store deler av finmassene vasket ut og kanten mot sjøen blir dermed mer ustabil i dette området. Denne prosessen gjør at området mellom kanalene også blir mer ustabil på grunn av redusert sidestøtte.

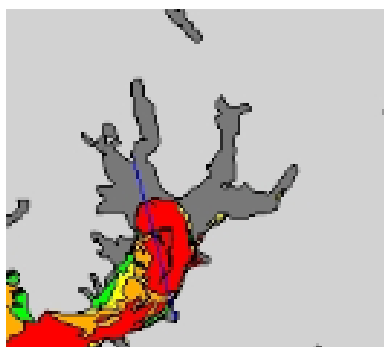
Erosjonsratene varierer relativt mye fra år til år og fra periode til periode. Dette kan sees i forhold til at temperatur, nedbør, lengde av isfri periode endrer seg fra år til år. Når det gjelder årlige variasjoner så inneholder denne undersøkelsen dessverre kun to perioder hvor erosjonsraten har vært målt fra ett år til den neste: 2010-2011 og 2011-2012. For disse målingene observeres en endring i erosjonsrate der raten for siste periode, målt i 2012, er 1/7-del av raten målt i 2011. Ved å se på den store endringen (nedgang) i erosjonsrate i forhold til klima, så viser gjennomsnittlig sommertemperatur for Svalbard de siste to år at sommeren 2012 var relativt kaldere enn sommeren 2011. Observasjoner knyttet til tilstedeværelse av fjordis mellom sommeren 2011 og sommeren 2012, viser unormal lang periode med isfri sjø både i Sassenfjordenen og Tempelfjorden, uten at dette førte til økt erosjonsaktivitet ved Fredheim. Alle disse observasjonene er viktige faktorer i diskusjonen om hvilke drivere som kan betraktes som viktigste i forhold til erosjon ved Fredheim, men i og med at det her er snakk om én observasjon, så er det umulig å bruke dette i en statistisk sammenheng. Andre viktige forhold for grunnlag til videre diskusjon og studier er tilstedeværelse og effekt av landfast is, dvs den del av sjøisen som er fastfrosset i kystlinjen. Mekanismer rundt denne, spesielt knyttet til dynamikk i forbindelse med tidevann kan påvirke erosjonsraten, på samme måte som snø i strandsonen vil påvirke temperaturregimet i den kystnære permafrosten, og dermed påvirke erosjonsratene. Alle disse faktorene er så interessante at tilsvarende malinger og observasjoner anbefales gjennomført de neste år. Iskart med observasjoner knyttet til is i Sassenfjorden og Tempelfjord er presentert i Figur 6 og Figur 7.



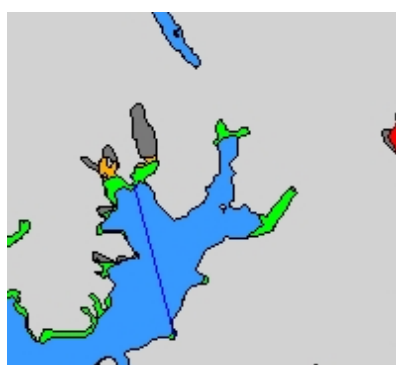
Figur 5 Sone med vannkanaler i jorden og utvasking.



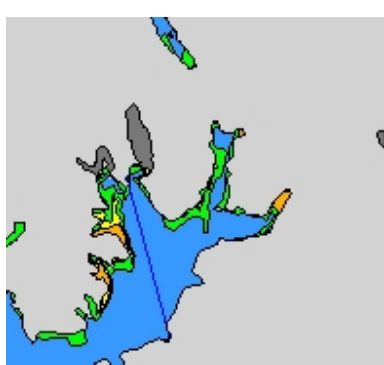
Figur 6 Iskart 1. februar 2011.



1. mars 2011.

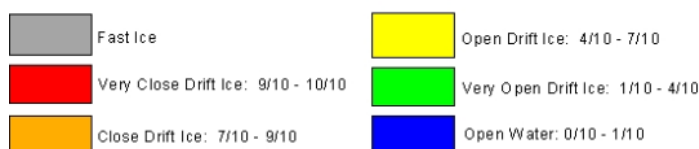


Figur7 Iskart 1. februar 2012.



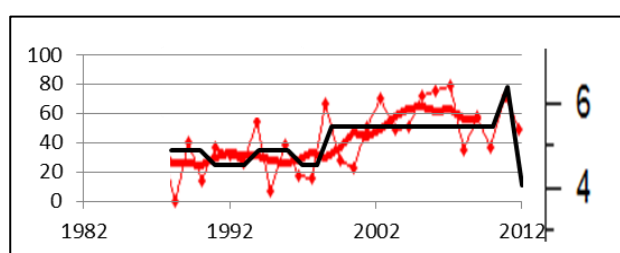
1. mars 2012.

Ice Categories:



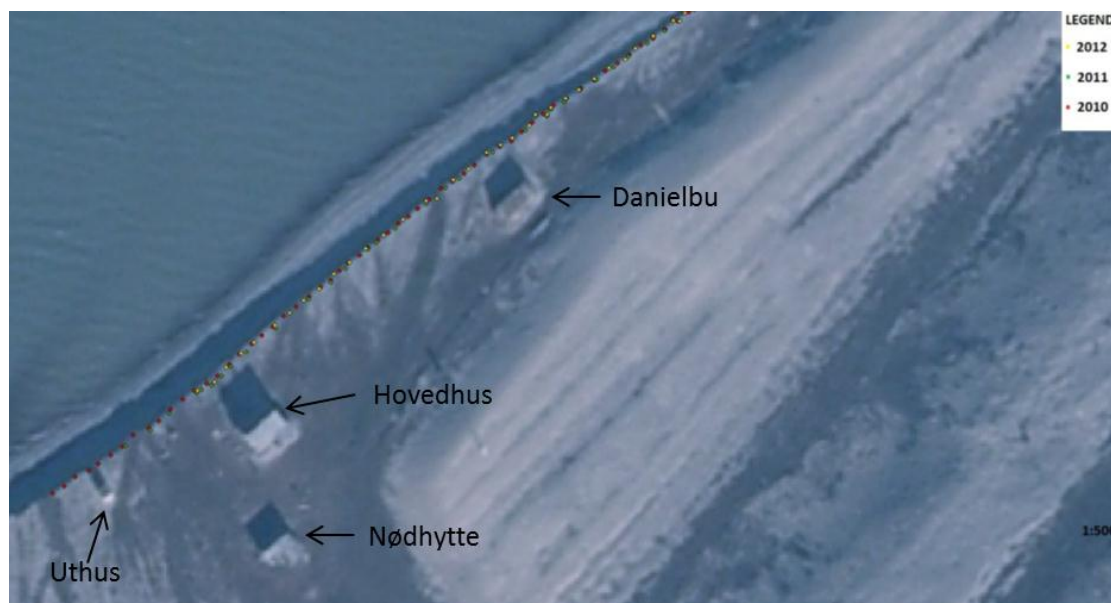
Figur8 Forklaring til iskart.

Temperaturen på Svalbard har stor årlige variasjoner og som tidligere nevnt i antas det at lufttemperaturen har store innvirkninger på erosjonsratene. I Figur 9, er gjennomsnittlig årlig erosjonsrate for de forskjellige perioder tegnet inn på plott sammen med årlige sommertemperaturer for Svalbard. Denne fremstillingen støtter antagelser om at høyere sommertemperatur, større smeltevannsstrømmer og smelting av permafrost kan være en av hoved-driverne for erosjon i dette området. En stor feilkilde i denne fremstillingen er naturlig nok opptegning av gjennomsnittlige erosjonsrater og ikke årlige målte rater.



Figur 9 Gjennomsnittlige erosjonsrater pr år i cm (venstre side), plottet mot sommertemperatur Svalbard (skala høyre side). (Temperaturer er hentet fra [www.climate4you.com](http://www.climate4you.com)).





Figur 10 Presentasjon av målepunkt utført med DGPS, 2010, 2011 og 2012 (Tangen og Justad et al. 2011 og 2012).

## Mulige fremtidige byggematerialer

Erosjonssikring av Fredheim er tenkt utført med en front utført i tre-materialer, alternativt med stein som byggemateriale. Tre er valgt med bakgrunn i to forhold: I strandsonen på Svalbard finnes mye drivtømmer og på enkelte steder er volumet av drivtømmer så stort at det preger naturen og kan regnes som et naturlig element. Det andre forholdet som favoriserer tre som byggemateriale er knyttet til tradisjonen ved bruk av tre som erosjonssikring ved eldre kystkonstruksjoner som finnes i alle bosetninger i og utenfor Isfjorden. Uansett valg av byggemateriale er det ved en eventuell bygging av erosjonssikring mulig å "ta tilbake" deler av det eroderte kystlandskapet.

Ved bruk av tre vil det være nødvendig å bruke lokale jordmasser hentet fra strandsonen og i sjøen som tilbake-fyllingsmaterialer. Dette er sand og grus som legges opp bak erosjonssikrings-vegg. Med bakgrunn i dette er det gjennomført undersøkelser og analyser av jordprøver både fra strandsone og fra sjøbunn og sammendrag fra analysen finnes i tabell under. Resultater fra selve analysen ligger i kapittel 0 og 0. Stein er også presentert som byggemateriale, men dette er mer tenkt som et visuelt alternativ enn ett konkret forslag til løsning for erosjonssikring. Geologien i området er av en slik karakter at det ikke vil være mulig å finne stein som har så god kvalitet at den kan fungere som en god erosjonssikring over mange år. Erfaring ved bruk av stein fra Svalbard til erosjonssikringformål, som blant annet er utprøvd i Svea, viser at det er vanskelig å finne stein som er egnet for dette formålet (Finseth, J. et. al, 2009: Preventing coastal erosion in arctic areas; protection by use of Geosynthetics).

Tabell 4 Tabell med beskrivelse av jordprøver

Prøve	Antall prøver	Beskrivelse
Prøver fra Sjøbunn	5	Jord som i hovedsak består av sand/silt
Prøver tatt 30 cm under topp skråning	5	Grus med lite innslag av sand
Prøver tatt 100 cm over vannlinje i skråning	5	Grus med innslag av sand, ca 30 %



Disse resultatene viser at store deler av den jord som er vasket ut i strandsonen kan brukes som byggematerialer i en eventuell erosjonssikring av området. Egenskapene som etterspørres i en slik sammenheng er velgraderte masser uten for høy finstoffandel. Dette gir mulighet for å bygge en stabil fylling, samtidig som vann kan renne relativt fritt gjennom den tilbakefylte jorden. Presentasjon av metode for erosjonssikring finnes i kapittel 0.

## Erosjonsrater

Kysterosjon truer bygningene på Fredheim med en hastighet som krever nødvendige tiltak hvis kulturarven skal forbli intakt i årene fremover. To erosjonsrater; 25 og 57 cm/år er tidligere rapportert (Johannessen 1997, Flyen 2009). Nyere studie utført av SINTEF og UNIS, 2010-2012 har målt et gjennomsnitt på ca 17,5 cm erosjon pr år. Det er viktig å merke seg at målinger ble utført med visuell bedømming av retning, parallelt med veggene av bygningene. På grunn av høye erosjonsrater, har Danielbu blitt flyttet tilbake fra kanten i 2002 (Woolley, 2002) og uthus ble flyttet etter måling i 2010, men det er ikke kjent hvor langt (Tangen og Justad et al. 2012). Målinger fra nødhytte til kant ble første gang gjennomført i 2011. I tabell under er minimum antall leveår for bygningene beregnet, i forhold til å bli tatt av erosjon. Disse tallene forutsetter at gjennomsnittlig erosjonsrate er konstant i årene fremover i forhold til de målte rater i alle tre studier (Johannessen 1997, Flyen 2009 og Tangen, Justad et al. 2012). Når det gjelder de beregninger som er gjennomført vil alle bygg være tatt av erosjon i løpet av de neste 150 årene, men ser en bort fra nødhytte så vil resterende bygg være borte innen de neste 40 - 50 år, igjen forutsatt konstante erosjonsrater basert på scenarioet basert på målinger de siste to år.

Tabell 5 Beregnet antall år før bygninger er tatt av kysterosjon forutsatt konstante erosjonsrater i årene fremover. Tabellen viser tre scenarioer basert på de tre gjennomførte studiene.

Bygning	Johannessen 1997	Flyen 2009	SINTEF/UNIS (2010-2012)
Uthus	14 år	6 år	20 år
Nødhytte	109 år	48 år	156 år
Hovedhus	35 år	15 år	50 år
Danielbu	29 år	13 år	42 år

Tabell 6 Maksimum gjennomsnittlig erosjonsrate og minimum antall år før husene er tatt av erosjon.

Bygning	Maks erosjon (cm) (studie 1986-2012)	Levetid (1987-2012)	Maks erosjon (cm) (studie 2010-2012)	Levetid (2010-2012)
Uthus	38 cm	9 år	6 cm	60 år
Nødhytte	-	-	37 cm	74 år
Hovedhus	51 cm	17 år	78 cm	11 år
Danielbu	31 cm	24 år	63 cm	12 år

Det er mange utenforliggende naturlige forhold som kan påvirke de tallene som er presentert i Tabell 5 og 6. For eksempel vil stadig utbredelse av deltaet for Sassen elven kunne beskytte kysten i større grad enn tidligere motbølger fra vest-sør/vest. På den annen side vil et mulig endret klima kunne føre til større nedbørsmengder og varmere sommertemperaturer, som igjen vil påvirke vannstrømningen i bakken, som altså er en negativ faktor i forhold til fremtidig erosjon. Fjelldybde under husene er også en viktig faktor som ikke er tatt inn i denne studien. Ved å gjennomføre borer i området vil det være mulig å bestemme dybde til fjell for å se om erosjonstrussel knyttet

til erosjon av løsmasser er reell, eller om dybde til fjell er så liten at erosjon av kysten vil stoppe opp i løpet av få år.

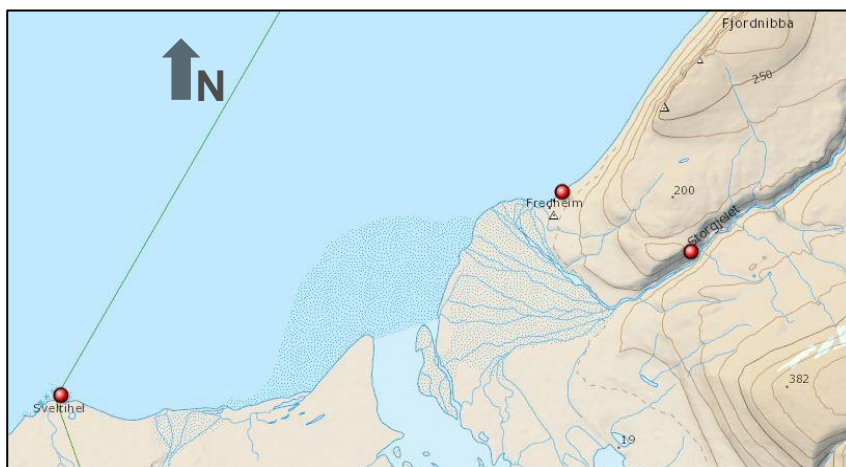
## Geologi

### Bedrock Geology of Fredheim

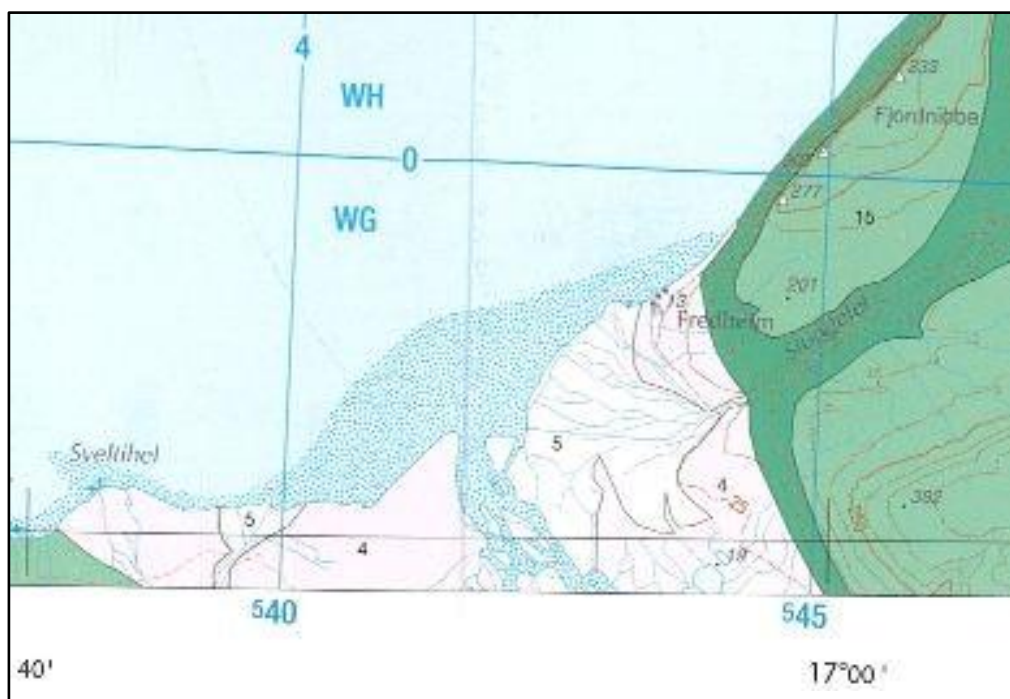
The bedrock in the vicinity of Fredheim has been identified as Gipshuken Fm. of Sakmarian – Artinskian age (Ma) of the Gipsdalen Group (Cutbill and Challinor 1965; Major and Nagy 1972; Dallmann, Kjærnet et al. 2001). The Gipshuken Fm. at Storgjelet and Sveltihel is described as platform deposits of limestone/dolomite containing marly, shaley or sandy interbeds and thin gypsum layers (Major 1972). This is representative of the upper section of the Fm. which has informally been named the Skansdalen Mb. by Dallman et al. (2001) who further describes the deposits as consisting of regularly bedded dolomites containing intercalated marly beds where bioturbation, algal mats and erosional surfaces are commonly found. The sediments represent cyclic deposits and are interpreted to have developed in a sabkha flat environment trending toward lagoonal deposition (Dallmann, Kjærnet et al. 2001; Hüneke, Joachimski et al. 2001; Blomeier, Scheibner et al. 2009).

Prior to this report, the formation in the area has been described at two locations: at Storgjelet in Nøis Valley South-east of Fredheim, and Sveltihel, on the coast west of Fredheim (Major 1972) (Figur 11). However, the most recent bedrock geology map of the Billefjorden area does not include the findings at Sveltihel but rather labels the entire Sassendalen mouth as Quaternary deposits (Lauritzen, Salvigsen et al. 1989) (Figur 12). It has only been within the last two decades that bedrock has become exposed on the coastal escarpment and beach directly in front of Fredheim and thereby linking the two locations. It is therefore apparent that an update in the geological map may be necessary in the near future. Having applied the use of ground penetrating radar (GPR) in combination with outcrop description and analysis it is proposed that the buildings in Fredheim sit on approximately 2 meters of unconsolidated alluvial sediments of the Quaternary that are underlain by the Gipshuken Fm. of the Late Carboniferous – Early Permian.

Up until this project there has been no evaluation of the rock and sediments at Fredheim in consideration of engineering or coastal protection. It has therefore been of interest to assess the bedrock quality and conduct grain size analysis of unconsolidated sediments for building assessment.



Figur 11 Red points mark geological outcrops made up of the Gipshuken Fm. at Svelthel, Storgjelet in the Nøis Valley and Fredheim. The main river is Sassen River, flowing from Sassen Valley. Image adapted from Norsk Polarinstitutt, Interaktiv Kart TopoSvalbard.



Figur 12 Geological map excerpt of Fredheim as created by Norsk Polarinstitutt (Lauritzen et al. 1989). Dark green is the Gipshuken Fm. and light green is the Kapp Starostin Fm. above. The off white areas represent fluvial and marine unconsolidated deposits. Note how there is no bedrock described at Svelthel or Fredheim.

## Methods

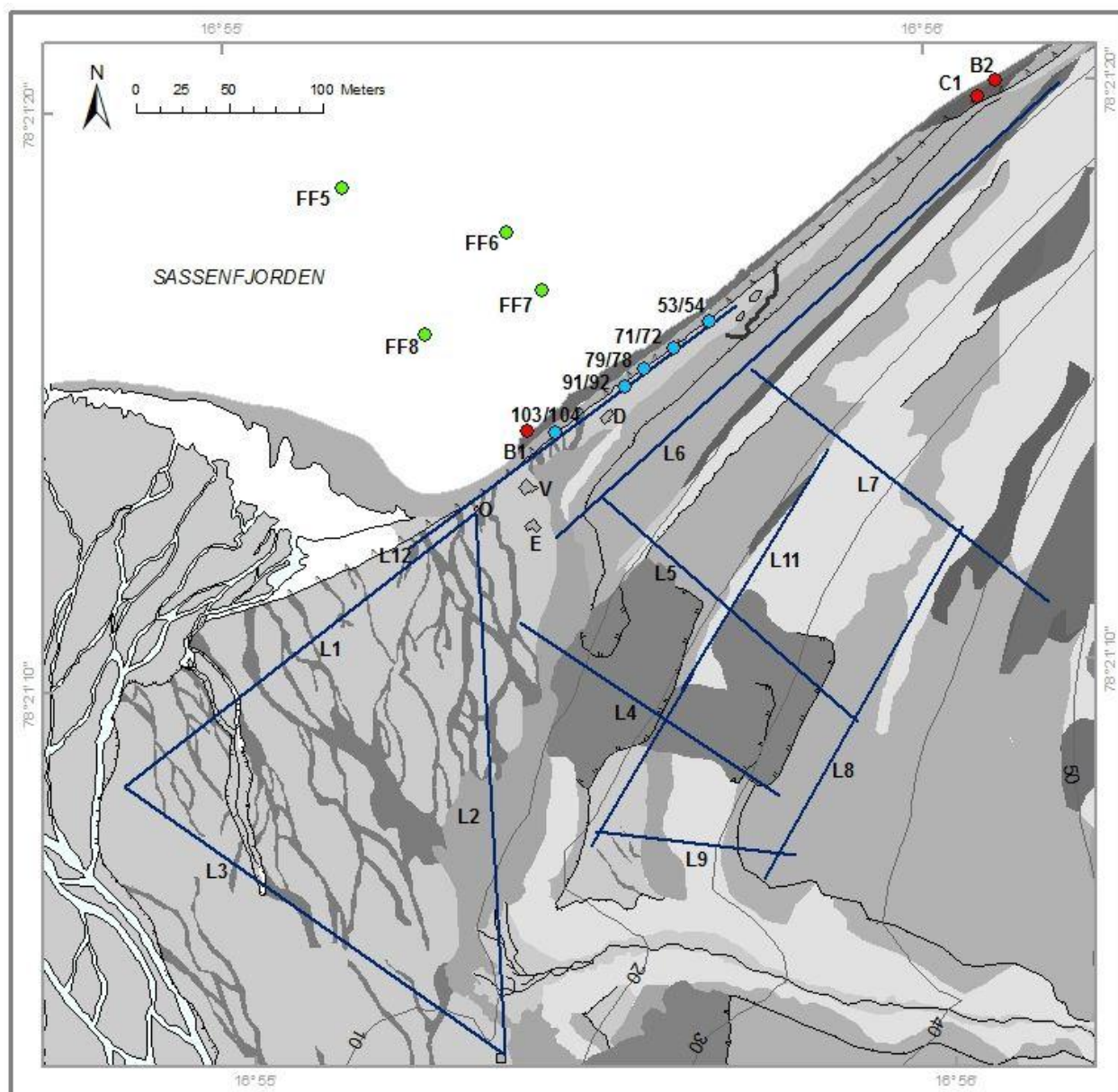
Fredheim has been visited on a number of occasions to conduct fieldwork for the *Fredheim Visualization Project*. In August 2011 and June 2012 sediment samples were collected from the coastal escarpment. Soil samples were sampled both from the escarpment and the sea bed, and brought to the Geotechnical laboratory at NTNU (University of Trondheim) for grain size distribution

analyses. Soil samples from escarpment were collected by shoveling and sea bed samples were sampled by use of a grab sampler. On the same field excursions, differential GPS measurements of the coastal cliff were taken to assess the erosion of the escarpment. GPS point references are given in the WGS84 datum and projected in UTM Zone 33X. Bedrock samples for further analysis were also taken in the same time periods and tested for carbonates using a diluted HCl solution.

Bedrock quality was estimated and results presented in Tabell 7 and 8, using the Q-system as described by (Barton and Choubey 1977) which states that

$$Q = (RQD/J_n) * (J_r/J_a) * (J_w/SRF) \quad [1]$$

Where  $Q$  is the rock quality,  $RQD$  is the rock quality designation determined by the percent of competent drill-core sticks > than 10 cm in length,  $J_n$  is the joint set number,  $J_r$  is the joint roughness number,  $J_a$  is the joint alteration number,  $J_w$  is the joint water reduction factor and  $SRF$  is the stress reduction factor.  $(RQD/J_n)$  provides a crude measure of block size,  $(J_r/J_a)$  produces an estimate of the roughness or friction of surfaces and  $(J_w/SRF)$  results in a ratio of two active stress parameters. This empirical system allows for a subjective evaluation of rock quality. The numerical value of the index  $Q$  varies in logarithmic scale from 0.001 to 1000 where low values are poor rock and high values have higher stability. In Fredheim, there is only one outcrop along the beach where samples have been taken, however if future work is planned it would be beneficial to drill a core to better understand rock quality for building and protection purposes.



- Bedrock, Gipshuken Fm.
- Marine beach material: well rounded tabular clasts
- Fluvial material, bi-modal sediment
- Organic material, high water content and vegetation
- Active layer detachment slide, vegetated overridden by gelifluction
- Gelifluction material, vegetated terrace
- Relict river/groundwater channel, loss of fines, high vegetation
- Beach deformation by ice
- Slide scarp
- Coastal erosion scarp
- Fluvial erosion scarp
- Terrace edge
- Water
- Cultural heritage infrastructure
- Marine sediment samples
- Terrestrial sediment samples
- Bedrock samples
- Georadar lines

Figur 13 Showing sediment deposits and sample locations. The buildings are marked as Outhouse (O), Main Villa (V), Emergency Hut (E) and Danielbu (D). Inside of the beach deformation area are two crushed boats. Note bedrock at the base of Marine deposit slopes. (Figure adapted from Sessford 2012, Master Thesis in Preparation).





Figur 14 Aerial image from 1990 displaying sediment plume from Nøiselva carried by longshore drift toward the east. Orange line indicates extent of the delta and coastal cliff in 2009 as measured with DGPS. (Image adapted from Norsk Polarinstitutt image S90 2207).

## Site Descriptions

Between 1990 and 2009 delta growth has been significantly high and Quaternary cliff sediments have undergone erosion (Figur 14) (This study). Two rates of erosion, 25 and 57 cm/year have been reported (Johannessen 1997, and Flyen 2009, respectively). Whichever rate may be the most accurate, it is apparent that the loose sediments are rapidly being washed to sea and thereby exposing the underlying bedrock unit. Bedrock exposure on the beach and shore face is visible from the Villa at  $16^{\circ} 56' 23,576''$  E,  $78^{\circ} 21' 13,91''$  N and extends eastward beyond the main cliff forming outcrop at  $16^{\circ} 56' 2,214''$  E,  $78^{\circ} 21' 19,763''$  N (Figur 13 and 15).



Figur 15 Bedrock outcrop at  $16^{\circ}56'2,214''$  E,  $78^{\circ}21'19,763''$  N, used for Q-system rock quality evaluation and samples C1 (detached from top of outcrop) and B2 (previously detached and found on beach below outcrop). (Photo: Sessford, July 2012).



Figur 16 Samples C1 (left) and B2 (right)



Figur 17 Sample B1

Three bedrock samples have been collected from the beach and shore face; one, directly in front of the Villa (B1), one from on top of the outcrop shown in Figur 16 (C1) and the third from directly below the cliff face (B2) (Figur 16 and Figur 17). Bedrock is exposed again higher up on the marine terraces between MT1 and MT2 (Figur 13). This is a blockfield like exposure that is heavily frost shattered and broken. This trend continues with all exposures of reoccurring bedrock, each at the base of the slope between two terraces, and heavily weathered both chemically and mechanically (Figur 18 and 19). Bedrock samples are described in the next section.



Figur 18 Chemical and mechanical weathering on bedrock outcrops on terraces (photo: Sessford 2012).



Figur 19 Bedrock outcropping on marine terrace (Photo: Sessford 2012).





Figur 20 Spring melt-water flowing from snowpack along relict river and flowing over escarpment edge (Photo: Sessford, June 2012).



Figur 21 Surface water flowing from spring meltwater into bog and then out toward the fjord along vegetated relict river channel (Photo: Sessford, June 2012).

Fredheim itself lies on pre-recent fluvial sediments, meaning that the current river is not reworking sediment deposits. However, relict fluvial channels continue to be used as ground and melt water runoff channels during the spring and summer seasons (Figur 20 and 21). Several terrestrial samples have been taken from the escarpment and are described in the terrestrial section of this report. A present day pro-grading river energy dominated delta fed by the River Nøis lies directly to the west of Fredheim (Figur 13, 14 and 22). Within the last two decades the delta has extended approximately 125 m toward the east and in the process, protecting sections of the coastal escarpment (Guegan and Sessford in prep.). Sassenfjordenen is a fjord branch from the main Isfjorden system in Western Spitsbergen. Fjord sediment samples are described in the marine description section of this report.



Figur 22 The Nøis River prograding delta has extended toward the east by approximately 125 metres in the last two decades (Photo: Sessford, August 2011).

## Bedrock Sample Descriptions

### Sedimentological Structure

Sample B1 and C1 were detached from the bedrock when sampled whereas B2 had already been disconnected from the main source and exhibits intense weathering by wave action (Figur 16 and Figur 17).

All samples are limestone/dolomite and clearly display sedimentological signs of the Gipshuken Fm. as the rocks are made up of undulating layers of shale, marl and algal mats. Cavities exhibiting mineral growth are present, varying in size up to 7 and 2 cm in length and width respectively. HCl tests resulted in varying effervescence (bubbles) strength indicated differences in carbonate content between samples. Samples B1 and C1 show strong effervescence and B2 display almost none. However, all other bedrock exposures from the marine terraces exhibit strong to violent effervescence, suggesting that overall, the rock has high carbonate content. It is therefore likely to be of the Gipsdalen Group of the Gipshuken Fm. as described by Dallmann (2001).

### Q-system Rock Quality

The outcrop used in rock quality evaluation is shown in Figur 16 and results are shown in Tabell 7. The quality is evaluated using Tabell 8. One can see from Tabell 7, that the rock quality designation (RQD) is considered relatively poor and that two joint sets ( $J_n$ ) dominate in the rock, yet there are some random joint sets scattered within the section. The joint roughness ( $J_r$ ) represents smooth planar to rough or irregular planar for rock wall contact. The least favourable joint alteration ( $J_a$ ) in the section is softening or low friction clay mineral coatings such as gypsum which coincides well with the limestone/dolomite of the Gipshuken Fm. Joint water pressure ( $J_w$ ) numbers suggest medium to large inflow or high pressure with occasional to considerable outwash of joint fillings. The stress reduction factor (SRF) indicates single weakness zones containing clay or chemically disintegrated rock when depth of excavation is less than or equal to 50 m. It can be seen from Figur 16, that the bedrock has been heavily weathered. This is due to a combination of chemical and mechanical weathering from wave action during storm events, sea ice thrusting and ride up, and periglacial processes due to permafrost such as frost shatter. It is likely that the effects of permafrost penetrate approximately 2 m into the bedrock from any exposed surface.

Tabell 7 Rock mass quality Q-system results for bedrock outcrop at Fredheim.

	RQD	$J_n$	$J_r$	$J_a$	$J_w$	SRF	Q
Outcrop Typical Range	40	1	0.5	2	0.33	5	0.165
Outcrop Most Frequent	30	4	1	4	0.33	5	0.231

Tabell 8                      Quality classes for Q-values as described by Barton (personal communication). From this table one can see that at Fredheim there is extremely poor Class F rock.

Q-Value	Class	Rock Mass Quality
400 ~ 1000	A	Exceptionally Good
100 ~ 400	A	Exceptionally Good
40 ~ 100	A	Very Good
10 ~ 40	B	Good
4 ~ 10	C	Fair
1 ~ 4	D	Poor
0.1 ~ 1	E	Very Poor
0.01 ~ 0.1	F	Extremely Poor
0.001 ~ 0.01	G	Exceptionally Poor

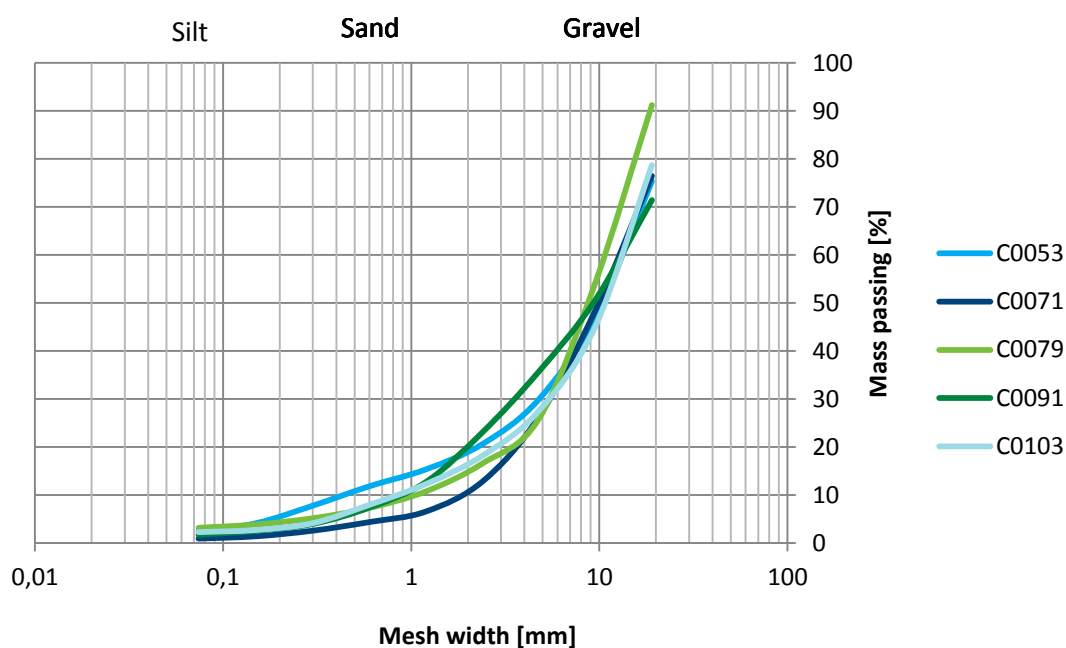
## Unconsolidated Sediments

### Terrestrial

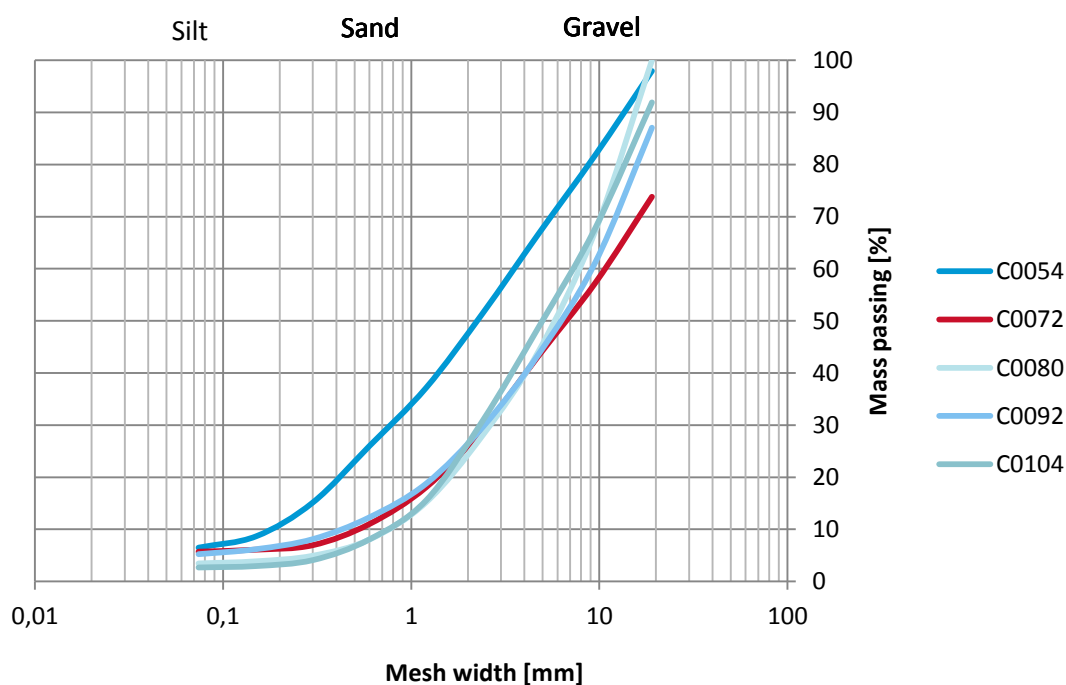
The buildings at Fredheim sit on unconsolidated relict fluvial deposits which are composed mainly of bimodal sand and gravel sediments (Figur 23). There are less than 10% fines entering into the silt fraction and none within clay (Figur 24 and 25). For this reason there is very little ground ice as water is well drained. Relict alluvial channels can be seen on the surface of the ground as highly vegetated elongated and braiding depressions, and in the escarpment clearly by typical rounded clasts and curved channel fill clast orientation. Channels have lower quantity of fines as they are washed out easier than the larger clasts. At the escarpment, back-cutting of channels causes higher erosion rates than inter-channel areas (Figur 26 and 27).



Figur 23                      Unconsolidated bimodal fluvial sediments that make up the coastal escarpment. Note the positioning of the stones indicated by the curved line in the cliff section (marked in red) which show a distinct channel deposition above which vegetation is growing. The blue section is scree deposits from erosion of the escarpment. (Photo: Sessford, October 2011).



Figur 24 Grain size analysis results for samples taken approximately 30 cm below escarpment top. Series labels correspond to DGPS measurement locations as shown in Figur 13.



Figur 25 Grain size analysis results for samples taken in the middle of the escarpment approximately 1m above the base and directly above scree accumulation. Series labels correspond to DGPS measurement locations as shown in Figur 13.





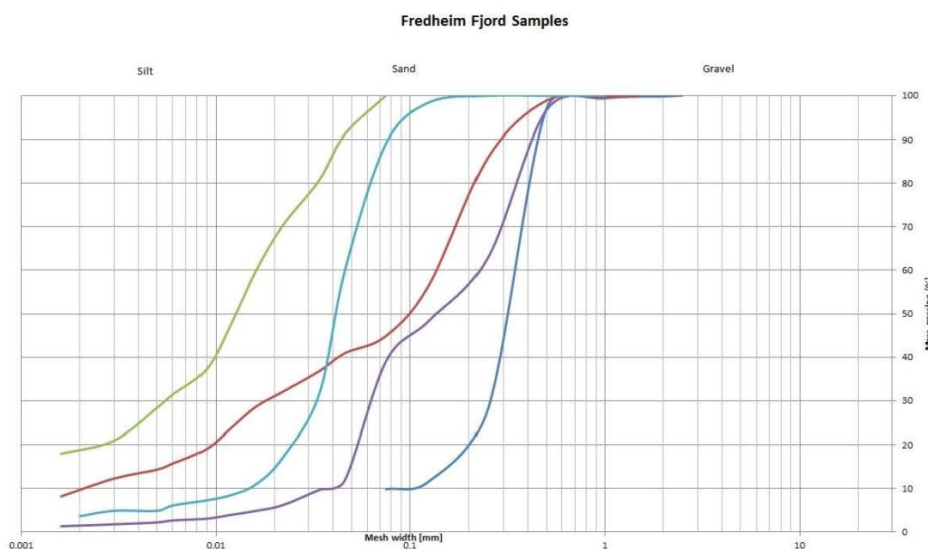
Figur 26 A relict channel that reaches the coastal escarpment and is undergoing higher erosion than inter-channel zones (un-vegetated). (Photo: Sessford, August 2011).



Figur 27 Oblique photo of Fredheim distinctly showing snow catchment areas in vegetated relict fluvial channels (Photo: retrieved from Pedersen Archives approx. date of image 1965).

## Marine

Fjord sedimentation in the vicinity around Fredheim is dominated by sediment input from Sassen River flowing out of Sassen Valley and the Nøis River that flows from Nøis Valley (Figur 11). Four sediment samples from the fjord in front of Fredheim have been analyzed through grain size distribution and hydrometer tests (Figur 28). The results show that the sediments have significantly high silt fraction with the exemption of sample FF6. As the delta is to the west of Fredheim, and presently building out toward the east it can be assumed that longshore drift is a commanding factor in sediment deposition in front of Fredheim during the summer months when sea ice is not present. In winter on the other hand, large deposits of sea ice pile/ride up inclusive of large icebergs are pushed onto the Nøis Delta from the east (Figur 29 and 30). Sample FF6 might represent an iceberg plunged deposit.



Figur 28 Grain size results for fjord floor sediments in front of Fredheim where FF5, FF6 and FF7 are the blue, red and green lines respectively.

Tabell 9 Percentage of fine grains in fjord sediment samples.

Sample	% < 0,075 mm	Dominant fine grain
FF4	100	Medium-coarse silt
FF5	44,87	Medium silt
FF6	9,82	No Hydrometer needed
FF7	89,06	Coarse silt
FF8	39,06	Coarse silt





Figur 29 Sea and glacier ice pushed up onto delta from the east (photo taken approximately 30 m from delta edge) (Photo: Sessford, March 2012).



Figur 30 Ice piling up on edge of delta in front of Fredheim. Note the absence of sea ice in March (Photo: Sessford, 2012).

## Hazards

It should also be noted, that the buildings are not only in danger of coastal erosion, but also of damage by active layer detachment slides. These are slides or earth flows along a shearing surface consistent with the active layer of permafrost. The marine terraces above the buildings have many active layer detachment scars and deposits indicating that the slopes are unstable (Figur 13 and 31). These detachments have also provided a channel system for spring melt-water to flow and gelifluction to actively cause creep of the surface sediments. With this in mind, one should be aware that moving the buildings to a new location to protect them from coastal erosion may not be the most preferable means of protection due to other hazards in the area.



Figur 31 Active layer detachment slides behind buildings. Note channel like vegetated areas below scarps with high gelifluction and vegetation. (Photo: Sessford 2011).



## Summary of Geology

Through this investigation it can be said with confidence that the bedrock at Fredheim has become exposed due to coastal erosion in the last two decades. This bedrock, of the Gipshuken Fm. is of poor quality and as it becomes more exposed to the elements is likely to deteriorate even more rapidly. It appears that as the limestone/dolomite becomes jointed it becomes more permeable and blocks become detached and fall off the escarpment. In regards to unconsolidated sediments, Fredheim rests upon approximately 2 m of bimodal fluvial sediments that when exposed to flowing water are exceptionally erodible. In addition to fluvial and coastal erosion the area is prone to gelifluction and active layer detachment slides causing unstable soil.

## Discussion Geology

After reviewing the bedrock geology and unconsolidated sediments in the Fredheim area it is necessary to discuss the processes affecting coastal erosion and the implications they may have on the cultural heritage buildings. Through word of mouth, it has been said that when Fredheim was built in 1924 it was approximately 60 m from the buildings to the coastal escarpment. If this is the case, it is apparent that coastal erosion used to be significantly higher than it has been in the last two decades. With this understanding, it can be presumed that since the Nøis River Delta has begun to pro-grade into the fjord it has undertaken the role of natural coastal protection from wave action. However, it is apparent that erosion is still occurring even though the delta has begun to expand and protect (Figur 14). It can be seen in the field, and from images that waves are not hitting the coastal escarpment so wave action may be negligible except perhaps in extreme storm events (Figur 32). The possibility of sea-ice and icebergs attaching itself to the cliffs and plucking sediments off is a much more probable form of erosion at present (Figur 33). On the other hand, it has been shown in Tangen et al. 2012 that there are higher erosion rates where relict channels are located. This suggests that ground and surface water flow from spring melt water are high erosion agents.

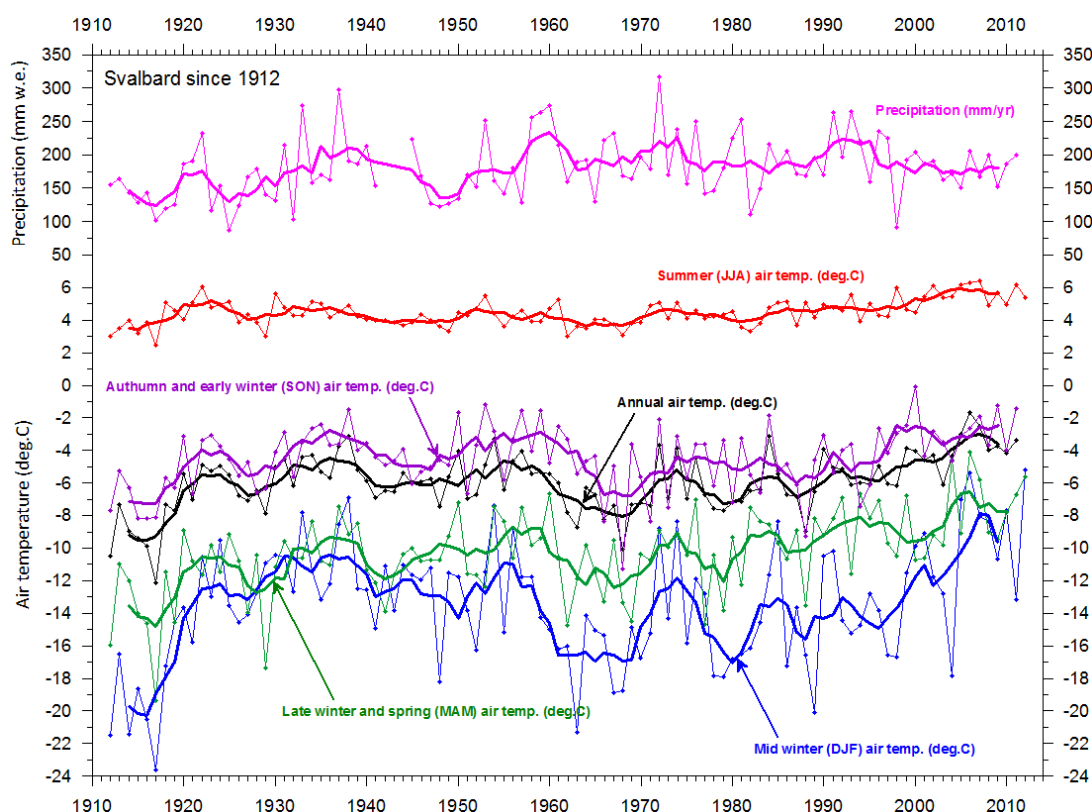
It seems probable that melt water runoff has increased in the past decades due to rising spring and summer temperatures coinciding with increased winter precipitation (Figur 34). If there is more melt going on upstream along Sassen River and Nøis River, it is likely that more sediment is entrained and transported to the mouth of the river thereby providing sediment for delta build-up. It also causes increased surface and groundwater flow along relict channels, and thereby contributing to higher erosion rates where these channels are located.



Figur 32 Waves do not hit coastal escarpment even at high tide. (Photo: Sessford, June 2012).



Figur 33 Ice foot attached to coastal escarpment possibly acting as an eroding agent through plucking of sediments. (Photo: Sessford March, 2012).



Figur 34 Precipitation and temperature data for Svalbard from 1912 to 2012 (Accessed on 27.11.2012 from [www.climate4you.com](http://www.climate4you.com)).

## Erosjonssikring av Fredheim

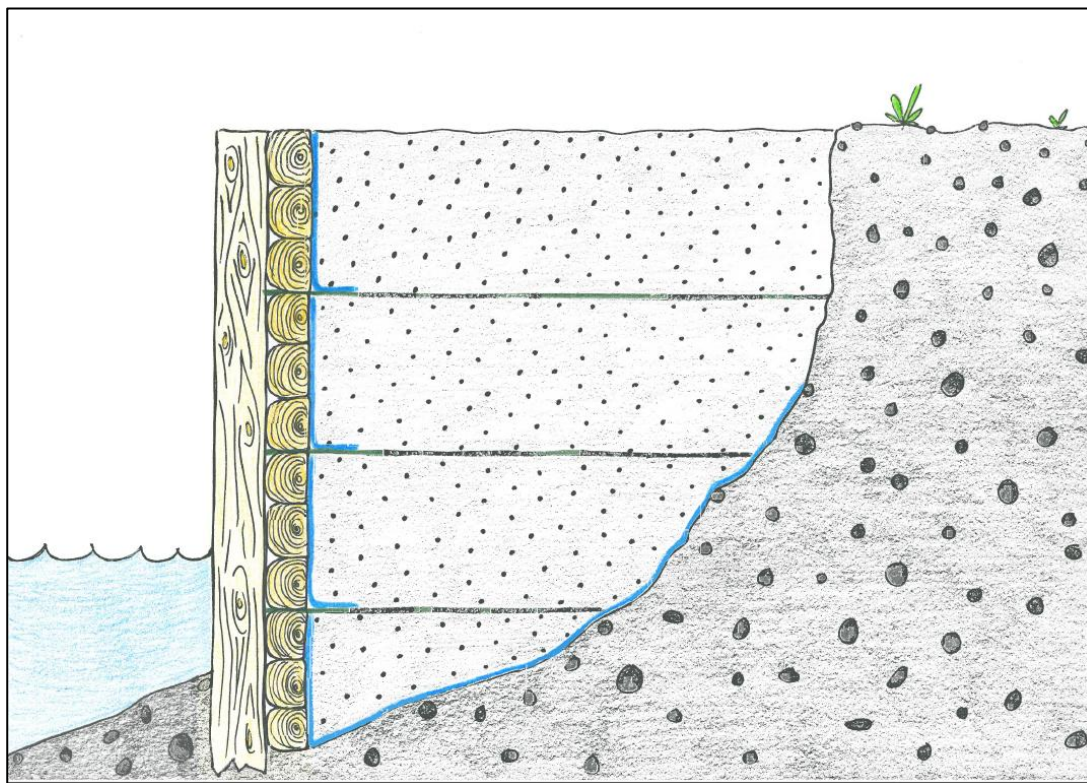
Med utgangspunkt i funn gjennom prosjektet "*Bygging i strandsonen på Svalbard – Hva forteller fortidens kaier oss om fremtidens anlegg*", ble det allerede på idestadiet til dette prosjektet besluttet av prosjektgruppen at en eventuell konstruksjon knyttet til erosjonssikring av Fredheim måtte ha treverk som hovedbyggemateriale. Spesielt erosjonssikringer av treverk viser en sterk evne til å motstå krefter fra sjø og is i Svalbards fjorder, som observert i Pyramiden og Barentsburg. I Pyramiden og Coles Bay er det i tillegg mulig å observere senkekaskekonstruksjoner, brukt som deler av kaikonstruksjon, der byggemåten viser en enestående evne til å motstå havets og polarvinterens krefter. Med dette som utgangspunkt presenterer denne rapporten et knippe forslag til mulige løsninger vedrørende erosjonssikringer utført med tre som materiale, gjengitt i hovedsak som manipulerede bilder, men også i skisseform. Det er ikke et mål i seg selv å kopiere eldre byggeskikk, da det har skjedd en stor utvikling vedrørende erosjonssikringsmetoder og muligheter for forsterkning av disse ved hjelp av moderne materialer og teknikker. Derimot kan en kombinasjon av materialer og teknikker gjennom et århundre forenes for å oppnå et godt teknisk resultat og en estetisk tilpasset sikring. I tillegg til å presentere mulige modeller utført hovedsakelig i treverk vil vi som et alternativ presentere en mer konvensjonell erosjonssikringsmetode, der hovedbestanddelen av byggemateriale er stein. Denne metoden er derimot ikke presentert på detaljnivå.

## Byggeteknikk

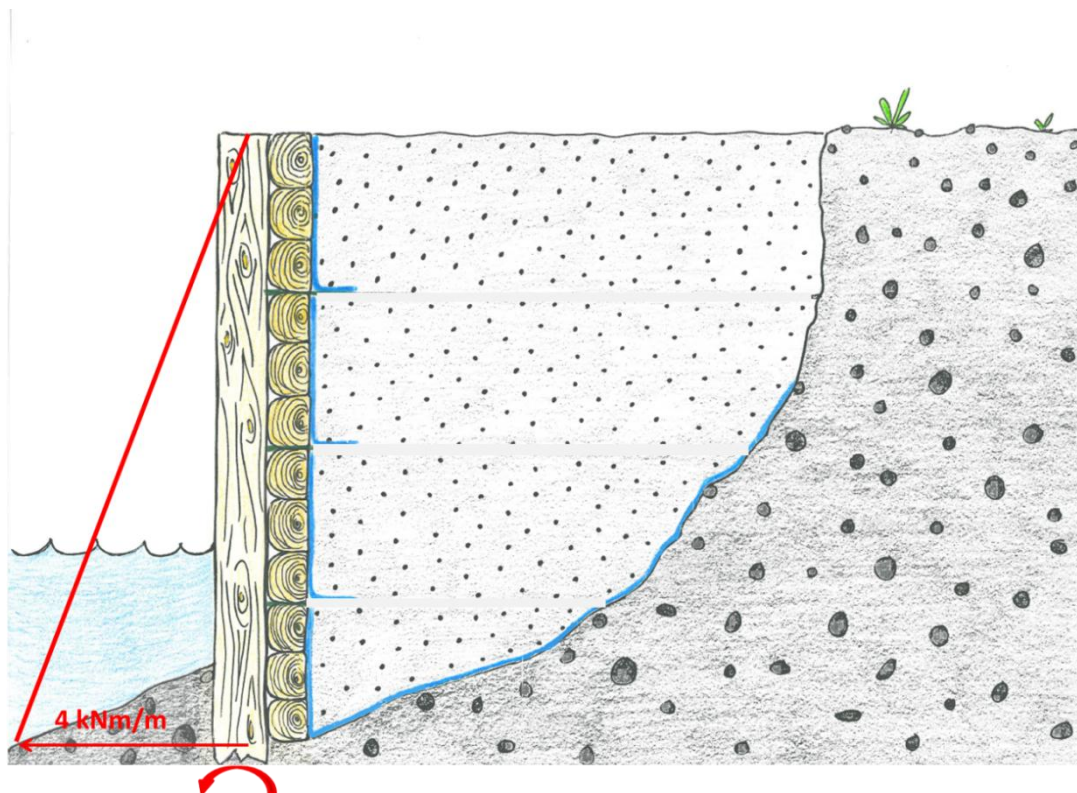
Som nevnt over vil tre, eller tømmer, være hovedmateriale i de forslagene som. En trekonstruksjon alene, som en vegg mot sjøen med bakenforliggende jordtrykk vil kunne bli påført store statiske og dynamiske krefter, spesielt vil trykk fra bakenforliggende jord være en stor utfordring. For å gi selve vegg i front mindre påkjenning bakfra foreslås det å kombinere treverk med geosynteter. Geosynteter er kjent blant folk flest som "veiduk", men produseres i et utall varianter og materialer, spesialdesignet for å ta opp krefter i jord brukt som armering, eller fungere som et separasjonslag, der jorden holdes på plass og vannet kan strømme fritt gjennom sand og grus. Figur 35 er en prinsippskisse av en mulig konstruksjon som muliggjør å "ta tilbake" ca 2 meter av kysten som er erodert.

I front av vegg bores peler ned til nødvendig dybde og bak disse etableres tømmer horisontalt, eventuelt en kombinasjon av horisontalt og vertikalt tømmervirke for å oppnå ønsket fasade av erosjonssikringen. Typisk for en slik konstruksjon er at pålen utsettes for et visst moment, dvs en kraft som vil bidra til at erosjonssikringsveggen vil ha et bakenforliggende trykk som kan føre til at pålen knekker hvis den ikke får tilstrekkelig hjelp til å motstå kreftene. Et eksempel på moment kan være en lyktestolpe i vind. Hvis vinden blir sterk nok så brekker lyktestolpen. Typisk måte å redusere faren for at stolpen brekker vil være å spenne den fast med vaiere, i flere høyder, for å redusere momentet. For å redusere momentet i erosjonssikringskonstruksjonen så er det nødvendig å legge inn flere anker for vegg slik at momentet reduseres. De horisontale grønne linjene representerer jordforsterkning og forankring av vegg, og de blå linjene representerer separasjonsduk, see Figur 35. Med denne type jordforsterkning reduseres momentet på stolpe til 0 kNm/m i nedre del av stolpen som illustrert i Figur 36 og Figur 37. Dette betyr at stolpen som bores ned kan ha mindre dimensjon og ikke behøver å bli installert dypere enn at laster fra is og sjø ikke flytter denne. Faren for at den brekker på grunn av jorden bak er ikke lengre til stede. Den røde linjen i figurer 36 viser momentkreftene nedover stolpen uten forankring, og de svarte linjene i 37 viser de reduserte momentkreftene for den forankrede stolpen. Jorden som er fylt inn bak er av en karakter og sammensetning som sørger for god gjennomstrømning av vann, samtidig som separasjonsduk holder jorden på plass.

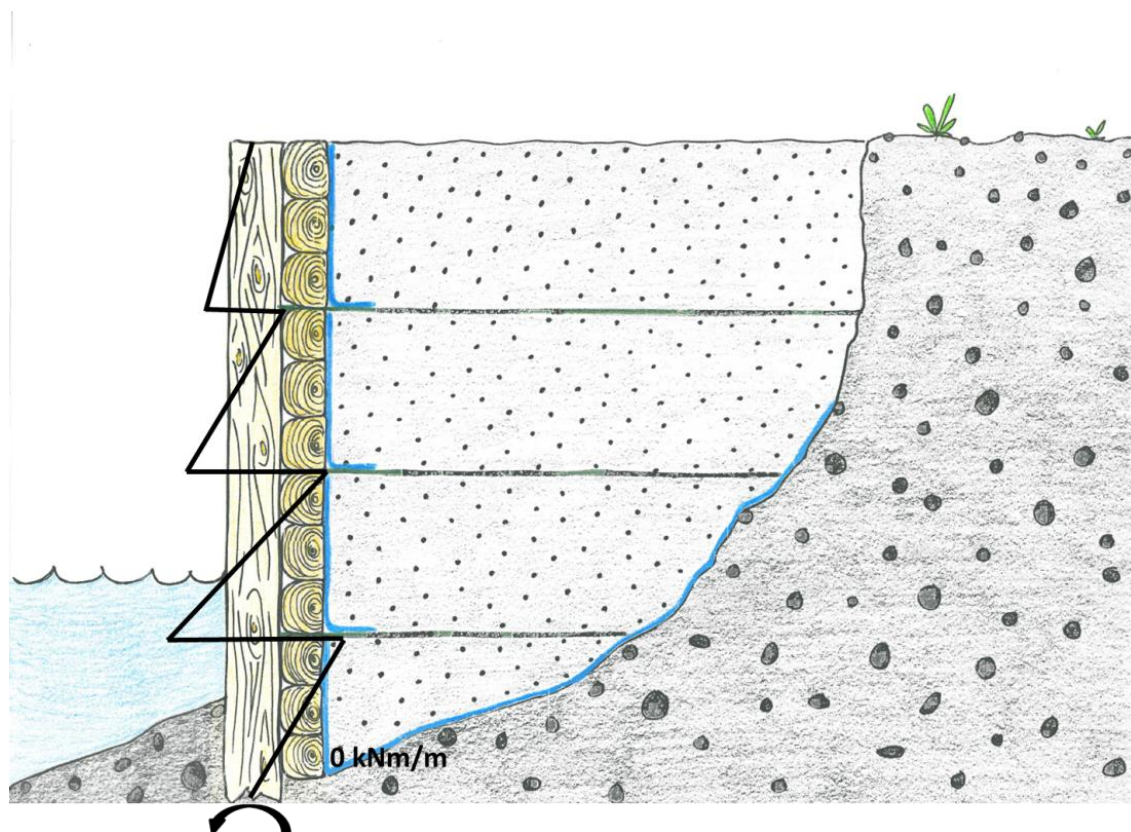




Figur 35 Prinsippskisse av erosjonssikring ved Fredheim.



Figur 36 Moment på stolpe uten forsterkning og forankring, eksempel.



Figur 37 Moment på stolpe med forsterkning og forankring, eksempel.

## Presentasjon av mulige løsninger for erosjonssikring av Fredheim

I dette kapittelet presenteres et knippe løsninger (fasader), basert på fotomontasje, for å illustrere en mulig erosjonssikring av Fredheim. De enkelte fasader, har fått navn etter hvor de er observert, og alle fasader i fotomontasjen er hentet fra eksisterende kaianlegg eller erosjonssikringer fra russiske bosetninger på Svalbard. Originale bilder fra de forskjellige bosetningene og fakta knyttet til disse er hentet fra rapporten *"Bygging i strandsonen på Svalbard – Hva forteller fortidens kaier oss om fremtidens anlegg"* (Finseth og Lothe 2011)

### "Barentsburg"

Det første forslaget som presenteres er utarbeidet av LPO Arkitekter i nord, ved Ingvild Sæbu Vatn, på oppdrag fra, og i samarbeid med SINTEF Byggforsk. Forslaget tar utgangspunkt i en eksisterende erosjonssikring i Barentsburg.





Figur 38 Erosjonssikring mellom to pirer i Barentsburg.

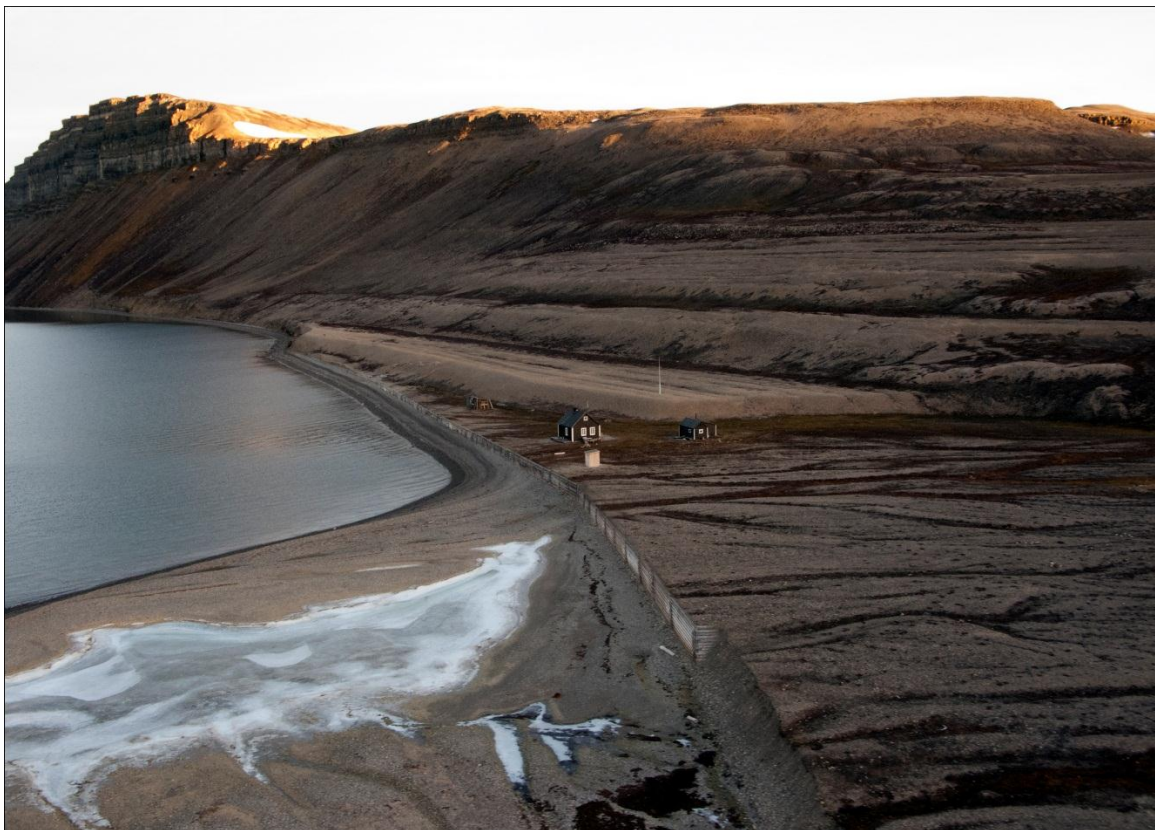


Figur 39 Visualisering: Sett fra nord, Tempelfjorden.





Figur 40      Visualisering: Sett fra vest, tempelfjorden.



Figur 41      Visualisering: Sett med fugleperspektiv fra sør.



Figur 42 Visualisering: Sett med fugleperspektiv fra sør.

## "Coles Bay"

De neste bildene som presenteres er utarbeidet av SINTEF Byggforsk ved landskapsarkitekt Bridget Thodesen. Det første alternativet tar utgangspunkt i en av senkekassene i Coles Bay, nordligste pir. Kassen er en del av brufundamentet og er et av de konstruksjonselementene som i særlig grad har tålt påkjenningene fra is og sjø gjennom mange tiår.





Figur 43      Motiv fra Coles Bay, nordligste pir.



Figur 44      Visualisering: Sett fra Vest, Sassenfjord.





Figur 45 Visualisering: Sett fra sør-vest, Sassenfjorden.



Figur 46 Visualisering: Sett fra nord, Tempelfjorden.

## "Pyramiden"

Denne erosjonssikringsfronten er laget med utgangspunkt i senkekassene som danner kaikonstruksjonen i Pyramiden. På samme måte som kaianlegget i Coles Bay har dette kaianlegget vist stor evne til å motstå naturkreftene, selv om forholdene i Billefjorden ikke kan sammenlignes med is og sjøpåkjenninger i Coles Bay. Senkekassene i kaikonstruksjonen ved Pyramiden har setningsskader, men dette tillegges fundamenteringsproblemer.



Figur 47      Visualisering: Kaikonstruksjon i Pyramiden etter senkekasse-prinsippet.





Figur 48      Visualisering: Sett fra Vest, Sassenfjorden.



Figur 49      Visualisering: Sett fra sør-vest, Sassenfjorden.





Figur 50 Visualisering: Sett fra nord, Tempelfjorden.

### Tradisjonell erosjonssikring

Det er vanskelig å komme utenom erosjonssikring bygget etter norske tradisjoner, med sprengstein, når ulike alternativer skal presenteres. Denne type sikring er en utfordring å bygge på Svalbard når steinmaterialet er av slik kvalitet at den ikke tåler den mekaniske påkjenningen, eller fryse-tine sykluser. Det finnes flere steinsatte kystområder i forbindelse med kaianlegg, både i Longyearbyen og i Svea, men disse er bygget opp med stein fra fastlandet.



Figur 51 Visualisering: Sett fra Vest, Sassenfjorden.



Figur 52 Visualisering: Sett fra sør-vest, Sassenfjorden.





Figur 53 Visualisering: Sett fra nord, Tempelfjorden.

## Diskusjon og konklusjon

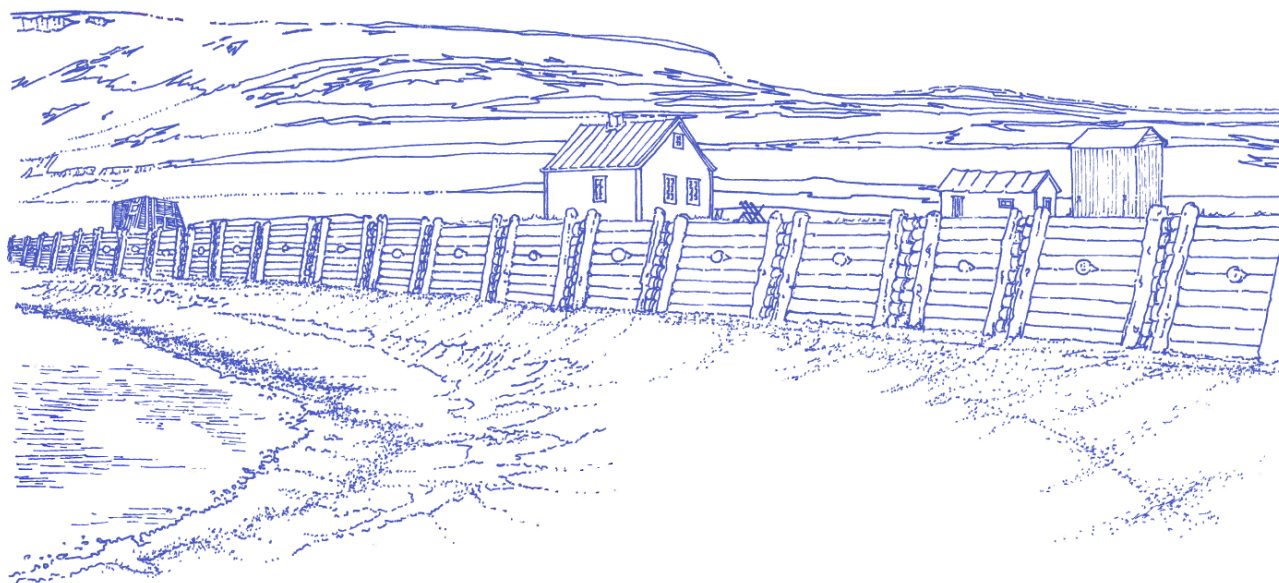
Målet med denne studien og rapporten har vært å se på nødvendigheten av, og muligheten for å bygge en erosjonssikring av Fredheim. Samtidig er visualisering av mulige løsninger tillagt stor vekt.

Mekanismer knyttet til erosjon av permafrost kyst finnes i mange variasjoner, de fleste, på detaljnivå, sannsynligvis særegen for den enkelte kystlinje. Funnene på Fredheim viser at den største driveren for erosjon sannsynligvis er knyttet til sommertemperatur, smeltevannskanaler i jorden og sekundært bølger som frakter bort de eroderte massene fra strandsonen og avsetter disse i fjorden der de største partiklene ligger nærmest land (grus/sand) og de fineste partiklene (sand/silt/leire) fraktes lengre ut i fjorden avhengig av størrelse.

I kapittel 0 presenteres funn knyttet til forskjellige risikoer for kulturminnet, ikke bare erosjon. Alle mulige risikoer er viktig å inkludere i en totalvurdering, men denne rapporten omhandler kun vurderinger og forslag til tiltak for å stoppe kysterosjon. I denne studien er det gjort et anslag av hvor lenge husene er trygge i forhold til erosjon, et anslag som kun bygger på tidligere målte erosjonsrater, og ikke tar inn over seg mulige forhold i, eller endringer i omgivelsene som for eksempel hvor ligger nivået for fjell under området hvor husene er plassert, endring av delta for Sassen-elven eller generelle klimaendringer. Skulle slike hensyn vært inkludert så ville dette nødvendigvis ført til en helt annen tilnærming til prosjektet enn den som er valgt i dette

visualiseringsprosjektet. Alle slike faktorer er viktige i forhold til å si kunne si noe om forventet levetid før en mulig ødeleggelse av husene på Fredheim, på den annen side vil et så stort arbeid, og analyse, kunne bli en større økonomisk belastning enn å gjennomføre tiltak.

Det økonomiske aspektet er ikke gjennomgått når det gjelder erosjonssikring av Fredheim, dvs at det ikke er gjort kalkyler eller anslag knyttet til kostnader ved å bygge erosjonssikring. Dette må ivaretas av en eventuell utbygger som også har ansvar for teknisk design. Dette var heller ikke en del av målet med denne studien. Målet har vært å lage en mulighetsstudie for erosjonssikring av Fredheim, med visualisering, og det arbeidet som er gjennomført viser at dette i høyeste grad er mulig å gjennomføre, selv om valg av fasade for en sikring blir avgjørende når det gjelder å bevare kulturminnet i mest mulig original stand ved et slikt inngrep. Anslag knyttet til levetid i forhold til erosjon tilsier at tiltak må gjennomføres og det vil i realiteten være kun to mulige løsninger; flytting eller erosjonssikring. Dette prosjektet har, bevisst, ikke tatt stilling til hvilken løsning som vil være mest forsvarlig, økonomisk og i forhold til kulturminneforvaltningen, men håper at rapporten kan være et viktig bidrag når det gjelder valg av løsning.



Figur 54 Skisse med erosjonssikring av Fredheim (Bridget Thodesen, 2012).

## Referanser

Barton, N. (2012). Personal communication. University Centre in Svalbard (AT-301) lectures in Rock Mechanics.

Barton, N. and V. Choubey (1977). The shear strength of rock joints in theory and practice. Rock Mechanics Meeting, Befo. Stockholm, Swedish Rock Mechanics Research Foundation: 95-117.

Bjerck, H. (1999). Erosjonsforebygning - Fredheim. Riksantikvaren. Longyearbyen, Sysselmannen På Svalbard: 1-7.

Blomeier, D., C. Scheibner, et al. (2009). "Facies arrangement and cyclostratigraphic architecture of a shallow-marine, warm-water carbonate platform: the Late Carboniferous Ny Friesland Platform in eastern Spitsbergen (Pyefjellet Beds, Wordiekammen Formation, Gipsdalen Group)." Facies **55**(2): 291-324.

Climate4you. (2012). Svalbard meteorological observations since 1912.  
[www.climate4you.com/SvalbardTemperatureSince1912.htm](http://www.climate4you.com/SvalbardTemperatureSince1912.htm). Accessed 01.11.2012.

Cutbill, J. L. and A. Challinor (1965). "Revision of the stratigraphical scheme for the Carboniferous and Permian rocks of Spitsbergen and Bjornoya." Geological Magazine **102**(5): 418-439.

Dallmann, W. K., T. Kjærnet, et al. (2001). Geological map of Svalbard 1:1000,000 Sheet C9Q Adventdalen. Temakart No. 31/32. Tromsø, Norwegian Polar Institute.

Finseth, J. and Lothe A. (2011) "*Bygging i strandsonen på Svalbard – Hva forteller fortidens kaier oss om fremtidens anlegg*". Rapport SINTEF Byggforsk og Svalbard Miljøvernfond.

Finseth, J. Andreassen, D., T., R., Wold, M., Øiseth, E., "Preventing coastal erosion in arctic areas; protection by use of geosynthetics", Strait Crossings 2009.

Flyen, A. C. (2009). Coastal erosion . a threat to the cultural heritage of Svalbard? Polar Research in Tromsø. J. Holmén. Oslo, Norwegian Institute for Cultural Heritage Research: 13-14.

Hüneke, H., M. Joachimski, et al. (2001). "Marine carbonate facies in response to climate and nutrient level: The upper carboniferous and permian of central spitsbergen (Svalbard)." Facies **45**(1): 93-135..

Johannessen, L. J. (1997). Villa Fredheim. Longyearbyen, Governor of Svalbard, Environmental Section, in cooperation with the Svalbard Tourist Board and Svalbard Museum: 1-15.

Lauritzen, Ø., O. Salvigsen, et al. (1989). Geological Map Svalbard 1:100 000, C8G Billefjorden. Oslo, Norsk Polarinstitutt.

Major, H. and J. Nagy (1972). "Geology of the Adventdalen map area." Norsk Polarinstitutt Skrifter(138).

Sessford, E. (2012). Master thesis in preparation. University of Oslo and the University Centre in Svalbard. Defence, May 2013.

Tangen, H. and J. Justad (2012). A survey on coastal erosion in Central Spitsbergen, Svalbard. SAMCot - Sustainable Arctic Marine and Coastal Technology. M. G. G. Bæverfjord, S. W. Danielsen and K. Heilemann. Trondheim, SINTEF: 61.

Tangen, H., J. Justad, et al. (2012). A survey on coastal erosion in Central Spitsbergen, Svalbard 2012. SAMCot. E. Balmand and A. Watn. Trondheim, SINTEF Building and Infrastructure: 54.

Woolley, R. (2002). Flytting og restaurering av Danielbua, Fredheim, Sassenfjorden, Svalbard, Kulturminne Nr. C9-077. Rapport fra den arkeologiske undersøkelsen Longyearbyen, Sysselmannen på Svalbard: 1-32.





Teknologi for et bedre samfunn

## **Appendix – (external disc)**

### **Automatic Camera Photos**

Fredheim time-laps 2012-2013(.jpeg images)

Skansbukta time-lapse 2011-2012 (.jpeg images)

### **Figures**

Map 1: Fredheim, Isfjorden, Svalbard Quaternary geology and geomorphology map, 1:3000 (PDF document)

Map 2: Skansbukta, Billefjorden, Svalbard Quaternary geology and geomorphology map, 1:2000 (PDF document)

Figure DR1: Guegan et al., (submitted, Geology) supplementary material (.jpeg image)

### **Measurements Sessford Thesis**

Active layer detachment slides (Excel file)

DR2 Supplementary material (Guegan et al., submitted (Geology)) (Excel file)

ErosionRates\_Fredheim (Excel file)

### **Pre-existing data sets**

Sea ice data 1986-2012 (Norwegian Ice Service) (Excel file)

SvalbardMetObs – Temperature and precipitation data from Longyearbyen airport (met.no) (Excel file)

### **Raw Data**

DGPS Raw (Differential GPS points for BASE station and Rover at both Fredheim and Skansbukta) (DBX files for processing in Leica GeoOffice Software, and RINEX files)

GPR MALAGS (Ground penetrating radar data, not used in thesis) (.rad files for processing in RadExplorer)

**NOTE:** All data originating from this study is available for future use by whosoever wishes.  
Please reference data sources accordingly.

